

Copyright Warning & Restrictions

The copyright law of the United States (Title 17, United States Code) governs the making of photocopies or other reproductions of copyrighted material.

Under certain conditions specified in the law, libraries and archives are authorized to furnish a photocopy or other reproduction. One of these specified conditions is that the photocopy or reproduction is not to be “used for any purpose other than private study, scholarship, or research.” If a user makes a request for, or later uses, a photocopy or reproduction for purposes in excess of “fair use” that user may be liable for copyright infringement,

This institution reserves the right to refuse to accept a copying order if, in its judgment, fulfillment of the order would involve violation of copyright law.

Please Note: The author retains the copyright while the New Jersey Institute of Technology reserves the right to distribute this thesis or dissertation

Printing note: If you do not wish to print this page, then select “Pages from: first page # to: last page #” on the print dialog screen

The Van Houten library has removed some of the personal information and all signatures from the approval page and biographical sketches of theses and dissertations in order to protect the identity of NJIT graduates and faculty.

ABSTRACT

A STUDY OF THE BIOFILTRATION PROCESS UNDER SHOCK-LOADING CONDITIONS

by
Helen Androutsopoulou

Biofiltration is a new technology for treating airstreams contaminated with emissions of volatile organic compounds (VOCs). It employs porous particles which are placed in reactors, in packed-bed configurations, after appropriate microorganisms have been immobilized on the solid support.

Biofiltration involves complex processes, and is not yet well understood. In this thesis the response of biofilter units to quantitative and qualitative changes in the inlet airstreams was examined. Steady state data were also analyzed through the use of an existing detailed model.

Experiments were performed with two small-scale biofilters, and with ethanol and butanol as model compounds. Each biofilter was dedicated to one compound for a period of eight months. Subsequently, and for a period of four months, the inlets to the two biofilters were switched.

It was found that biofilters respond very successfully to quantitative shock-loading conditions, and less effectively to qualitative shock-loads. Adsorption/desorption of VOCs on the packing material was found to be a key factor for the transient response. Excellent agreement was found between steady state data and model predictions.

**A STUDY
OF THE BIOFILTRATION PROCESS
UNDER SHOCK-LOADING CONDITIONS**

by
Helen Androutsopoulou

**A Thesis
Submitted to the Faculty of
New Jersey Institute of Technology
in Partial Fulfillment of the Requirements for the Degree of
Master of Science in Chemical Engineering**

**Department of Chemical Engineering,
Chemistry, and Environmental Science**

May 1994

APPROVAL PAGE

**A STUDY OF THE BIOFILTRATION PROCESS
UNDER SHOCK-LOADING CONDITIONS**

Helen Androutsopoulou

Dr. Basil C. Baltzis, Thesis Advisor Date
Professor of Chemical Engineering, NJIT

Dr. Piero M. Armenante, Committee Member Date
Professor of Chemical Engineering and Graduate
Advisor for Chemical Engineering, NJIT

Dr. Demetri Petrides, Committee Member Date
Assistant Professor of Chemical Engineering, NJIT

BIOGRAPHICAL SKETCH

Author: Helen Androutsopoulou
Degree: Master of Science in Chemical Engineering
Date: May 1994

Undergraduate and Graduate Education

- Master of Science in Chemical Engineering,
New Jersey Institute of Technology,
Newark, New Jersey, 1994
- Bachelor of Science in Chemical Engineering,
National Technical University of Athens,
Greece, 1992

Major: Chemical Engineering

Presentations and Publications:

Baltzis, B.C., and H. Androutsopoulou. "A Study on the Response of Biofilters to Shock-Loading." *To be presented at the 87th A&WMA Annual Meeting*. Cincinnati, OH (June 1994).

Shareefdeen, Z., H. Androutsopoulou, and B.C. Baltzis. "Solvent Emissions Control with a Packed-Bed Biofilter: Steady-State and Transient Behavior." *Presented at the American Institute of Chemical Engineers 1993 Annual Meeting*. St. Louis, Missouri, November 7-12, 1993.

ACKNOWLEDGMENT

I would like to express my sincere gratitude to my advisor, Basil C. Baltzis, for his invaluable support and guidance during the course of my research work. I am also thankful to Professors Piero M. Armenante and Demetri Petrides for serving as members of my committee.

I want to deeply thank all the members of the Biodegradation Laboratory, for devoting their time and effort in helping me, whenever I needed them.

I am also grateful to the Emission Reduction Research Center (ERRC), an NSF Industry/University Cooperative Research Center headquartered at the New Jersey Institute of Technology, for funding this project.

Finally, I would like to say a special thank you to my family, Victor Papaconstantinou, and all my friends, here and back home, for their moral support throughout this difficult experience.

TABLE OF CONTENTS

Chapter	Page
1 INTRODUCTION.....	<u>1</u>
2 LITERATURE REVIEW.....	<u>7</u>
3 OBJECTIVES.....	<u>14</u>
4 MATERIALS AND METHODS.....	16
4.1 Microorganisms and Medium.....	<u>16</u>
4.2 Kinetics Determination.....	16
4.3 Biofilter Set-Up.....	<u>18</u>
5 KINETIC EXPERIMENTS.....	20
5.1 Mathematical Modeling.....	20
5.2 Results.....	24
6 BIOFILTER EXPERIMENTS.....	28
6.1 Mathematical Description of the System at Steady State.....	28
6.2 Results and Discussion.....	<u>34</u>
7 CONCLUSIONS AND RECOMMENDATIONS.....	<u>63</u>
APPENDIX A.....	65
APPENDIX B.....	80
REFERENCES.....	91

LIST OF TABLES

Table	Page
1 Composition of the nutrient medium.....	16
2 Kinetic parameters.....	24
3 Model parameter values used for predicting steady state concentrations and removal rates.....	33
4 Experimental and model predicted steady state removal rates for butanol vapor in a biofilter exposed to butanol only.....	35
5 Experimental and model predicted steady state removal rates for ethanol vapor in a biofilter exposed to ethanol only.....	36
6 Experimental and model predicted steady state removal rates for butanol vapor in a biofilter exposed to ethanol prior to the switch to butanol.....	37
7 Experimental and model predicted steady state removal rates for ethanol vapor in a biofilter exposed to butanol prior to the switch to ethanol.....	37
A-1 Experimental and regressed data from kinetic runs on ethanol.....	66
A-2 Experimental and regressed data from kinetic runs on butanol.....	66

LIST OF FIGURES

Figure	Page
1 Schematic of the experimental fixed-bed biofilter unit.....	18
2 Specific growth rate of biomass on ethanol under no oxygen limitation.....	25
3 Specific growth rate of biomass on butanol under no oxygen limitation.....	25
4 Schematic of the biofilm concept at a cross section along the biofilter column.....	29
5 Transient response of the ethanol concentration in the air exiting the biofilter when the ethanol concentration in the air supplied to the biofilter is varied. Data from a biofilter exposed to ethanol only. The space time was kept constant at 1.86 min ($F = 0.030 \text{ m}^3 \text{ h}^{-1}$).....	40
6 Transient response of the ethanol removal rate in a biofilter exposed to ethanol only when the concentration in the inlet air is varied. The graph is an alternate representation of the data shown in Figure 5.....	41
7 Transient response of the butanol concentration in the air exiting the biofilter when the butanol concentration in the air supplied to the biofilter is varied (A: 1.59 g m^{-3} , B: 2.61 g m^{-3} , C: 5.09 g m^{-3} , D: 3.13 g m^{-3} , and E: 0.98 g m^{-3}). Data from a biofilter exposed to butanol only. The space time was kept constant at 1.96 min ($F = 0.030 \text{ m}^3 \text{ h}^{-1}$).....	42
8 Transient response of the ethanol removal rate in a biofilter exposed to ethanol only when the concentration in the inlet air is varied (A, B, C, D, E correspond to the same concentrations as in Figure 7). The graph is an alternate representation of the data shown in Figure 7.....	43
9 Transient response of the ethanol concentration at the exit of the biofilter (curve 1), and of the ethanol removal rate (curve 2) when the ethanol concentration in the inlet air is kept constant at about 4.2 g m^{-3} while the air flowrate varies. Data from a biofilter exposed to ethanol only. Units of C_{exit} : g m^{-3} ; R: $\text{g h}^{-1} \text{ m}^{-3}$ -packing.....	44
10 Transient response of the butanol concentration at the exit of the biofilter (curve 1), and of the butanol removal rate (curve 2) when the butanol concentration in the inlet air is kept constant at about 1.1 g m^{-3} while the air flow rate varies. Data from a biofilter exposed to butanol only. Units of C_{exit} : g m^{-3} ; R: $\text{g h}^{-1} \text{ m}^{-3}$ -packing.....	45
11 Response of a biofilter to changes in the identity of the solvent vapors (qualitative shock loading). The unit originally treated butanol vapors. Last experiment before switching to ethanol was performed with inlet butanol	

LIST OF FIGURES
(Continued)

Figure	Page
<p>concentration $C_{Bin} = 0.25 \text{ g m}^{-3}$ and $\tau = 1.63 \text{ min}$ ($F = 0.036 \text{ m}^3 \text{ h}^{-1}$). At a certain instant of time (designated as zero) the inlet stream was switched to ethanol with inlet concentration $C_{Ein} = 0.53 \text{ g m}^{-3}$. The space time for the new stream was 2.45 min ($F = 0.024 \text{ m}^3 \text{ h}^{-1}$).....</p>	46
<p>12 Response of a biofilter to changes in the identity of the solvent vapors (qualitative shock loading). The unit originally treated ethanol vapors. Last experiment before switching to butanol was performed with inlet ethanol concentration $C_{Ein} = 0.67 \text{ g m}^{-3}$ and $\tau = 1.6 \text{ min}$ ($F = 0.036 \text{ m}^3 \text{ h}^{-1}$). At a certain instant of time (designated as zero) the inlet stream was switched to butanol with inlet concentration $C_{Bin} = 0.49 \text{ g m}^{-3}$. The space time for the new stream was 2.33 min ($F = 0.024 \text{ m}^3 \text{ h}^{-1}$).....</p>	47
<p>13 Concentration profile of butanol vapor in the air along a biofilter column at constant flow rate of $0.048 \text{ m}^3 \text{ h}^{-1}$.....</p>	49
<p>14 Concentration profile of ethanol vapor in the air along a biofilter column at constant flow rate of $0.024 \text{ m}^3 \text{ h}^{-1}$.....</p>	50
<p>15 Model predicted concentration profiles in the biolayer at the middle point of the biofilter. The experimental conditions were, air flow rate $0.024 \text{ m}^3 \text{ h}^{-1}$, and inlet ethanol concentration 2.34 g m^{-3}.....</p>	51
<p>16 Model predicted concentration profiles in the biolayer at the middle point of the biofilter. The experimental conditions were, air flow rate $0.048 \text{ m}^3 \text{ h}^{-1}$, and inlet butanol concentration 0.38 g m^{-3}.....</p>	52
<p>17 Radial profiles of the ethanol concentration in the biofilm at increasing bed heights. The residence time is kept constant at 0.45 min with $F = 84,585 \text{ m}^3 \text{ h}^{-1}$.....</p>	54
<p>18 Axial profiles of active biofilm thickness at different inlet pollutant concentrations, loads, and τ. The values of V_p for the three curves are: (1) 638 m^3; (2) 980 cm^3; and (3) 556 m^3.....</p>	56
<p>19 Predicted required biofilter volume at constant conversion and constant values of rate of mass of VOC supply.....</p>	58
<p>20 Sensitivity analysis of the effect of the kinetic parameters on the removal rate of butanol. Conditions for this graph are discussed in the text.....</p>	59
<p>21 Sensitivity analysis of the effect of parameters A_S, X_V, and m on the</p>	

LIST OF FIGURES
(Continued)

Figure	Page
removal rate of butanol. Conditions for this graph are discussed in the text.....	60
22 Sensitivity analysis of the effect of the kinetic parameters on the removal rate of ethanol. Conditions for this graph are discussed in the text.....	62
23 Sensitivity analysis of the effect of parameters A_S , X_V , and m on the removal rate of ethanol. Conditions for this graph are discussed in the text.....	62
A-1 Transient response of the butanol concentration in the biofilter exit when the butanol concentration in the incoming air stream is varied. Data from a biofilter exposed to butanol only. The space time was kept constant at 0.89 min ($F = 0.066 \text{ m}^3 \text{ h}^{-1}$).....	67
A-2 Transient response of the butanol removal rate when the concentration in the inlet air is varied. This graph is an alternate representation of the data shown in Figure A-1.....	67
A-3 Transient response of the ethanol concentration in the biofilter exit when the ethanol concentration in the incoming air stream is varied. Data from a biofilter exposed to ethanol only. The space time was kept constant at 2.33 min ($F = 0.066 \text{ m}^3 \text{ h}^{-1}$).....	68
A-4 Transient response of the ethanol removal rate when the concentration in the inlet air is varied. This graph is an alternate representation of the data shown in Figure A-3.....	68
A-5 Transient response of the butanol concentration at the exit of a biofilter which was switched from ethanol to butanol. The space time was kept constant at 2.33 min ($F = 0.024 \text{ m}^3 \text{ h}^{-1}$).....	69
A-6 Transient response of the ethanol concentration at the exit of a biofilter which was switched from butanol to ethanol. The space time was kept constant at 2.45 min ($F = 0.024 \text{ m}^3 \text{ h}^{-1}$).....	69
A-7 Transient response of the butanol concentration at the exit of a biofilter which was switched from ethanol to butanol. The space time was kept constant at 2.33 min ($F = 0.024 \text{ m}^3 \text{ h}^{-1}$).....	70
A-8 Transient response of the ethanol concentration at the exit of a biofilter which was switched from butanol to ethanol. The space time was kept constant at 2.45 min ($F = 0.024 \text{ m}^3 \text{ h}^{-1}$).....	70

LIST OF FIGURES
(Continued)

Figure	Page
A-9 Transient response of the butanol concentration at the exit of a biofilter which was switched from ethanol to butanol. The space time was kept constant at 1.86 min ($F = 0.030 \text{ m}^3 \text{ h}^{-1}$).....	71
A-10 Transient response of the ethanol concentration at the exit of a biofilter which was switched from butanol to ethanol. The space time was kept constant at 1.96 min ($F = 0.030 \text{ m}^3 \text{ h}^{-1}$).....	71
A-11 Concentration profile of butanol vapor in the air along a biofilter column at constant flow rate of $0.024 \text{ m}^3 \text{ h}^{-1}$	72
A-12 Concentration profile of butanol vapor in the air along a biofilter column at constant flow rate of $0.072 \text{ m}^3 \text{ h}^{-1}$	72
A-13 Concentration profile of butanol vapor in the air along a biofilter column at constant flow rate of $0.066 \text{ m}^3 \text{ h}^{-1}$	73
A-14 Concentration profile of butanol vapor in the air along a biofilter column at constant flow rate of $0.072 \text{ m}^3 \text{ h}^{-1}$	73
A-15 Concentration profile of butanol vapor in the air along a biofilter column at constant flow rate of $0.036 \text{ m}^3 \text{ h}^{-1}$	74
A-16 Concentration profile of butanol vapor in the air along a biofilter column at constant flow rate of $0.024 \text{ m}^3 \text{ h}^{-1}$	74
A-17 Concentration profile of butanol vapor in the air along a biofilter column at constant flow rate of $0.030 \text{ m}^3 \text{ h}^{-1}$	75
A-18 Concentration profile of butanol vapor in the air along a biofilter column at constant flow rate of $0.048 \text{ m}^3 \text{ h}^{-1}$	75
A-19 Concentration profile of butanol vapor in the air along a biofilter column at constant flow rate of $0.072 \text{ m}^3 \text{ h}^{-1}$	76
A-20 Concentration profile of ethanol vapor in the air along a biofilter column at constant flow rate of $0.015 \text{ m}^3 \text{ h}^{-1}$	76
A-21 Concentration profile of ethanol vapor in the air along a biofilter column at constant flow rate of $0.015 \text{ m}^3 \text{ h}^{-1}$	77
A-22 Concentration profile of ethanol vapor in the air along a biofilter column at constant flow rate of $0.024 \text{ m}^3 \text{ h}^{-1}$	77

LIST OF FIGURES
(Continued)

Figure	Page
A-23 Concentration profile of ethanol vapor in the air along a biofilter column at constant flow rate of $0.030 \text{ m}^3 \text{ h}^{-1}$	78
A-24 Concentration profile of ethanol vapor in the air along a biofilter column at constant flow rate of $0.024 \text{ m}^3 \text{ h}^{-1}$	78
A-25 Model predicted concentration profiles in the biolayer at the middle point of the biofilter. The experimental conditions were, air flow rate $0.012 \text{ m}^3 \text{ h}^{-1}$, and inlet ethanol concentration 9.59 g m^{-3}	79
A-26 Model predicted concentration profiles in the biolayer at the middle point of the biofilter. The experimental conditions were, air flow rate $0.030 \text{ m}^3 \text{ h}^{-1}$, and inlet butanol concentration 1.59 g m^{-3}	79

CHAPTER 1

INTRODUCTION

Several industrial plants, such as the pharmaceutical industry, wastewater and sewage treatment works, and a few categories of the food industry, constitute a continuous source of emission of large volumes of waste gases containing volatile organic compounds (VOCs). VOCs contribute to a variety of air quality problems. VOC containing off-gas streams, in addition to the unpleasant odors that they emit, contain toxic compounds which pose possible health hazards on treatment plant employees, and neighboring residents. Additionally, as Moretti and Mukhopadhyay (1) mention in their recent study on VOC control, photochemically reactive volatile organic compounds are precursors to ground level ozone, contributing significantly to the formation of smog. Due to all these harmful impacts, VOC emissions have become a major target of regulations under local, state, and federal programs. Specifically, the Clean Air Act Amendments of 1990 (CAAA) impose strict laws, and force thousands of currently unregulated sources of VOC emissions to meet the regulatory limits.

Ethanol and butanol are two characteristic examples of volatile organic compounds that can serve as precursors to ozone, while as mentioned in the study of Leson et al. (2), when ethanol is present at levels higher than 1,000 ppmv ($\sim 1900 \text{ mg m}^{-3}$), it imposes a possible danger for the people working or living in the emission area. Commercial bakeries are sources of ethanol emissions, since ethanol is a fermentation by-product released to the atmosphere. In their survey, Wooley et al. (3) mention that ethanol is the component of many consumer products. It is widely used as solvents in liquid laundry and hand-dish washing detergents, constituting more than ten percent of their mass, and is released to the environment upon its use. Similarly, as solvents, ethanol and butanol are used in the pharmaceutical industry, as well as in dry-cleaning operations. In an effort to eliminate the

harmful emissions of ethanol, a ruling was recently issued in the San Francisco Bay Area, requiring the installation of control devices in large bakeries, in order to reduce their emissions by an estimated total of one metric ton per day (3).

In order to address the problems caused by the dangerous VOC emissions, a number of different technologies, employing physical and chemical methods for treating contaminated air streams, have been developed. Among these technologies the most widely applied are thermal incineration, catalytic oxidation, ultraviolet oxidation, chemical scrubbing by means of chlorine and ozone, condensation, and adsorption/absorption processes. Although these technologies offer effective means for VOC control, they also have certain disadvantages that impose the need for an alternate control process. The most serious drawbacks of the conventional methods are their high installation, maintenance, and operating costs, as well as the production of toxic and hazardous substances, or the creation of secondary pollution needing further treatment.

A very promising solution to these problems, seems to be offered by the implementation of biological methods for the purification of polluted air streams. Biological degradation of different chemical, organic and inorganic, compounds is a process occurring naturally in physical environments for billions of years. Millions of microbial species present in the soil and plants, are continuously involved in microbiological processes which constitute a natural method for purification of the atmosphere from existing compounds. Through the evolution process, microorganisms (mainly bacteria and to a small extent, filamentous fungi and yeasts) have developed enzymatic systems to degrade biogenic (naturally originated), as well as anthropogenic (man made) compounds, and convert them under aerobic conditions to mineral end-products (e.g. H_2O , CO_2 etc.).

The ability of microorganisms to degrade organic substances can be exploited by using them in specially designed systems for the removal of environmentally undesired compounds. Such an application would offer the advantage of low operation and

maintenance costs, as well as environmentally safe end-products. In fact, this concept has already been successfully established in the area of waste water treatment and remediation of contaminated soil, but only very recently gained attention for the treatment of polluted air (4). Actually, only a few years ago "biofiltration", i.e., the biological removal of air contaminants from effluent air streams in a solid phase reactor, became an accepted air pollution control technology, predominantly in the Netherlands and West Germany.

Biofiltration is defined as the removal and oxidation of pollutants present in contaminated air, by the use of microorganisms immobilized on solid support, e.g. soil, compost, peat, bark, etc. Biofilters are beds, open or closed, of porous packing material on which appropriately selected microorganisms are immobilized. The bed constitutes an extensive network of fine pores, having large surface areas onto which VOCs sorb, along with an excess of water, and get oxidized by microorganisms. The carrier particles are surrounded by a wet biolayer, created by the adsorption of the water present in their pores. This water layer is where biodegradation happens. More specifically, as the waste gas flows through the bed, continuous mass transfer takes place between the gas phase and the biolayer. Pollutants, as well as the oxygen present in the air are dissolved in the biofilm and are consumed by the microorganisms also contained in the water layer. The second removal process, which is of great importance too in the remediation process, is the adsorption of the contaminants onto the carrier surface. Biofilters, unlike conventional air pollution control techniques which employ only unique physicochemical methods, simultaneously wash, adsorb, and oxidize pollutants. This way, biofilters offer a cheap, safe, and very effective alternate solution for treating polluted off-gas streams.

However, biofiltration is not as simple as it appears, and its design should successfully meet certain requirements, otherwise it can end up being a very expensive and poorly performing process. These design considerations are extensively described by Leson and Winer, in their recent review (6), as well as in a survey by Bohn (7). Basically, what should be considered in the biofilter design is the need to provide the

microorganisms with a hospitable environment, and the optimum conditions for the oxidation of the carbon source. The packed bed configuration should fulfill certain requirements, the most important of which are proper temperature and pH levels, presence of needed oxygen and nutrients, low pressure drop, high surface area, and maintenance of adequate moisture contents.

Based on the above considerations, the ideal packing should consist of special materials offering a high adsorption capacity, assuring the presence of the necessary nutrients for the growth of the microorganisms, and containing minerals and bases that can neutralize any acidity resulting from the oxidations and offer buffering capacity. The packing should be porous, and the bed should have enough voids, so that there is minimal pressure drop, uneven aeration, or channeling which can lead to the development of anaerobic zones operating at inadequate oxygen concentrations. The oxygen concentrations in the inlet gas stream should be at least 5 to 10 percent by volume (4), and the temperature between 25-35°C (8), which is the temperature range for microbial maximum growth rates. Furthermore, one of the most important considerations is to maintain a moisture content which is optimal at 40 to 60 percent of the bed by weight. Too little moisture results in the development of dry zones where the microbial activity stops, while excessive water levels can lead to compaction, breakthroughs of incompletely treated raw gas, and the formation of anaerobic zones. Since the microbial processes are exothermic, a large amount of the moisture content of the bed is being carried by the gas, and additional moisture should be provided, either by saturating the raw gas by passing it through water, or by spraying water at the top of the vessel. Moreover, the packing material should be hydrophilic enough, in order to be able to maintain the provided moisture, and be easily rewetted when dried. Finally, the kinetic limitations of the microbial reactions should be considered, and adequate reactor volume be provided, so that sufficient residence time is offered for the desired removal rates to be achieved.

Biofiltration could also be applied for the treatment of air streams from batch

operations, such as the pharmaceutical industry, provided that biofilters are able to respond to frequent variations in the quantitative and qualitative characteristics of the air streams. This application could be useful for cases where different solvents are utilized at different time periods (qualitative changes in the composition of the air streams), or where the operating flow rates and concentrations are varying with time (quantitative changes). Sudden variations in the flow rate or concentration of pollutants in the inlet air stream imply changes in the load, and are known as shock-loading effects. Bohn (5) suggests in a recent review on biofiltration, that biofilters are quite resistant to shock loads, as the excess of oxygen, nutrients, and microbial population can absorb sudden VOC increases and respond quite effectively. This is a claim which needs further investigation.

The term which is used for the measurement of the efficiency of biofilters has already been introduced by other researchers (4,11), and is known as the removal rate, or elimination capacity. It is defined as the amount of pollutant converted per unit time and per unit volume of the packing material; it can be calculated through the following equation,

$$R = \frac{F}{V_p} (C_{ji} - C_{je}) \quad (1.1)$$

where, C_{ji} and C_{je} are the concentrations of compound j in the air stream at the entrance and exit of the biofilter, respectively; F is the flow rate of the air supplied to the biofilter; V_p is the volume of the packing material.

One more term which is very often mentioned through this thesis, is the load, and needs to be defined here. The load is the amount of the pollutant supplied to the biofilter unit per unit time and per unit volume of packing material. In mathematical terms, the load is defined via the following equation,

$$L = \frac{F}{V_p} C_{ji} \quad (1.2)$$

As can be seen from equations (1.1) and (1.2), if the pollutant is completely

removed in a biofilter unit, the removal rate and the load are identical.

This thesis is a systematic investigation of the response of biofilters to quantitative and qualitative shock-loading conditions. Two packed-bed biofilters were set-up and operated over a period of eight months with airstreams containing ethanol and butanol, respectively, at varying flow rates and inner pollutant concentrations. Eventually, the identities of the solvents in the incoming streams were switched and the effect of qualitative shock-load was studied for a period of four months. Prior to biofilter experiments, two series of batch experiments were performed in closed serum bottles, and the biodegradation kinetics were revealed for ethanol and butanol separately. Using the determined kinetic expressions, extensive numerical work, based on a preexisting model (24), was done, and the experimental steady state data of the biofilters were analyzed in detail.

CHAPTER 2

LITERATURE REVIEW

The concept of biofiltration was originally proposed for odor control purposes, and even this occurred relatively recently, in 1923, when Bach (6) suggested the use of biological methods to treat H₂S emissions from a sewage treatment plant. More than 25 years after this report, in 1950, the first patent was issued in West Germany, aiming at the realization of the concept of biofiltration. At about the same time, in 1957, Pomeroy (9) published in the US the first patent for a soil bed concept which was successfully implemented in the construction of the first biofilter unit in California. In 1959 a soil bed reactor was also installed in West Germany, mainly for odor control.

Carlson and Leiser (10) in the early 1960s conducted in the US the first systematic research on biofiltration, and the results of their work were applied in the installation of several biofilters at a waste water treatment plant near Seattle, CA. A number of studies on the soil bed concept, along with full-scale applications, were demonstrated in the 1960s and 1970s, and these are reviewed in detail in a study published by Ottengraf (11).

Although the main principles of biofiltration were qualitatively well understood since the 1960s, the design of commercially applied systems was predominantly done empirically up to the early 1980s. At that time, the first detailed theoretical studies on biofiltration were published, along with mathematical models. These models could describe the process, and could be used in sizing full scale systems. The first important contributions to the development of a thorough knowledge of biofiltration were made by Ottengraf and his co-workers, in the Netherlands. In their first study, Ottengraf and Van den Oever (12) used a peat-compost biofilter to investigate the removal of organic compounds from air emissions in laqueries. A biofilter was used for treatment of a synthetic waste gas stream containing vapors of a mixture of toluene, ethyl acetate,

butanol, and butyl acetate. The peat-compost biofilter mediated to achieve high VOC removal rates, and a low pressure drop, while it kept its microbial activity constant over a period of two years. Also, after a two week period of inactivity, the microbial activity in the filter bed showed no signs of decrease. The (macro)kinetics of the elimination process, along with the corresponding kinetic parameters were experimentally determined, and found to follow a zero-order model. The same authors, proposed a theoretical model for describing the behavior of the system. Experimentally, it was found that the maximum elimination rate of each component amounted to ca. 20-40 g h⁻¹ m⁻³-packing, and the theoretical curve representing the pollutant's concentration profile along the biofilter bed was in good agreement with the experimentally measured values.

In another investigation (13), Ottengraf and his co-workers examined the ability of biofilter to eliminate volatile xenobiotic compounds. Among the compounds which proved susceptible to microbial activity were the following: 2-propanol, ethyl-acetate, ethyl-lactate, diacetone alcohol, and 1-ethoxy-2-propanol. The accompanying kinetic study concluded that all these compounds were eliminated according to zero-order reaction kinetics, while the elimination capacity in the bed was found to be dependent on both the organic load to the filter bed, and the gas flow rate. In the same work, the performance of multistage biofilters for treatment of a waste gas stream containing acetone, ethanol, 2-propanol, and dichloromethane was also studied. It was found that acetone was eliminated in the first stage at a maximum rate of 164 g h⁻¹ m⁻³-packing, ethanol and 2-propanol were completely degraded in the second stage (removal rate, 57 g h⁻¹ m⁻³-packing), and dichloromethane was partially converted in the third stage after inoculation with a specific culture. Discontinuous biofilter operation was also studied, and it was concluded that fluctuations in the gas inlet concentrations can be smoothed by the sorptive capacity of the biofilter. Furthermore, addition of activated carbon was reported to provide storage capacity for VOCs. Adsorption of the pollutant during peak loads, followed by desorption during reduced loads was reported to lead to treatment of the excess load. It was also

suggested that the system could be further improved by dividing the processes of adsorption/desorption and biodegradation into two different stages.

In another series of studies, Ottengraf and Diks (14-16) investigated the ability of biological trickling beds to treat waste gases contaminated with dichloromethane vapors. The trickling filter bed is a type of packed bed reactor, being different from the classical biofilters in the sense that the aqueous phase present in the bed is moving instead of staying stationary. This feature of the trickling filters offers the advantage of pH control in cases of acidic products. These products can be dissolved in the continuous water phase which is recirculated through the packed bed. There are actually three different types of waste gas biotreaters (biofilters, bioscrubbers, and trickling filters), and their characteristics are discussed again by Ottengraf in a different study (17). In their investigation about the ability of trickling filters to remove dichloromethane vapors, Diks and Ottengraf showed that a stable dichloromethane elimination performance can be achieved, with the start-up period of the system being only a few weeks long. They found that the elimination capacity of the system had a maximum value of $157 \text{ g h}^{-1} \text{ m}^{-3}$ -packing. They also developed a simplified steady state model for predicting the performance of the system, under the assumption of existence of very low gas-liquid mass transfer resistances. They examined cases of inlet gas concentrations much higher than the kinetic constant in the Monod expression, and thus, they assumed that the biological reaction kinetics inside the biofilm were zero-order with respect to the substrate concentration. It should be mentioned though, that low gas phase concentrations do not necessarily imply low concentration values in the biofilm. The model predictions for the elimination capacity of the trickling filter were very close to the experimental measurements, under various conditions. It was also shown that the degree of conversion achieved in the system could be described as a function of the total superficial gas contact time. After being unable to treat mixtures of dichloromethane and methylmethacrylate in the same system, these investigators concluded that an accurate knowledge of the intrinsic growth parameters, as

well as the characteristics of the biofilm formed on the packing, is necessary for the design of a trickling filter.

Another researcher, also in the Netherlands, van Lith (18,19), studied the ability of biofilters to eliminate more than 40 different substances, and presented useful information concerning the design of biofilters. For his modeling work he used the zero-order kinetic approach developed by Ottengraf. The theoretically predicted removal rates that he calculated, were in close approximation with the experimental results, even for cases of treatment of mixtures. The removal rate of methylformiate that he reported, was $500 \text{ g h}^{-1} \text{ m}^{-3}$ -packing, the highest ever measured. He also tested mixtures of methanol and isobutanol, and came to the conclusion that isobutanol influences the degradation of methanol, and that at high levels of isobutanol presence the break-down of methanol stops completely. Finally, van Lith suggested that the filter material in the reactor was capable of adsorbing VOCs to a certain extent. As a result, high removal rates measured after increases in inlet concentration, could be only apparent. For some experimental data a negative elimination (production) of methanol was detected, something which could only be explained by the assumption that desorption phenomena occurred.

Biofiltration studies in the US started only in the very recent years. Kambell published in 1987 a study (20), in which he investigated the removal of propane, isobutane, and n-butane from a polluted air stream in a small-scale soil bed set-up. The results indicated that light aliphatic hydrocarbons and trichloroethylene, a compound originally resistant to aerobic biological treatment, could be removed. Biodegradation kinetics were found to be of first order. The bioreactor was able to reduce the hydrocarbon concentration in the air stream by at least 90 percent, with a residence time of 15 minutes. A substantial pressure drop of 85 cm of water was observed.

Utgikar et al. (21), published a study in which they developed a steady state model describing the biodegradation of VOCs in a biofilter. For the development of the model they primarily used the assumptions made by Ottengraf, with few modifications. They

assumed for example, that the biodegradation reaction follows a first-order expression with respect to the substrate, and that the adsorption of the pollutant vapors on the carbon support follows the Freundlich isotherm. In order to describe the steady state behavior of the system, they performed a number of numerical studies. The results were subsequently used in sizing a biofilter for 90 percent removal of VOCs from air stripper off-gases of landfill leachates. The most common constituents of these gases were benzene, toluene, acetone, higher ketones, chloroform, methylene chloride, chloroalkanes, and chlorobenzene. Detailed experimental data for the removal of toluene and methylene chloride in a bench scale biofilter were also presented. The results were in good agreement with the model predictions.

Hartmans and Tramper (22) simulated the mass transfer and degradation of VOCs in a trickling-bed bioreactor by calculating the volumes of a series of identical, ideally-stirred tank reactors required to give the desired conversion. In another study by Ockeleon et al. (23), a simulation model of a fixed-bed bioscrubber was presented. This model was an extension of the modeling approach of Diks and Ottengraf (14-16). Results of computer simulations, showed that as the solubility of the pollutant decreases, the removal efficiency decreases. Furthermore, with less soluble compounds co-current operation of the unit is more efficient. These authors also proved that the simplified model of Diks and Ottengraf, which assumes uniform liquid concentration, is only applicable for short columns in which, the removal efficiencies are independent of the liquid and gas relative flow directions. They also concluded that the zero-order assumption may not be valid in cases where the actual kinetics are of Monod type, and the half-saturation coefficient is significant compared to the liquid concentration.

In their work with biofilters, Baltzis et al. (24-26) studied the removal of methanol, as well as mixtures of toluene and benzene vapors, in both small and large scale laboratory biofilters. This group developed a mathematical model for the description of the process, and for sizing biofilter units operating at desired removal rates. The model predictions

were experimentally validated for both cases of single compounds and mixtures. Unlike the rest of the theoretical approaches, these authors took more realistically into account the issue of oxygen availability inside the moist biolayer, and considered its potential limiting effects on the process. They did not assume, like in the rest of the studies, that oxygen in the biofilm is in excess at all times. Instead they developed their model in terms of both the electron donor (carbon source), and the electron acceptor (oxygen). Furthermore, at the kinetic level, they used actual expressions (mostly of the inhibitory type), instead of the widely used simplified assumptions of zero or first order macro kinetics. Finally, for the case of mixtures, they introduced a model considering the potential interactions among solvents, rather than assuming that each pollutant in the mixture is being degraded independently of the presence of the others. In fact, the experimentally determined kinetic model showed that toluene inhibits the removal of benzene much more strongly than benzene does for toluene, when both solvents are treated simultaneously.

In a very recent study, Deshusses and Hamer (27) investigated the removal efficiency of a biofilter treating a mixture of methyl ethyl ketone (MEK) and methyl isobutyl ketone (MIBK). The maximum elimination capacities that they reported were $50 \text{ g h}^{-1} \text{ m}^{-3}$ -packing for MEK, and $20 \text{ g h}^{-1} \text{ m}^{-3}$ -packing for MIBK. They came to the conclusion that the degradation of each compound was strongly affected by the presence of the other. They also suggested that for describing the complex processes involved in biofiltration of multicomponent mixtures, detailed knowledge of the degradation kinetic rates for both single, and multiple pollutants, is required.

In another recent work, Smith et al. (28) developed a modeling approach for a trickle bed biofilter. This model takes into account the effect of microbial growth on the hydrodynamics of the flow, and considers Monod type kinetic expressions for the description of the VOC consumption inside the biofilms. A relationship between the flux into the biofilm, and the corresponding biofilm thickness was also introduced. It was

shown that removal rates were very low for cases of low inlet substrate concentrations, most probably due to the existence of a limit in the pollutants gas phase concentration, under which the biofilms cannot be sustained.

There are a few more studies on biofiltration, mostly qualitative, that were published in the last one or two years, establishing the fact that biofilters can be very effectively used for treating a number of different VOCs. Leson et al. (2) demonstrated in their work the ability of biofilters to achieve more than 90 percent removal efficiencies upon treating ethanol containing air streams. They additionally suggested that concentrations up to 2 g m^{-3} are economically preferable, and also have a lower potential for overloading and acidifying the filter material. In a study by Ergas et al. (29), biofiltration was shown to be effective for simultaneously controlling emissions of toluene and dichloromethane, at concentrations between 3 and 50 ppmv. Trichloroethene (TCE) vapors were also present in the inlet gas stream, but no TCE removal was observed, although the reactor was inoculated with the proper TCE degrading microbial culture. Togna and Frisch (30), investigated the effectiveness of a field-pilot biofilter containing 30 ft^3 of packing material to treat styrene contaminated air streams. They reported an overall removal efficiency greater than 95 percent, and that the biofilter was able to respond very successfully to rapid changes in styrene concentration, as well as in intermittent daily and weekly operation. It appeared that the biofilter, upon restarting after being shut down for more than two weeks, needed only 5 to 8 hours to recover more than 90 percent of its removal efficiencies.

As biofiltration appears to have a great potential for treating VOCs, an increasing number of research groups is engaged in studies for a better understanding of the intricacies of this process. The work presented in this thesis is a step in this direction.

CHAPTER 3

OBJECTIVES

The objectives of the present study were the following.

- I. A detailed investigation of the response of biofilter units to frequent variations in the flow rate of the air stream passed through the filter, and in the concentration of the pollutants in the inlet airstream (quantitative shock-loading).

This objective was met by setting-up two packed-bed biofilters, one of which operated with airstreams containing ethanol, while the second removed butanol vapor from air. Each unit operated continuously over a period of eight months. During this period the air flow rate and the presence of ethanol, or butanol in it were varied, in most cases every five days.

- II. A detailed analysis of steady state data obtained during the experiments performed for meeting objective I.

In order to meet this objective, kinetic expressions describing biodegradation of ethanol and butanol were needed. In order to obtain the kinetic expressions, another objective had to be met.

- III. Determination of kinetic expressions and constants for describing the aerobic degradation of ethanol and butanol by the microbial consortia used in the biofiltration experiments.

This objective was met by performing two series of batch experiments, in closed serum bottles. The data from these experiments were analyzed, and the biodegradation kinetics were revealed.

Once objective III was met, detailed numerical studies were performed in order to meet Objective II. In these studies, a model developed earlier (24) was used. The steady state biofiltration data were presented, and extensive computer simulations were

performed so that the sensitivity of the model to the various parameters could be determined. Once the model was validated, it was used in some preliminary design calculations.

IV. A preliminary investigation of the response of biofilters to qualitative shock-loading conditions.

This objective was met by using the biofilter which removed ethanol for eight months, to remove butanol. Also the biofilter which removed butanol for eight months, was subsequently subjected to ethanol containing airstreams. These experiments lasted for a period of four months.

The results of the work performed to meet Objectives I, II, and IV are presented in Chapter 6. Chapter 5 deals with the work done to meet Objective III.

CHAPTER 4

MATERIALS AND METHODS

4.1 Microorganisms and Medium

A microbial consortium of butanol degrading organisms was obtained from the microbiology laboratory of Professor R. Bartha, at Rutgers University. Part of this consortium was acclimated to ethanol, and found to be quite effective in removing it. Inocula of both cultures were maintained by periodically transferring 5 ml of every old suspension to 100 ml of fresh medium which contained 10 μ l liquid volume of the corresponding substrate. After transfer, the cultures were kept in sealed serum bottles, stored in an incubator at 30° C. The aqueous medium used for cultivation was the same for both cultures, and its composition is shown in Table 1.

Table 1 Composition of the nutrient medium.

Component	Concentration (kg m ⁻³ -H ₂ O)
Na ₂ HPO ₄	4.0
KH ₂ PO ₄	1.5
NH ₄ Cl	1.0
MgSO ₄ ·7H ₂ O	0.2
CaCl ₂	0.01
FeNH ₄ -nitrate	0.005

4.2 Kinetics Determination

The microbial consortia were first used in small scale shake flask experiments for the determination of the kinetics of the removal of each one of the two substrates. For each run, 10 ml of fresh medium were added to a 160-ml serum bottle. The bottle was then

sealed with aluminum crimp caps (Wheaton Manufacturers, Millville, NJ), placed upon butyl teflon-faced 20 mm-stoppers (Wheaton Manufacturers, Millville, NJ). One milliliter of the corresponding inoculum was then transferred by syringe to the bottle, so that the initial biomass concentration was in the range of 200 to 250 mg dry biomass/l. Next, a specific liquid volume of the solvent was added to the serum bottle, which was placed in a rotary shaker incubator (250 rpm) at 28° C. Each bottle received a different liquid volume of solvent, so that experiments could be performed at different initial substrate concentrations. The volume of the culture suspension in each bottle (10 ml), and shaking were appropriately selected so that growth was neither kinetic, nor mass transfer limited by oxygen.

The utilization of each solvent was monitored by withdrawing 0.2 ml head space gas samples from the bottles, using a 0.5 ml precision gas-tight syringe (Fisher Scientific, Springfield, NJ), equipped with a side-port needle (id. 0.25 mm, length 50 mm). The gas sample was subsequently assayed by injection into a Hewlett-Packard 5890 gas chromatograph (GC) equipped with a Chromosorb 108 80-100 mesh column (6' × 1/8" × 2 mm stainless steel, Chrompack Inc., Bridgewater, NJ) and a flame ionization detector. The carrier gas was nitrogen (24.4 ml min⁻¹), while the rest of the operating conditions were: oven 180° C; injector 200° C; and detector 220° C. Under these conditions, the retention time of butanol was 5 min, and that of ethanol 1.7 min. Standard curves were prepared, prior to the kinetic experiments, by injecting into sealed serum bottles of known volume, precise amounts of the corresponding compound, allowing the solvent to evaporate completely at room temperature, and then sampling the air space with a gas tight syringe.

For the kinetic runs, gas sampling continued until substrate concentrations dropped below the detection limit (~ 0.015 ppm). Biomass concentration was measured only in the beginning, and at the end of each batch experiment, and determined by monitoring the optical density of the liquid samples. The optical density was measured by using a

spectrophotometer (Varian-DMS200) at a wavelength of 540 nm, with deionized water as the reference sample. For optical densities up to 0.6 there was a linear relationship between optical density and biomass concentration, with a slope of 273 g m^{-3} per unit optical density. In cases where the optical density of the sample exceeded 0.6, the sample was diluted with deionized water to a specific ratio, mixed, and the measurement was repeated.

4.3 Biofilter Set-Up

A schematic representation of the experimental set-up used in this study is shown in Figure 1. The columns used were glass manifolds with side ports (Ace Glass, Vineland, NJ), and their dimensions were 60 cm in height and 5 cm in internal diameter.

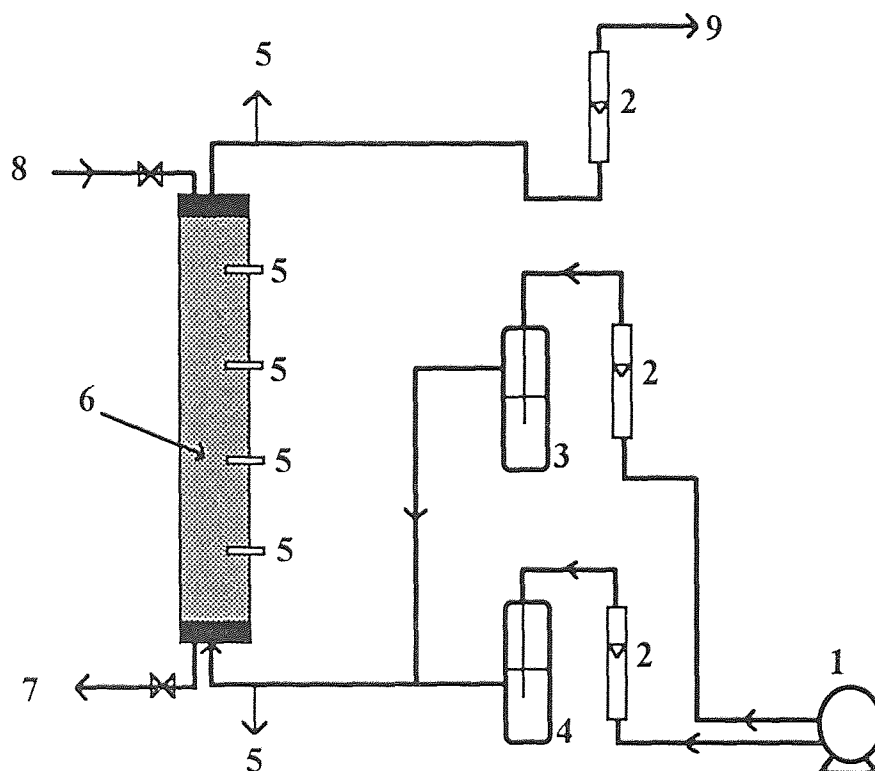


Figure 1 Schematic of the experimental fixed-bed biofilter unit: (1) air pump; (2) air flow meters; (3) solvent tank; (4) water tank; (5) sampling ports; (6) column packing material; (7) water drain; (8) water supply (when needed); (9) exhaust.

An amount of biomass was first prepared in a 3 L fermentor, harvested by centrifugation, and resuspended in fresh mineral medium. The new suspension had a volume equal to 30 percent the volume of the packing material. The packing material was a mixture of peat and perlite, 2:3 volume ratio before mixing. The solids were first steam sterilized, and then a volume of 950 cm³ was mixed with the prepared suspension. After mixing, the solids (with the biomass) were used in packing the biofilter columns.

The biofilter columns were installed in exhaust hoods and their temperature was maintained between 20 and 25° C, although in a few occasions some temperature extremes could not be avoided. In the arrangement shown in Figure 1, compressed oil free air was saturated with water vapors by passing through an 1 L flask containing deionized water. This gas stream consisted of the major humidified air stream, and was passed upwards through the column, after it was mixed with a smaller air stream sparged through a 100 ml flask containing the solvent. Two air flow meters (65-mm direct reading flow meters, Cole-Parmer, Niles, IL), allowed the control of the air flow passing through the water and the solvent. By varying the flow of the air sparged into the solvent, the concentration of the pollutant in the influent stream could be changed. A soap film flow meter (1-10-100 ml, Fisher Scientific, Springfield, NJ) was connected at the top of the column, and was used to determine the total air flow rate. The presence of the contaminant in the stream passing through the bed was monitored via GC analysis of air samples taken from the entrance, exit, and four equally spaced positions along the column.

In most cases, the prehumidification of the inlet air stream was enough to maintain proper moisture levels inside the packing media. In few occasions though, when signs of bed dryness were visually observed, especially at the bottom of the column, water had to be added at quantities of 10 to 15 ml at a time. Incidents of column flooding never occurred. No other nutrients beside the contaminants were supplied to the columns throughout their operation, which lasted about a year. Pressure drop was often monitored and found to be negligible. Actually, it never exceeded a value of 0.25" water/m-packing.

CHAPTER 5

KINETIC EXPERIMENTS

5.1 Mathematical Modeling

In order to be able to better understand, and mathematically predict, biofiltration of VOCs, one needs to determine the kinetic parameters for biological elimination of these compounds. For this reason, separate shake-flask experiments were performed with each one of the compounds studied subsequently in biofilter columns. The data from these experiments were analyzed according to the following theory.

Making the usual assumption that the specific growth rate μ of a culture remains constant during a batch run, one can write

$$\ln \frac{b}{b_0} = \mu(S_j)t \quad (5.1)$$

Equation (5.1) is the integrated form of the following equation, which describes the balance on the biomass in a batch vessel,

$$\frac{db}{dt} = \mu(S_j)b \quad (5.2)$$

In the above two equations, b is the concentration of the biomass at time t ; b_0 is the initial cell concentration; $\mu(S_j)$ is the specific growth rate at a substrate concentration S_j ; S_j is the concentration of the substrate in the aqueous environment of the growth; and t is the time since the start of the reaction.

According to equation (5.1), if biomass concentration data are plotted versus time on a semilogarithmic scale, the constant μ can be determined as the slope of the resulting line. The value of the specific growth rate derived by this method is attributed to the concentration of the substrate at the beginning of the run. This way, from several runs at different initial substrate concentrations, a plot of μ versus S_j can be generated and from

it, the prevailing kinetic expression can be determined.

In the case of volatile substrates, like alcohols, a sealed reactor should be used, in order to control the continuous tendency of the solvent to leave the liquid phase, a behavior that would cause problems upon calculating the amount of the compound degraded as opposed to that evaporated. In such cases, the volume of the liquid phase in the closed system needs to be very small, so that oxygen in the head space stays in excess through the entire run, and its availability does not create reaction limitations. There is, though, a serious problem with a system like this, and it is imposed by the fact that it is very difficult for one to collect a large number of data regarding biomass concentrations at different times during the course of the reaction. This happens because for the determination of the biomass concentration via optical density measurements, the volume of each sample needs to be at least 1 ml, and since the total liquid volume of the reacting medium was just 10 ml, in the experiments performed, frequent sampling was impossible.

In the experiments performed, the volume of the gas phase was 150 ml and for every head space sample only 0.2 ml were needed. As a result, it was very easy to monitor the concentration of the volatile substrate in the gas phase, C_j . These measurements needed to be translated into biomass data. This was done as follows.

Assuming that the degrading substance is following the ideal gas law, and that it is distributed between the two phases according to thermodynamic equilibrium, the substrate concentration in the liquid phase can easily be calculated from the relationship:

$$S_j = \frac{C_j}{m} \quad (5.3)$$

where, m is the distribution coefficient of the compound concerned, and it can also be given as:

$$m = \frac{H}{RT} \quad (5.4)$$

where, H is the Henry's law constant; R is the ideal law constant; and T is the absolute

temperature of the system.

Furthermore, the substrate concentration, S_j , can be related to the biomass concentration, b , if one introduces the yield coefficient, Y , defined as the ratio of the amount of biomass produced per unit amount of substrate consumed. Considering equation (5.2), and using the notion of Y , one can write the following mass balance

$$\frac{dM}{dt} = \frac{1}{Y} \mu b V_l \quad (5.5)$$

where, M is the total mass of the volatile substrate in the flask; and V_l is the volume of the liquid phase. The total mass of the compound is the sum of the amounts present in the gas and the liquid phase, and can be expressed as

$$M = V_l S_j + V_g C_j \quad (5.6)$$

where, V_g is the volume of the head space.

In cases where the liquid phase is sampled no more than one to two times, V_l and V_g can be taken as being constant, and equations (5.3), (5.5), and (5.6) can be combined to give

$$\frac{dC_j}{dt} = \frac{mV_l}{V_l + mV_g} \frac{1}{Y} \mu(S_j) b \quad (5.7)$$

Combining equations (5.2) and (5.7), one gets

$$\frac{dC_j}{dt} = - \frac{mV_l}{V_l + mV_g} \frac{1}{Y} \frac{db}{dt} \quad (5.8)$$

which upon integration yields

$$Y = \frac{m(b - b_0)V_l}{(C_{j0} - C_j)(V_l + mV_g)} \quad (5.9)$$

where, C_{j0} is the concentration of the volatile compound in the head space at the beginning of the experimental run.

Equation (5.9) suggests that there is a linear relationship between C_j and b , and that, once Y is determined, gas phase concentrations can be converted to biomass

concentrations through expression (5.10), which is a rearrangement of equation (5.9).

$$b = b_o + \frac{Y(V_l + mV_g)}{mV_l}(C_{j0} - C_j) \quad (5.10)$$

For the determination of Y , at least two data points giving measurements of the biomass concentration should be available for each run. If one samples the liquid phase in the beginning and at the end of the run, then Y can be calculated from equation (5.9). Subsequently, from the frequently obtained measurements of the concentration of the substrate in the gas phase, the corresponding values of b can be calculated [from equation (5.10)] and plotted as a function of time, in a semilogarithmic scale. As explained before, the slope of the resulting line represents the specific growth rate attributed to the concentration of the substrate in the liquid phase in the beginning of the particular run.

If the μ versus S_j data show that μ reaches a constant value at high substrate concentrations, they should be regressed to the Monod expression, in order to calculate the kinetic constants μ_m and K_m :

$$\mu = \frac{\mu_m S_j}{K_m + S_j} \quad (5.11)$$

If on the other hand, the data indicate that μ reaches a maximum, and after that decreases as S_j increases, then the data should be regressed to the Andrews' expression, shown in expression (5.12)

$$\mu = \frac{\mu^* S_j}{K + S_j + S_j^2 / K_I} \quad (5.12)$$

where, μ^* , K , and K_I are kinetic parameters, having units of inverse time, concentration, and inverse concentration, respectively.

5.2 Results

Two series of batch experiments were performed, one with ethanol and one with butanol.

The values of Y , and μ for each run were determined according to the methodology discussed in the previous section, and are given in Tables A-1 and A-2. For each compound, the value of Y used, is the average of the values determined in the various runs with that compound. The μ versus S_j data indicated that μ goes through a maximum for both ethanol, and butanol. For this reason, the data were regressed to Andrews' expressions of the form of (5.12). The values of the kinetic parameters determined, are given in Table 2. Using these values for the parameters, the specific growth rate curves were generated according to expression (5.12), and are plotted in Figures 2 for ethanol, and 3 for butanol. In these graphs, the experimental points are also indicated, and one can easily see that they are nicely described by the curves.

Table 2 Kinetic parameters.

Parameter	Ethanol	Butanol
μ^* (h^{-1})	0.67	0.60
K (kg m^{-3})	0.69	0.95
K_I (kg m^{-3})	1.27	0.86
Y	0.385	0.458

There is a study reported in the literature (35), regarding the growth of *C. utilis* ATCC 8205 on butanol, in which kinetic data are regressed to an inhibitory type model, and the corresponding kinetic parameters are determined. If this model is brought into the form of the Andrews' expression, the calculated values for μ^* , K , and K_I are 1.03 h^{-1} , 0.41 kg m^{-3} , and 2.52 kg m^{-3} , respectively, which are of the same magnitude with the values determined in the present work. The only other parameter value which can be compared with values reported in the literature is the yield coefficient on ethanol. Bailey and Ollis (36) report values of yield factors for aerobic growth of two different cultures on ethanol as 0.68 and 0.49 g dry biomass/g ethanol. The value of 0.385 determined in the present study, compares relatively well with the reported values.

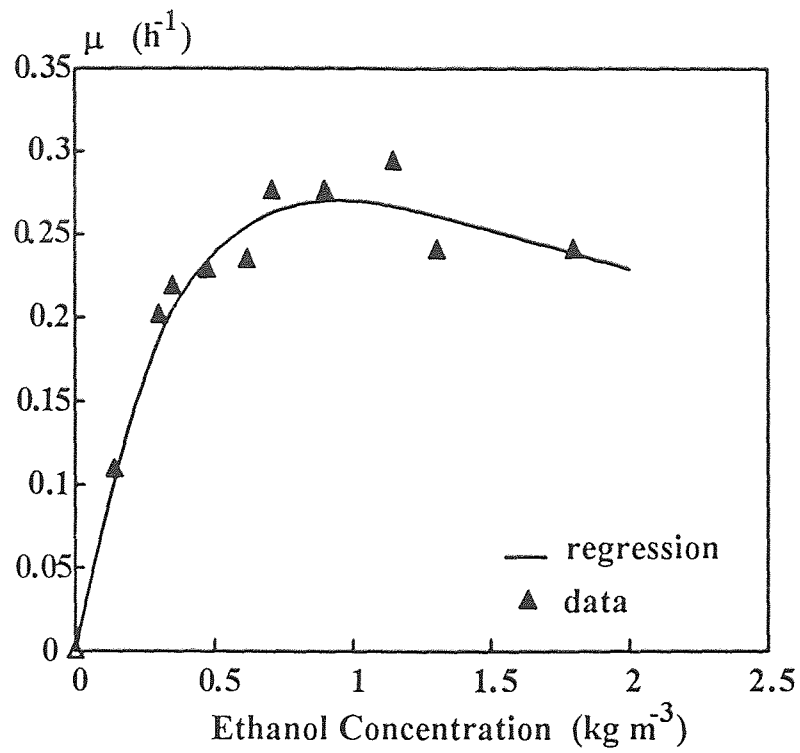


Figure 2 Specific growth rate of biomass on ethanol under no oxygen limitation.

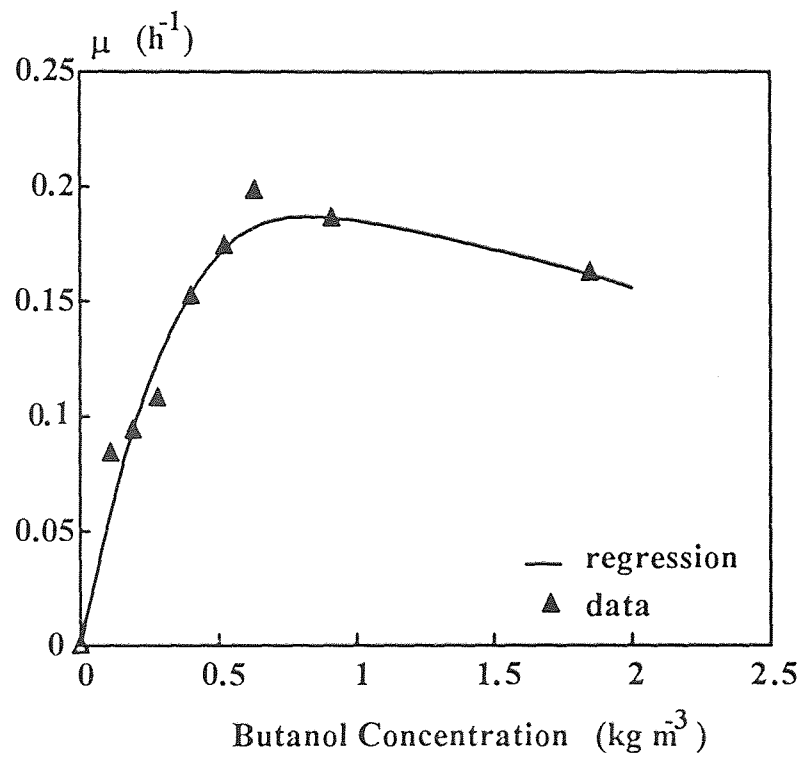


Figure 3 Specific growth rate of biomass on butanol under no oxygen limitation.

When aerobic biodegradation of a substrate occurs under conditions of low oxygen availability, the specific growth rate can be expressed by an interactive model (46), as

$$\mu(S_j, S_o) = \mu(S_j)f(S_o) \quad (5.13)$$

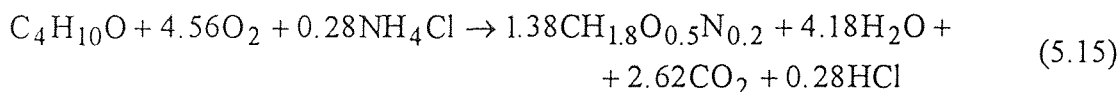
where S_o is the oxygen concentration, and $f(S_o)$ is the functional dependence of the specific growth rate on oxygen; $f(S_o)$ has been reported to follow a Monod-like expression (39, 40), i.e.,

$$f(S_o) = \frac{S_o}{K_o + S_o} \quad (5.14)$$

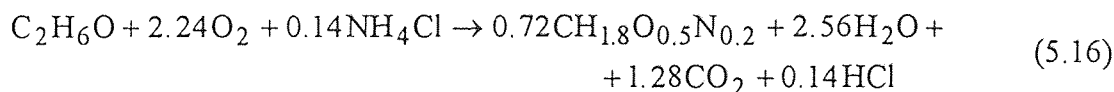
For the description of ethanol and butanol biofiltration which is discussed in the next chapter, the value of K_o was needed. Since this value was not determined from kinetic runs, a value of 0.26 mg/L was used. This is an average of reported values, as discussed by Livingston (40).

When oxygen plays an important role in the biodegradation of a compound, the data cannot be described unless one knows the yield coefficient, Y_o , of biomass on oxygen. As discussed by Shareefdeen et al. (24), the value of Y_o can be calculated through reaction stoichiometry, once the yield of biomass on the carbon source is known. Since the nitrogen source in the kinetic runs was NH_4Cl , if one represents the biomass composition as $\text{CH}_{1.8}\text{O}_{0.5}\text{N}_{0.2}$ (36), the values of Y_o can be determined as follows.

For butanol degradation ($Y_B = 0.458$ g dry biomass/g butanol = 1.38 mole dry biomass/ mole butanol), one can write



Similarly for ethanol ($Y_E = 0.385$ g dry biomass/g ethanol = 0.72 mole dry biomass/mole ethanol)



Based on equations (5.15) and (5.16) the values of the yield coefficients on oxygen can be calculated as follows:

$$Y_o = \frac{1.38 \text{ mole biomass}}{4.56 \text{ mole O}_2} \frac{1 \text{ mole O}_2}{32 \text{ g O}_2} \frac{24.6 \text{ g biomass}}{1 \text{ mole biomass}} = 0.232 \text{ g biomass / g O}_2 \text{ for}$$

butanol, and

$$Y_o = \frac{0.72 \text{ mole biomass}}{2.24 \text{ mole O}_2} \frac{1 \text{ mole O}_2}{32 \text{ g O}_2} \frac{24.6 \text{ g biomass}}{1 \text{ mole biomass}} = 0.247 \text{ g biomass / g O}_2 \text{ for}$$

ethanol.

This method of estimating Y_o has been found to be very accurate when methanol is the carbon source (24).

The kinetic expressions derived in this chapter were used in describing biodegradation of ethanol and butanol in biofilters (see Chapter 6). In biofilters the biomass is immobilized forming a biolayer, while the kinetic experiments discussed in this chapter are performed with suspended cultures. There are various reports (14, 24), which suggest that the kinetics of degradation of a substance by a particular culture are the same, regardless of whether this culture is immobilized or not.

CHAPTER 6

BIOFILTER EXPERIMENTS

6.1 Mathematical Description of the System at Steady State

Data from experiments which were allowed to reach steady state conditions, were analyzed through the model of Shareefdeen et al. (24). The computer code used in solving the model equations was originally developed by Z. Shareefdeen, and is given in Appendix B of this thesis.

The mathematical model is based on the following assumptions (24).

1. Both the VOC and oxygen exert rate limitation on the kinetics of biodegradation. This dual limitation can be described by a non-interactive model for the specific growth rate of the biomass (46).
2. The thickness, δ^* , of the biolayer formed on the exterior surface of the solids used as packing material is small when compared to the main curvature of the particles, thus planar geometry can be used (12).
3. Reaction does not necessarily occur throughout the biolayer. If oxygen, or the VOC get depleted before the biolayer/solid interface, there is an effective biolayer thickness (δ), in the sense of Williamson and McCarty (37). In the biolayer, all compounds are transferred through passive diffusion.
4. No boundary layer exists close to the air/biolayer interface.
5. Concentrations of both oxygen and the VOC at the air/biolayer interface follow Henry's law.
6. Air passes through the biofilter bed in plug flow.
7. Biofilm density is constant throughout the biofilter.
8. There is no net accumulation of biomass in the biofilter, and thus steady (or quasi-steady) state conditions can be reached. This implies that the biomass formed is equal

to that which undergoes decay.

A schematic representation of the biofilm model concept is shown in Figure 4.

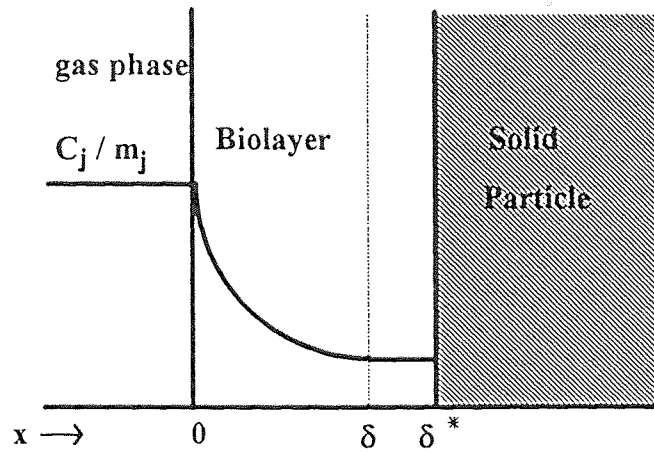


Figure 4 Schematic of the biofilm concept at a cross section along the biofilter column.

Under the assumptions above, steady state biofiltration of a single VOC is described by the following four mass balances for the VOC and oxygen.

In the biolayer at a position h along the packed bed,

$$f(X_V)D_j \frac{d^2 S_j}{dx^2} = \frac{X_V}{Y_j} \mu_j(S_j, S_o) \quad (6.1)$$

$$f(X_V)D_o \frac{d^2 S_o}{dx^2} = \frac{X_V}{Y_{oj}} \mu_j(S_j, S_o) \quad (6.2)$$

with corresponding boundary conditions,

$$S_j = \frac{C_j}{m_j} \quad \text{at } x = 0 \quad (6.3)$$

$$\frac{dS_j}{dx} = 0 \quad \text{at } x = \delta \quad (6.4)$$

$$S_o = \frac{C_o}{m_o} \quad \text{at } x = 0 \quad (6.5)$$

$$\frac{dS_o}{dx} = 0 \quad \text{at } x = \delta \quad (6.6)$$

Along the biofilter column,

$$\frac{F}{S} \frac{dC_j}{dh} = A_S f(X_V) D_j \left[\frac{dS_j}{dx} \right]_{x=0} \quad (6.7)$$

$$\frac{F}{S} \frac{dC_o}{dh} = A_S f(X_V) D_o \left[\frac{dS_o}{dx} \right]_{x=0} \quad (6.8)$$

with corresponding boundary conditions,

$$C_j = C_{ji} \quad \text{at } h = 0 \quad (6.9)$$

$$C_o = C_{oi} \quad \text{at } h = 0 \quad (6.10)$$

The specific growth rate $\mu(S_j, S_o)$, which appears in equations (6.1) and (6.2) is given by

$$\mu(S_j, S_o) = \frac{\mu_j^* S_j}{K_j + S_j + S_j^2 / K_{Ij}} \frac{S_o}{K_o + S_o} \quad (6.11)$$

The symbols appearing in the model equations are defined as follows. D_o and D_j are the diffusion coefficients of oxygen and compound j , respectively, in the water; $f(X_V)$ represents a correction factor for the diffusion coefficients, and stands for the relative diffusivity, i.e., the diffusivity of a compound in the biofilm divided by the diffusivity of the same compound in water; $f(X_V)$ can be calculated through a correlation proposed by Fan et al. (38); m_o and m_j are the Henry's law constants for the distribution of oxygen and substrate j , respectively, between the gas phase and the biolayer; S_o and S_j are the concentrations of oxygen and substrate j , respectively, at a position x along the biolayer; $x = 0$ denotes the position of the air/biofilm interface; δ is the effective biolayer thickness; Y_j is the yield coefficient of biomass on the VOC, indicating the amount of biomass produced per unit amount of contaminant removed; Y_{oj} is the yield of biomass on oxygen, and it indicates the amount of biomass produced per unit amount of oxygen consumed due to the

removal of the pollutant; C_o and C_j are the concentrations of oxygen and pollutant j , respectively, in the airstream at position h along the column; F is the volumetric rate of air supplied to the column; S is the cross sectional area of the biofilter; F/S stands for the superficial velocity, u_g , of the airstream in the biofilter unit; A_S is the biolayer surface area per unit volume of packing material; C_{oi} and C_{ji} are the concentrations of oxygen and compound j , respectively, in the air at the entrance of the biofilter, i.e., at $h = 0$; h is the position along the biofilter column.

The values of the kinetic constants appearing in expression (6.11), and those of the yield coefficients assume the values determined and discussed in Chapter 5.

It has been shown (24), that equations (6.1), (6.2), (6.7), and (6.8) are related via two algebraic stoichiometric relations between oxygen and the carbon source for growth (VOC). Hence, one needs in actuality to solve two, instead of four, coupled differential equations. This reduction of the dynamical dimensionality of the problem from 4 to 2, reduces substantially the computer time needed for solving the model equations, as discussed elsewhere (24, 25). Based on this approach, Shareefdeen (46) developed a code for solving the model equations. The equation in the biolayer is solved by a multiple shooting technique, while that for the gas phase is solved by a fourth-order Runge-Kutta method. The method proceeds from the inlet ($h = 0$) of the column, to its exit ($h = H = V_p/S$, where V_p is the volume the filter bed), in 100 equal steps. This code was used in the present study for describing the data, and in model sensitivity studies. Based on the exit concentrations of the VOC, the removal efficiency of the biofilter was calculated via equation (1.1).

The values of the various parameters used in solving the model equations were either determined during the course of the present study, or found in the literature, and are shown in Table 3. Some comments should be made here regarding the values used for parameters X_V , A_S , and δ . The biofilm density, X_V could not have been measured during the course of this study, because even if solid sampling was possible at various column

locations, it could easily lead to disturbances in the air/solids contact pattern. Also, the irregularity in the shape of the solids, and their wide size distribution made the biolayer volume determination impossible. As a solution, for the needs of the present study a value of $X_V = 100 \text{ kg m}^{-3}$ was used, calculated as the average of the values of biofilm densities reported in the literature (24).

Regarding parameters A_S and δ , it should be mentioned that it is very hard to measure them experimentally, and they cannot be taken from the literature, since they are characteristic of the particular packed bed. In the present study, A_S and δ were determined during the process of solving the model equations. As far as δ is concerned, a trial and error approach was used at each position along the biofilter, and its value was determined as the thickness which leads to 99 percent decrease in the concentration value of either oxygen or the pollutant (whichever happens first), relative to the concentration at the air/biolayer interface. Regarding A_S , its value was estimated by using a data-fitting procedure. Only four of the experimental sets for a particular compound were used in determining, by trial and error, the value of A_S . This value was the one which minimized the sum of the squares of the error between experimental and model predicted concentration values in all four sets. The reasoning for this approach was that since all four data sets had been taken from the same column which was operating for a fairly long period of time, the specific biofilm surface area, A_S , should be the same in all four of them. This value of A_S , determined from the chosen four sets, was subsequently used in predicting concentration profiles in all other data sets, and in comparing data and model predictions.

Table 3 Model parameter values used for predicting steady state concentrations and removal rates.

Parameter	Value	Units	Reference
A_S (ethanol)	39	m^{-1}	Present study
A_S (butanol)	38	m^{-1}	Present study
C_{oi}	275×10^{-3}	$kg\ m^{-3}$	24
D_j (ethanol)	1.00×10^{-9}	$m^2\ s^{-1}$	41
D_j (butanol)	0.77×10^{-9}	$m^2\ s^{-1}$	42
D_o	2.41×10^{-9}	$m^2\ s^{-1}$	24
$f(X_V)$	0.195	—	38
μ^*_j (ethanol)	0.67	h^{-1}	Present study
μ^*_j (butanol)	0.60	h^{-1}	Present study
K_j (ethanol)	0.69	$kg\ m^{-3}$	Present study
K_j (butanol)	0.95	$kg\ m^{-3}$	Present study
K_{Ij} (ethanol)	1.27	$kg\ m^{-3}$	Present study
K_{Ij} (butanol)	0.86	$kg\ m^{-3}$	Present study
K_o	0.26	$kg\ m^{-3}$	24
m_j (ethanol)	0.00033	—	43
m_j (butanol)	0.00036	—	44
m_o	34.4	—	24
Y_j (ethanol)	0.385	$kg\ kg^{-1}$	Present study
Y_j (butanol)	0.458	$kg\ kg^{-1}$	Present study
Y_{oj} (ethanol)	0.247	$kg\ kg^{-1}$	Present study
Y_{oj} (butanol)	0.232	$kg\ kg^{-1}$	Present study
S	19.63×10^{-4}	m^2	Present study
V_p (butanol)	980×10^{-6}	m^3	Present study
V_p (ethanol)	930×10^{-6}	m^3	Present study
X_V	100	$kg\ m^{-3}$	24

6.2 Results and Discussion

The two biofilter units were in continuous operation for almost one year and during this period, the inlet pollutant concentrations, as well as the air flow rates, were varied, one at a time and at fairly large intervals, in order to allow the columns to reach a steady state. After approximately three to four days of operation at each one of the operating conditions tested, the system appeared to reach steady state. At that point the outlet concentrations of the compound tested were used in determining the removal rate achieved. These steady state data for the different sets of applied conditions are listed in Tables 4 and 5 for butanol and ethanol, respectively, according to the chronological order in which they were taken. In the same tables, the model predicted values for the removal rates are also shown along with the percent error between experimental and model predicted values. Once enough data were collected from each column which operated with a specific compound (either ethanol or butanol), experiments were performed with the same columns under qualitative shock-loading. Data on butanol removal in the column which originally operated with ethanol, are presented in Table 6. Table 7 shows the data on ethanol removal in the column which was originally operated with ethanol. The calculated removal rates shown in Tables 6 and 7, are based on the assumption that the kinetic characteristics of removal of a certain VOC by a culture, do not change even if the culture is only exposed to another VOC over long periods of time.

As can be seen from Table 4, removal rates of butanol achieved in the column which was started-up with this compound, ranged from 9 to 73 $\text{g h}^{-1} \text{m}^{-3}$ -packing. The removal rate achieved in a column depends on the load, and the residence time. Data reported in the literature under similar values for the load, indicate removal rates between 20 and 40 $\text{g h}^{-1} \text{m}^{-3}$ -packing (12), hence they agree nicely with the results of the present study.

Ethanol removal rates achieved in the column which was started-up with ethanol, ranged between 19 and 76 $\text{g h}^{-1} \text{m}^{-3}$ -packing, as can be seen from Table 5. Comparing the

results shown in Tables 4 and 5, one could conclude that ethanol is removed easier than

Table 4 Experimental and model predicted steady state removal rates for butanol vapor in a biofilter exposed to butanol only.

τ (min)	C_{Bin} (g m ⁻³)	R_{exp} (g h ⁻¹ m ⁻³ -packing)	R_{model}	Error (%)
0.49	0.07	8.6	12.8	48.8
1.63	0.92	13.2	20.3	53.8
1.63	0.52	15.8	18.8	19.0
0.33	0.05	9.1	11.2	23.1
1.63	1.06	25.4	24.6	-3.1
0.82	1.06	25.6	22.5	-12.1
0.82	0.58	24.2	26.1	7.9
0.89	0.78	21.6	25.0	15.7
0.89	0.48	19.6	25.92	32.2
0.89	0.35	23.6	22.9	-0.03
1.96	1.59	24.8	21.9	-11.7
1.96	2.61	44.7	16.0	-64.2
1.96	5.09	73.2	11.4	-84.4
1.96	3.13	37.3	15.3	-58.9
1.96	0.98	24.2	23.3	-3.7
1.18	0.51	25.9	24.6	-5.0
2.45	0.95	21.8	23.3	6.9
1.96	0.80	24.5	24.2	-1.2
1.47	0.48	19.6	23.0	17.3
1.23	0.69	22.4	25.7	14.7
0.98	0.38	23.3	22.8	-2.1

Table 5 Experimental and model predicted steady state removal rates for ethanol vapor in a biofilter exposed to ethanol only.

τ (min)	C_{Ein} (g m ⁻³)	R_{exp} (g h ⁻¹ m ⁻³ -packing)	R_{model}	Error (%)
2.33	1.52	23.2	30.2	30.2
2.33	1.61	19.4	29.0	49.4
2.33	2.34	22.5	25.3	12.4
2.33	3.63	24.5	22.4	-8.5
2.33	6.11	19.1	17.3	-9.4
0.47	0.31	40.0	35.7	-10.8
1.86	9.75	75.8	15.7	-79.3
1.86	5.96	38.1	28.8	-24.4
1.86	4.15	25.8	22.5	-12.8
3.72	4.34	19.0	20.9	9.1
4.65	9.59	19.0	16.1	-15.3

butanol. Nonetheless, this may not necessarily be the case, because the rates on ethanol were obtained with inlet concentrations which were higher than those for butanol. In a pilot study on the feasibility of ethanol removal from airstreams coming from a bakery (2), removal rates as high as 150 g h⁻¹ m⁻³-packing were reported. It should be mentioned though, that the unit was much bigger (7 m³ of packing, 1 m-high bed) than the one used in the present study, and the average inlet concentrations low (~ 2 g m⁻³). In addition, the authors mention that the high rates obtained, could possibly be considered as artifacts caused by the fluctuations in ethanol concentration in the off-gas, the short sampling duration, and the high retardation of ethanol in the biofilter.

From the data presented in Tables 4 and 5, it becomes clear that there is a very good agreement between theory and experiments. For both ethanol and butanol, the

percent error between the experimental and model predicted removal rates does not exceed, in most cases, 15 percent, which is very small considering the complexity of the

Table 6 Experimental and model predicted steady state removal rates for butanol vapor in a biofilter exposed to ethanol prior to the switch to butanol.

τ (min)	C_{Bin} $g\ m^{-3}$	R_{exp} $g\ h^{-1}\ m^{-3}\text{-packing}$	R_{model}	Error (%)
2.33	0.49	7.2	24.0	233.3
2.33	0.76	7.3	25.3	246.6
2.33	1.49	8.3	21.8	162.7
1.86	0.63	8.1	24.9	207.4

Table 7 Experimental and model predicted steady state removal rates for ethanol vapor in a biofilter exposed to butanol prior to the switch to ethanol.

τ (min)	C_{Ein} $g\ m^{-3}$	R_{exp} $g\ h^{-1}\ m^{-3}\text{-packing}$	R_{model}	Error (%)
2.45	0.53	7.3	32.6	346.6
2.45	3.5	9.8	21.3	117.3
2.45	6.5	8.6	15.6	81.4
1.96	5.4	7.7	17.0	132.9

process. There are, of course, a few situations where the percent error reaches values as high as 79 , or even 84 percent for butanol, but these rare incidents do not imply that the model is incorrect; these cases should be considered as exceptions. For both ethanol and butanol, a large positive percent error appears in the first two sets of data, indicating that the model overestimated the removal efficiency for these cases. However, these data were taken during the first weeks of the columns' operation and it would be very reasonable to claim that during that period not enough biofilm had formed in the columns, hence the A_S value was less than that used in predicting the removal rates. As a result, the concentrations of the contaminants were high, and performance of the biofilters was poor when compared to that achieved later. Indeed, after the first couple of weeks, the removal

rates consistently reached higher values, which were much closer to the predicted ones.

As for a few other couples of intervening cases in which there are large discrepancies between the predicted and experimentally observed removal rates, their deviations could be explained by the possibility that either not enough time had been allowed for the columns to reach a steady state, or that the biofilters were either dry or overflowed and thus, their operating and physical characteristics were changed. Both of these claims suggest that either there was a reason for a steady state not to be reached, or that the steady state reached was different than that expected under the normal operating conditions (e.g. water content) of the columns.

It should be emphasized that during the course of this study it was observed that in order to be able to get consistent results, maintaining an optimum moisture content in the filter bed is of vital importance. In fact, it was found that without providing additional moisture to the packing material, the incoming gas would dry out the filter bed very quickly, because most of the times the inlet air does not get saturated after passing through the water containing vessel. Insufficient moisture always leads to a decrease in the degradation activity, and to reduced removal rates. Since the gas stream flows upwards, the lower part of the column provides the air with the necessary additional moisture to get saturated and consequently, this part of the column gets dry first. This can be very easily detected by simply observing the biofilters, which appear to have a lighter color in their lower sections, an indication that this part is drier and needs to be wetted. Most of the times though, the humidification of only this lower section proved to be quite strenuous, because the water supplied from the top of the column is usually retained by the upper layers of the packing media and thus, it does not reach the bottom. It was also observed that, even when water supplied to the top of the columns managed to get to their lower parts, the dry sections of the compost could not retain moisture easily. Hence, the columns became flooded, unless the excess water was drained.

Due to these problems, a special effort was made to provide the biofilter units with

small amounts of water at regular time intervals, so that even the lower parts were not allowed to dry out. However, during the one-year period of the operation of the biofilters, there were a few times when the packing material did temporarily dry out, or got flooded in some of its segments. These were some of the cases in which large deviations in the pollutants exit concentrations from their normally expected values, as well as the off-range removal rates, were observed.

Probably, what is happening in cases of column dryness is that along with the water, the pollutant is also being desorbed from the pores of the packing material. As a consequence, the contaminant concentration in the biofilter increases abruptly and this leads to values of outlet concentration much higher than the ones expected for the particular operating conditions. As a proof of this, it should be mentioned that there were a few cases in which the off-stream concentration appeared to be temporarily larger than the one in the incoming flow, while none of the operating conditions (residence time and inlet concentration) was changed. Obviously, measurements for such cases were not listed as steady state data; more time was allowed for the transients to smother, and data were recorded after the water content of the column was stabilized to its normal level.

From the forgoing discussion it becomes clear that adsorption/desorption phenomena are of major importance to the process of biofiltration. As mentioned in the introduction, although the most important remediation process during biofiltration is the transport of the contaminant from the gas phase into the wet biolayer surrounding the carrier particles, transient removal rates are strongly affected by the process of adsorption of the pollutants onto the carrier surface. Figures 5 and 6 show data from the response of the biofilter removing ethanol, to changes in the inlet pollutant concentration, while the air flow rate is kept constant. The changes were made in the direction of smaller loads. Figure 5 shows transient exit ethanol concentrations versus time, while Figure 6 describes the transient response of the removal rates.

The curves in Figures 5 and 6 are only interpolations through the experimental

points, and do not represent any kind of model predictions. An interesting observation that one can make from these graphs is that when the load is abruptly decreased the first response of the biofilter is such that it leads to substantially lower removal rates. This phenomenon can be interpreted as follows. When at a specific set of operating conditions a steady state is reached, then there is also adsorption equilibrium between the solvent in the gas phase and that adsorbed on the packing material. When the inlet pollutant concentration decreases, the adsorption equilibrium shifts to lower values and thus, an amount of the originally adsorbed material desorbs into the air stream, leading to lower observed removal rates. In fact, measurements at points along the column during transient phases have shown that after an inlet concentration decrease, concentration values along the column may, for short time periods, be higher than those at the entrance. Eventually, a

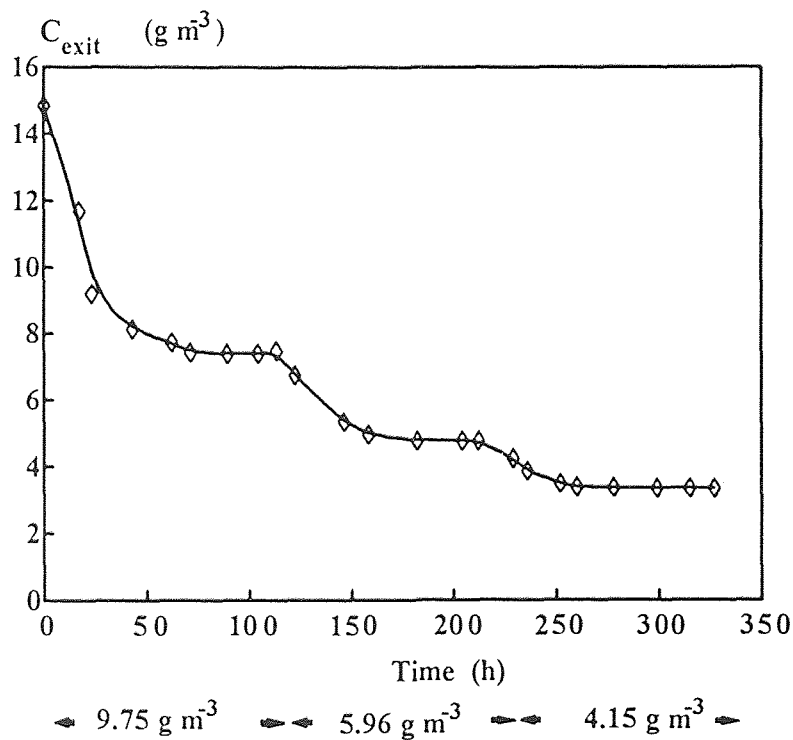


Figure 5 Transient response of the ethanol concentration in the air exiting the biofilter when the ethanol concentration in the air supplied to the biofilter is varied. Data from a biofilter exposed to ethanol only. The space time was kept constant at 1.86 min ($F = 0.030 \text{ m}^3 \text{ h}^{-1}$).

steady state is reached, and the removal rates stabilize at lower values as the load decreases. This last remark is consistent with earlier studies showing that only if the load is above a minimum value, its changes do not affect the removal rate (15, 25).

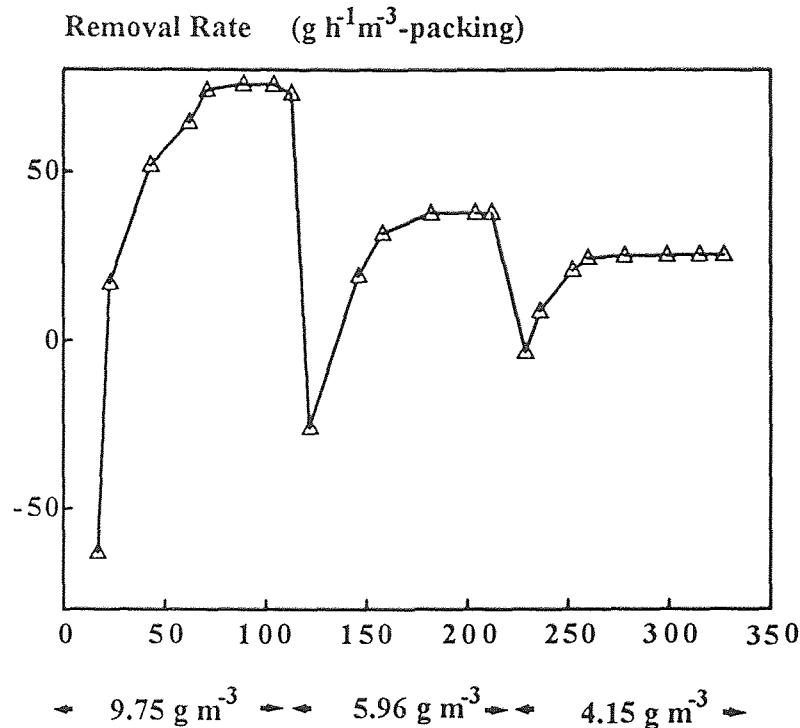


Figure 6 Transient response of the ethanol removal rate in a biofilter exposed to ethanol only when the concentration in the inlet air is varied. This graph is an alternate representation of the data shown in Figure 5.

Figures 7 and 8 show the response of a biofilter removing butanol vapors, to load changes. The load changes were made under a constant value of the air flow rate. As in the case of ethanol, the columns seem to be able to respond successfully after each change in the load, and they manage to achieve a new steady state in approximately 3 days. It can also be observed (Figure 8) that the initial response to load reduction is leading to drastically lower removal rates. Conversely, when the load increases (from region A to B and from B to C), the immediate response of the biofilter leads to substantially higher removal rates. Using the same arguments as before, this behavior can be attributed to the

fact that after a shock-load increase, an amount of the solvent is simply adsorbed on the packing material, shifting the adsorption equilibrium to higher values. One should observe that these temporary increases can lead to apparent removal rates as high as $110 \text{ g butanol h}^{-1} \text{ m}^{-3}\text{-packing}$.

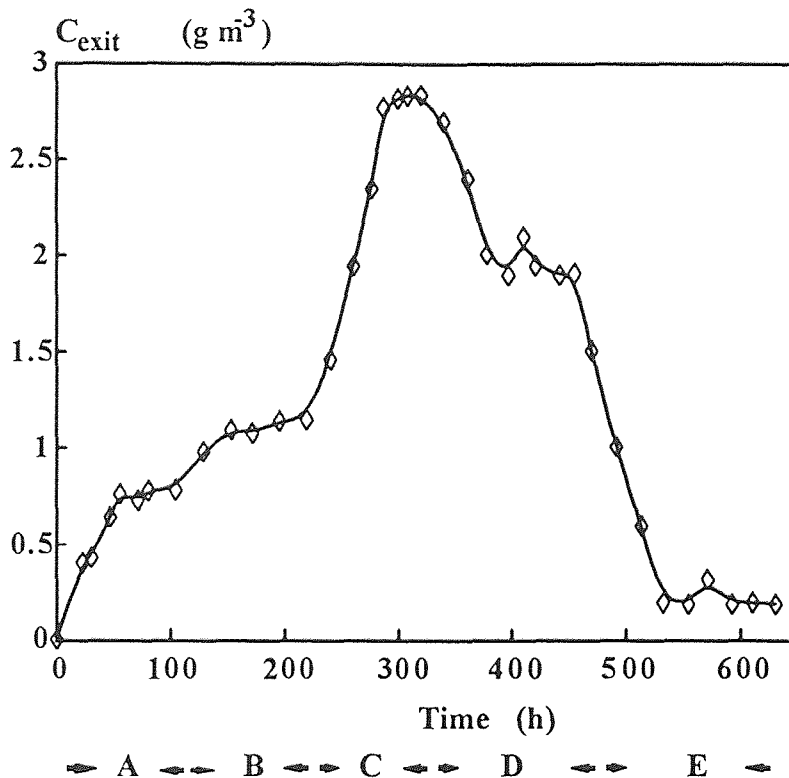


Figure 7 Transient response of the butanol concentration in the air exiting the biofilter when the butanol concentration in the air supplied to the biofilter is varied (A: 1.59 g m^{-3} , B: 2.61 g m^{-3} , C: 5.09 g m^{-3} , D: 3.13 g m^{-3} , and E: 0.98 g m^{-3}). Data from a biofilter exposed to butanol only. The space time was kept constant at 1.96 min ($F = 0.030 \text{ m}^3 \text{ h}^{-1}$).

The behavior of the biofilters discussed in conjunction with Figures 5 through 8, was also observed under other operating conditions, namely, higher residence time and lower inlet concentrations. The results are shown in Figures A-1 and A-2 for butanol, and A-3 and A-4 for ethanol. Except for the characteristics which were already discussed before, it is interesting to observe from Figures A-2 and A-4, that within certain ranges of

the inlet concentration values, the removal rates are essentially constant after the initial period of the transients. This happens despite the fact that the outlet concentrations change substantially (e.g., Figure A-3), due to the change in the load.

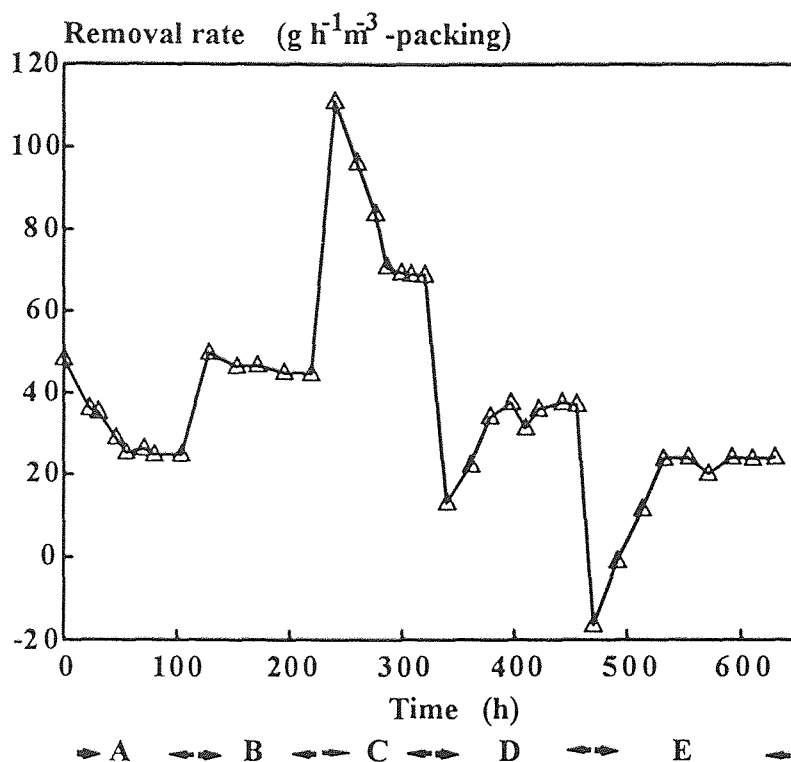


Figure 8 Transient response of the butanol removal rate in a biofilter exposed to butanol only when the concentration in the inlet air is varied (A, B, C, D, E correspond to the same concentrations as in Figure 7). This graph is an alternate representation of the data shown in Figure 7.

In another set of experiments with both columns, transient response under load changes was studied by varying the air flowrate, while keeping the inlet concentration unchanged. The results from these experiments are shown in Figure 9 for ethanol, and 10 for butanol. When the flowrate decreases, the residence time increases, and the solvent concentrations in the air present in the biofilters decrease, thus shifting the adsorption equilibrium to lower values. Desorption occurs, and the immediate response of the filter beds is to exhibit appreciably lower removal rates (Figure 9). From the same graph, one

can observe that after the transient phase is passed, the outlet concentrations observed at steady state are lower for the lower flow rates, which imply also lower loads. This observation can be easily explained by the fact that when the flow rate decreases, the residence time increases and the pollutant spends more time in the columns and consequently, better conversions are achieved. Despite this fact, the removal rate appears to change in the direction of the changes in the load.

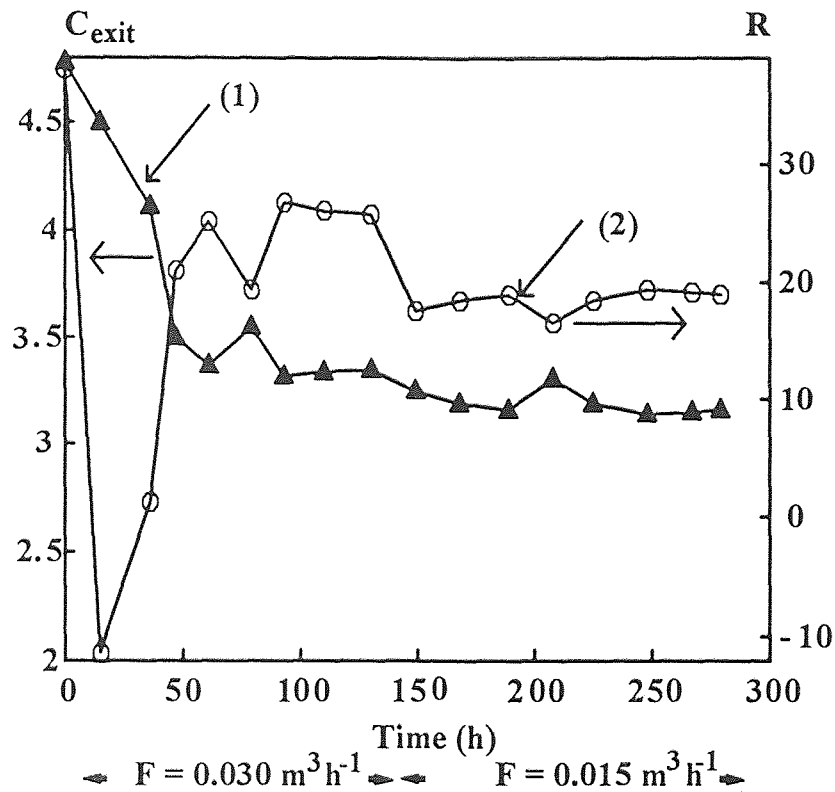


Figure 9 Transient response of the ethanol concentration at the exit of the biofilter (curve 1), and of the ethanol removal rate (curve 2) when the ethanol concentration in the inlet air is kept constant at about 4.2 g m^{-3} while the air flowrate varies. Data from a biofilter exposed to ethanol only. Units of C_{exit} : g m^{-3} ; R : $\text{g h}^{-1} \text{m}^{-3}\text{-packing}$.

As can be seen from Figure 10, flowrate increases lead to higher VOC concentrations in the air inside the column (less biodegradation) and thus, significant initial increases in the removal rate appear, due to adsorption of an amount of the vapor onto the packing particles. After the initial transients though, the system ends up almost at the same

level of removal rate as before the change in the flowrate. This behavior depends on the conditions, but appears to be consistent with the observations of other researchers (4, 12, 25), according to which, at high loads the steady state elimination capacity reaches a constant value which is independent of the value of the load.

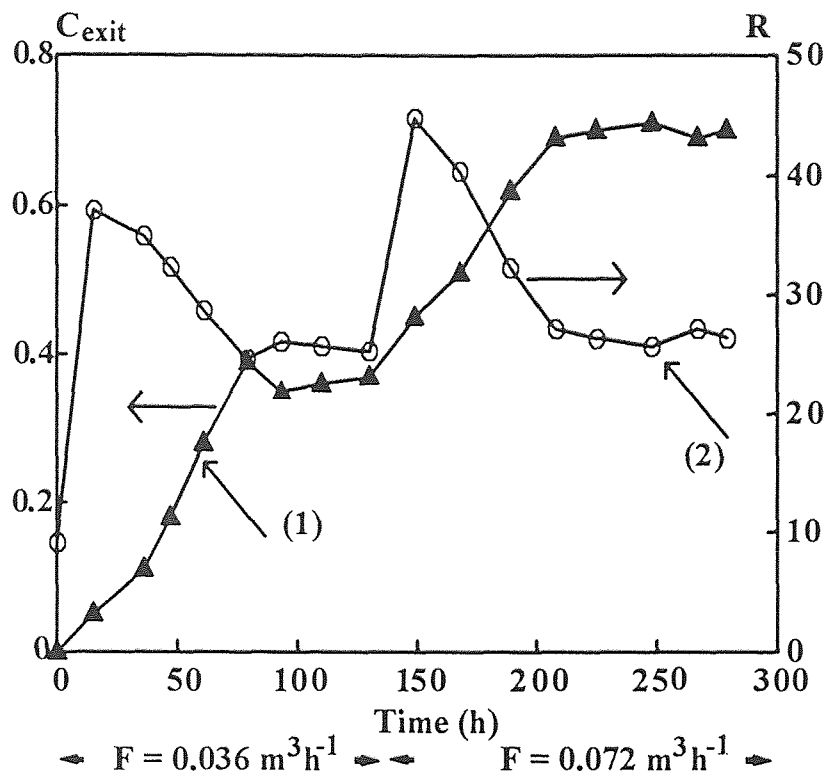


Figure 10 Transient response of the butanol concentration at the exit of the biofilter (curve 1), and of the butanol removal rate (curve 2) when the butanol concentration in the inlet air is kept constant at about 1.1 g m^{-3} while the air flowrate varies. Data from a biofilter exposed to butanol only. Units of C_{exit} : g m^{-3} ; R : $\text{g h}^{-1} \text{ m}^{-3}\text{-packing}$.

Figures 11 and 12 show the response of the biofilters operating on ethanol and butanol, respectively, to changes in the identity of the pollutant in the incoming air stream (qualitative shock-loading). Figure 11 shows the response of the column originally dedicated to treatment of butanol, when ethanol containing air is forced through it. Several useful conclusions can be derived by observing this graph. Initially, and although supply of butanol vapors has stopped, it can be observed that substantial butanol presence is being

detected at the exit. In fact, it turns out that butanol concentration levels are up to more than three times higher than the inlet concentration of butanol before the switch to ethanol. This again can be explained by the fact that butanol which was adsorbed on the packing material, desorbs when there is no butanol supply to the biofilter. Conversely, ethanol is initially being adsorbed on the packing, and thus, its concentration at the exit appears to be very low. Eventually transients decay and biological removal of ethanol is the only process occurring. A steady state is subsequently achieved, and it should be mentioned that the removal rate of ethanol obtained in this experiment is lower than the rate of ethanol removal obtained (under similar residence time and inlet ethanol concentration), in the biofilter which was originally dedicated to ethanol.

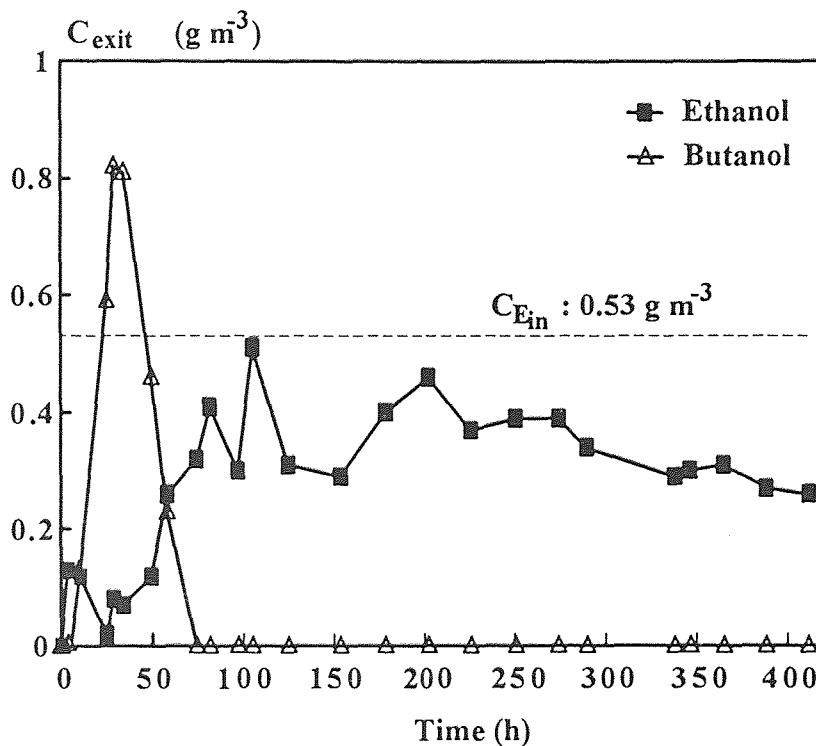


Figure 11 Response of a biofilter to changes in the identity of the solvent vapors (qualitative shock loading). The unit originally treated butanol vapors. Last experiment before switching to ethanol was performed with inlet butanol concentration $C_{Bin} = 0.25\ g\ m^{-3}$ and $\tau = 1.63\ min$ ($F = 0.036\ m^3\ h^{-1}$). At a certain instant of time (designated as zero) the inlet stream was switched to ethanol with inlet concentration $C_{Ein} = 0.53\ g\ m^{-3}$. The space time for the new stream was $2.45\ min$ ($F = 0.024\ m^3\ h^{-1}$).

The same behavior can be observed when the column dedicated to the removal of ethanol is subjected to ethanol vapors (Figure 12). It is interesting to observe here that the initial increase in the concentration of ethanol in the exit of the biofilter is not as drastic as that for the case of butanol shown in Figure 11. It is also interesting to stress the fact that initially, butanol in the experiment shown in Figure 12, is not being detected at the exit air stream for a long period of time, while ethanol in the experiment shown in Figure 11, is detected in the exit much sooner. It is worth noticing that the levels of flow rate and inlet concentration are the same in both experiments. These observations lead one to conclude that butanol shows a higher tendency for adsorption on the packing material than ethanol.

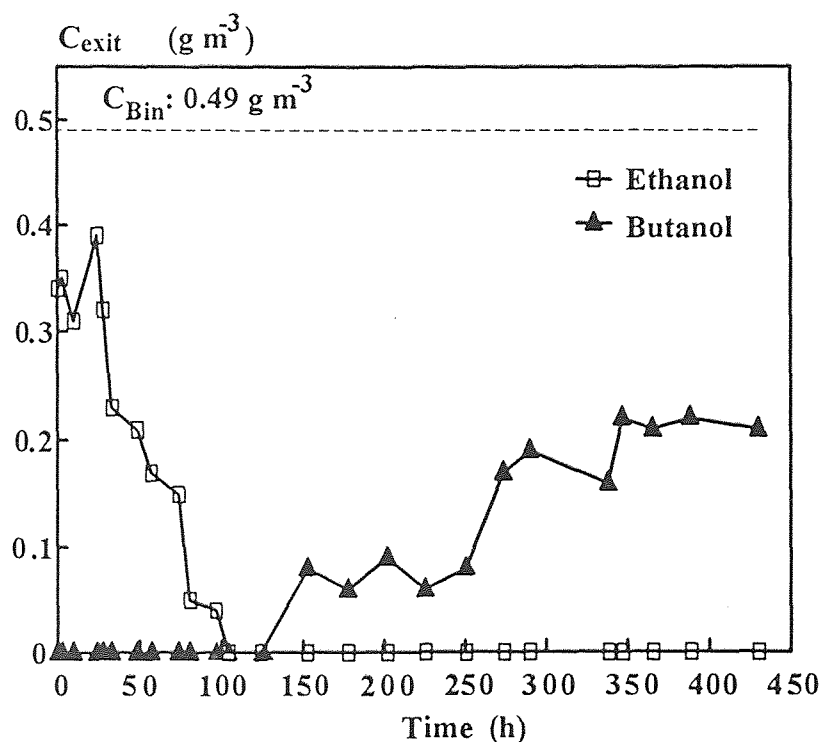


Figure 12 Response of a biofilter to changes in the identity of the solvent vapors (qualitative shock loading). The unit originally treated ethanol vapors. Last experiment before switching to butanol was performed with inlet ethanol concentration $C_{Ein} = 0.67\ g\ m^{-3}$ and $\tau = 1.6\ min$ ($F = 0.036\ m^3\ h^{-1}$). At a certain instant of time (designated as zero) the inlet stream was switched to butanol with inlet concentration $C_{Bin} = 0.49\ g\ m^{-3}$. The space time for the new stream was $2.33\ min$ ($F = 0.024\ m^3\ h^{-1}$).

The two biofilters were subjected, after the switch in the identity of the VOC, to three more sets of operating conditions, and their response is presented in Figures A-5 through A-10. These graphs show the sequence of experiments under the conditions discussed in Tables 6 and 7. If one considers the removal rates achieved by the two columns after the qualitative shock-loading, it is obvious that their values are much lower than the ones achieved before the shock. Comparisons are based on sets of similar inlet concentrations and residence time. This can be also seen from the large discrepancy between the experimental and model predicted values for the removal rates, shown in Tables 6 and 7. These predictions were made by solving the steady state model equations under the assumption that the biomass in the two biofilters was the same, and thus, had the same kinetic characteristics towards the two substrates with a culture newly acclimated to these two substances. This was clearly an incorrect assumption. In fact, after the first two months of operation, the biofilter degrading ethanol had developed a distinct green color, clearly different from that of the other column, which retained the dark brown color of the packed compost. This difference in the color of the two filter beds suggests that the cultures were not the same. Although the two columns were originally inoculated with essentially the same consortium, after the long period of operation (8 months), ethanol and butanol degraders prevailed in the columns operated with ethanol and butanol, respectively. This prevalence occurred certainly at the outer biofilm parts giving a different color to the two columns. The species which did not prevail, remained further inside the biolayer, and some of them probably died, due to lack of oxygen. This is possibly the reason why after the switch from ethanol to butanol and vice versa, both columns retained their former color. One could also suggest that, most probably, the species enhancing the biodegradation of butanol, for example, had become extinct in the column used for months for ethanol depletion. On the other hand, the fact that some removal was obtained after the qualitative shock-loading indicates that the culture which developed as more efficient for treating ethanol or butanol, has not completely lost its ability to degrade the other

substance, albeit with an efficiency lower than that of the original consortium. The fact that the removal rates remained low even after three months of operation beyond the qualitative shock-loading, seems to suggest that acclimatization of the culture in the columns, if it occurs at all, proceeds at rates so slow that practically the biofilters never regain the expected high efficiencies of removal. This also suggests that if a biofilter is to be used for removing different VOCs at different time intervals, the columns may have to be, frequently, and hopefully briefly, purposely exposed to all VOCs so that they maintain their properties.

Since in the case of columns which are started-up on a given VOC, and operate on this compound over long periods of time, the model discussed earlier can nicely predict exit VOC concentrations and removal rates at steady state, this model can be used in other

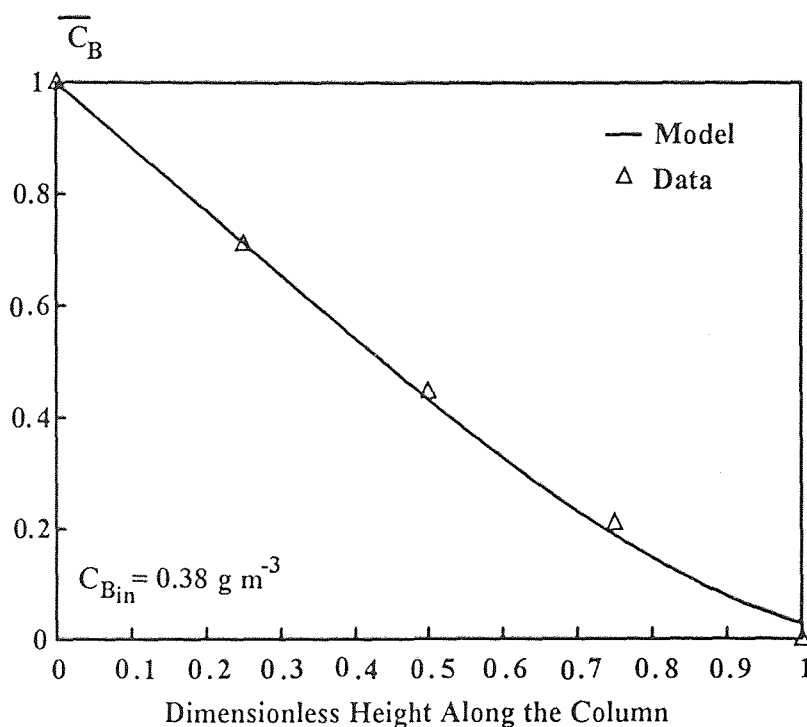


Figure 13 Concentration profile of butanol vapor in the air along a biofilter column at constant air flow rate of $0.048 \text{ m}^3 \text{ h}^{-1}$.

calculations as well. For example, the model can predict the theoretically expected

substrate concentrations not only at the exit, but also at intermediate points along the columns. This way, one can compare the predicted and experimental concentration profiles of the dimensionless pollutant gas phase concentration along the biofilter bed. An example for butanol is given in Figure 13, and for ethanol in Figure 14. Similar profiles have been produced for most of the steady state data appearing in Tables 4 and 5, and are presented in Figures A-11 through A-24 in the appendix.

In these graphs, the continuous line describes the profile predicted by solving the model equations for a specific set of values for the flow rate and inlet concentration, while the individual points represent the data obtained from the experiments, under the same operating conditions. In all these graphs, the dimensionless gas phase concentration of the VOC stands for the actual concentration value divided by that at the entrance of the biofilter bed. On the x-axis of these graphs, zero represents the entrance, and one the exit from the biofilter bed.

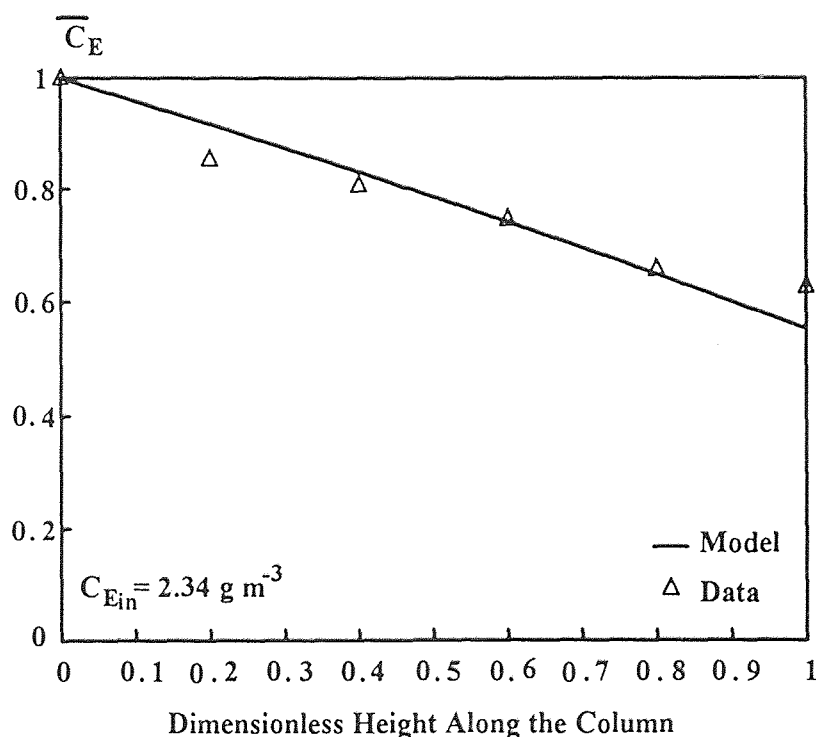


Figure 14 Concentration profile of ethanol vapor in the air along a biofilter column at constant air flow rate of $0.024 \text{ m}^3 \text{ h}^{-1}$.

By observing most of these figures, one can see clearly that there is a very good agreement between the model and the experiments, at every position and not only the biofilter exit. It is also obvious that the model predicts a concentration profile that is for most cases approximately linear with respect to the height along the column. A similar result has been also obtained in other studies (12, 27, 28) which assumed a type of kinetics (zero order or the Monod type) simpler than the inhibitory Andrews' model, that is used in the present study. However, at low inlet concentrations, the highest proportion of removal occurs near the top of the column, and in such cases the concentration profile is no longer linear, especially towards the exit of the biofilter bed, as shown in Figure 13. The profile in this graph resembles more an exponential form of behavior, suggesting that the rate determining step in the biodegradation process probably changes at low substrate concentrations.

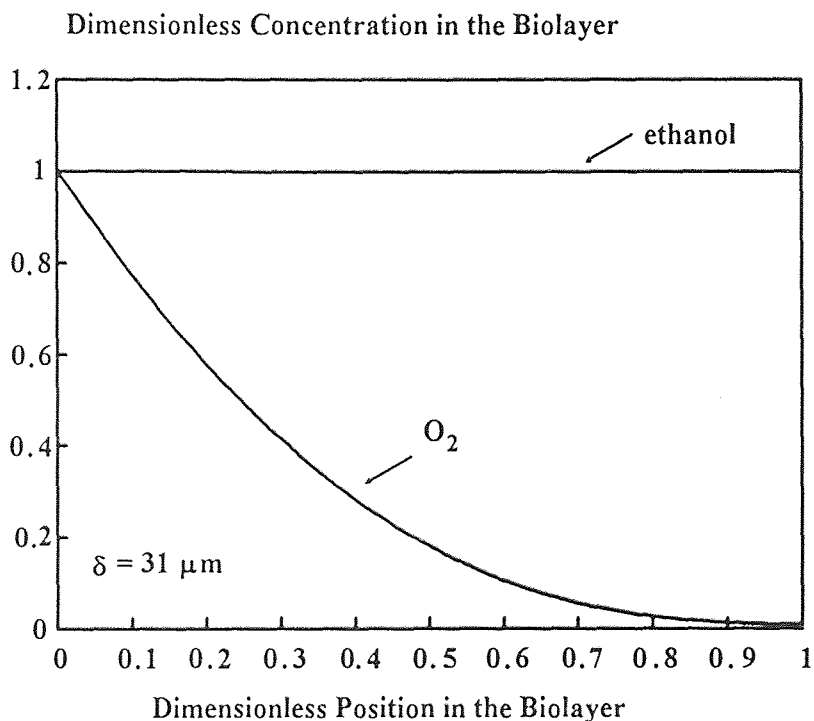


Figure 15 Model predicted concentration profiles in the biolayer at the middle point of the biofilter. The experimental conditions were, air flow rate $0.024 \text{ m}^3 \text{ h}^{-1}$, and inlet ethanol concentration 2.34 g m^{-3} .

A much better insight into the biofiltration process under steady state conditions can be gained by using the model equations to predict concentration profiles in the active part of the biolayer. Figures 15, 16, A-25, and A-26 show profiles of oxygen and either butanol, or ethanol, at the middle point of biofilters operated under four sets of conditions reported in Tables 4 and 5. In these graphs, the concentration values have been made

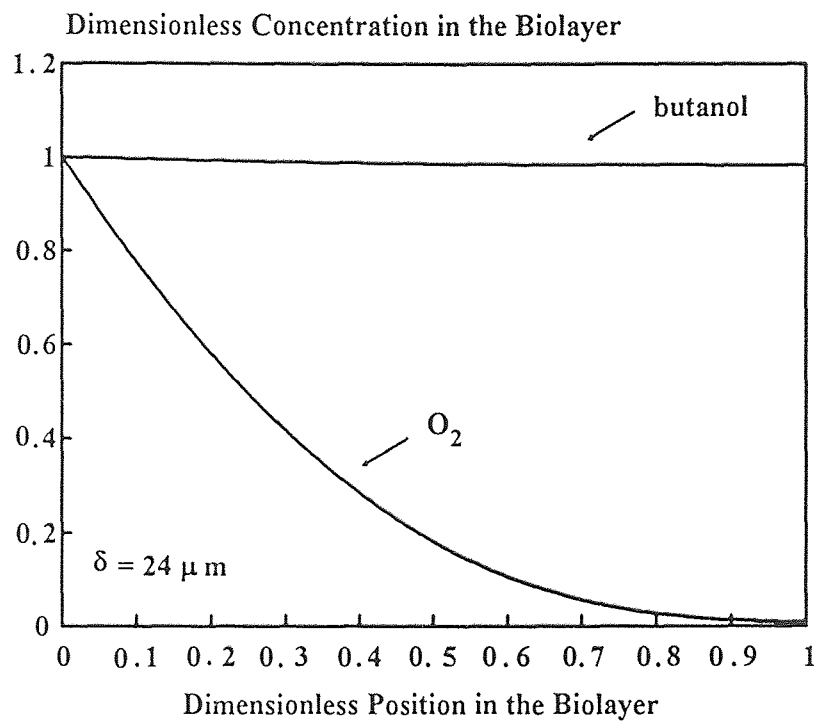


Figure 16 Model predicted concentration profiles in the biolayer at the middle point of the biofilter. The experimental conditions were, air flow rate $0.048 \text{ m}^3 \text{ h}^{-1}$, and inlet butanol concentration 0.38 g m^{-3} .

dimensionless by dividing actual values by the corresponding value at the air/biolayer interface. The values in the x-axis are also dimensionless, and represent the ratio of the actual position in the biolayer to the active biofilm thickness δ . By looking at these figures, one can easily notice that oxygen gets depleted in very small biofilm thicknesses, leaving the concentration of the carbon source almost unchanged. Of course, once oxygen is no longer present, the reaction ceases instantly, and thus, oxygen should be characterized as the limiting factor for the reaction. Similar profiles were found invariably, for both ethanol

and butanol, at all positions along the column, and regardless of the inlet concentration values. This observation regarding oxygen's limiting contribution, confirms one of the primary principles of the model used, according to which, one should consider oxygen when setting up the equations to describe the system.

Although this point will be elaborated in detail later, it should be mentioned here that the active biolayer thickness (δ) is not constant along the biofilter bed, and its value depends on the VOC concentration in the air. For most of the sets of inlet concentrations and flow rates studied in this thesis, the maximum δ values predicted, ranged between 25 and 65 μm in the case of butanol, and 29 to 64 μm in the case of ethanol. For butanol, only in two cases (inlet concentrations of 0.07 and 0.05 g m^{-3}), the thickness of the active biolayer reached values of 130 and 143 μm . For ethanol, the largest value of biofilm thickness was predicted for a case of an inlet concentration of 0.51 g m^{-3} , and it was 115 μm .

Based on the values of δ reported above, one can again show the importance of oxygen for the process, as follows. As mentioned above, for most experimental sets with butanol the maximum value of δ was between 25 and 65 μm , hence the average was 45 μm . Using this value for δ , one can calculate the value of the Thiele modulus, defined as: $\phi^2 = \delta^2 \mu_j^* X_V/D_j K_j Y_j$, for butanol, and $\phi^2 = \delta^2 \mu_j^* X_V/D_o K_o Y_o$ for oxygen (24). Considering the values of the system parameters given in Table 3, one can calculate the Thiele modulus based on butanol as 0.72, and on oxygen as 34.4. These values seem to indicate that the whole process is limited by the kinetics of butanol, since the corresponding value of ϕ is less than $\sqrt{2}$, and the diffusion of oxygen (45). This means that oxygen is a very important factor in the biofiltration process, and should be always included in the equations describing the system. In the exceptional cases where δ reaches values of 140 μm , the calculated Thiele moduli are 2.20 and 107.8 for butanol and oxygen, respectively. These values correspond to very low inlet solvent concentrations

(0.07 g m^{-3}), and the value of 2.20 indicates that diffusion of butanol also becomes important. Similar conclusions can be reached for the case of ethanol biofiltration.

The fact that the process seems to be oxygen diffusion limited except at very low gas phase VOC concentrations, explains the concentration profiles shown in Figures 13, 14, and A-11 through A-24. Moreover, since at very low gas phase VOC concentrations both VOC diffusion and kinetics of removal are important, the curvature of the gas phase concentration profiles towards the biofilter exit seems to be explained (e.g., Figures 13, A-11, A-16, and A-19). These results are a theoretical justification for writing the model equations in terms of both solvent and oxygen, and are in complete agreement with findings of previous investigations on methanol (24).

As mentioned above, the active biolayer thickness varies along the biofilter bed. This is shown in Figure 17. The y-axis of this figure shows ethanol concentrations in the

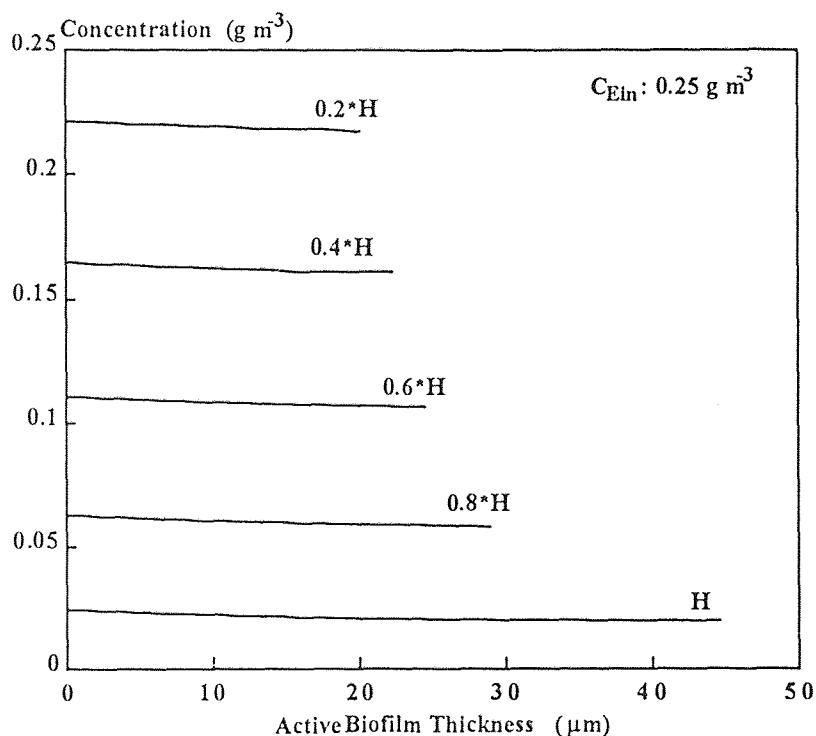


Figure 17 Radial profiles of the ethanol concentration in the biofilm at increasing bed heights. The residence time is kept constant at 0.45 min with $F = 84,585 \text{ m}^3 \text{ h}^{-1}$.

air along the biofilter bed. When these values are divided by 3.3×10^{-4} (distribution coefficient of ethanol), one gets the ethanol concentration values in the biolayer. The biolayer ethanol concentration profiles at five positions along the column are shown by the various curves of the graph. The end of these curves represents the active biofilm thickness. Since these curves are practically horizontal lines, it means that at all locations the biolayer concentration profiles are like the one shown in Figure 15, i.e., oxygen gets depleted first, and determines the active biolayer thickness. As can be seen from Figure 17, the active biolayer thickness (δ), increases in the direction of the air flow (i.e., towards the exit of the biofilter).

The behavior of δ shown in Figure 17 is not general. In fact, depending on the operating conditions, δ may increase, or decrease first and then increase in the direction of the air flow. These various types of behavior are shown in Figure 18. The results shown in this graph, as well as those shown in Figure 17, are based on numerical calculations with the model, and do not represent conditions under which experiments were performed. The various types of behavior of δ , can be explained based on the biodegradation kinetic expression. As can be seen from expression (6.11), the reaction rate becomes maximum for a particular value of the VOC concentration; let this concentration be S_j^* . This concentration is valid in the biolayer, and corresponds to a value $m_j S_j = C_j^*$ in the gas phase. If the concentration of the pollutant in the air entering the biofilter is less than C_j^* , then as the airstream goes through the biofilter, at all locations the biolayer concentrations are less than S_j^* and decrease in the direction of the flow. As these concentrations decrease, the rate of VOC consumption drops. Consequently, the rate of oxygen consumption also decreases and thus, oxygen gets depleted in biolayers of increasing thickness. This is what happens in the case shown in Figure 17, and in the case of curve 1 of Figure 18. If the outlet VOC concentration is larger than C_j^* , then biolayer VOC concentrations at all locations are larger than S_j^* . Since the concentrations decrease in the direction of flow, the rates of VOC degradation increase in this case. This results in a

higher rate of oxygen depletion and thus, in decreasing active biolayer thicknesses towards the biofilter exit. Such cases correspond to curve 2 of Figure 18. Finally, if the concentration of the VOC is higher than C_j^* at the inlet of the biofilter, but less than C_j^* at its exit, then by using the same reasoning as above, one can see that the active biolayer thickness first decreases, and then increases in the direction of the flow. Such a case is shown by curve 3 of Figure 18.

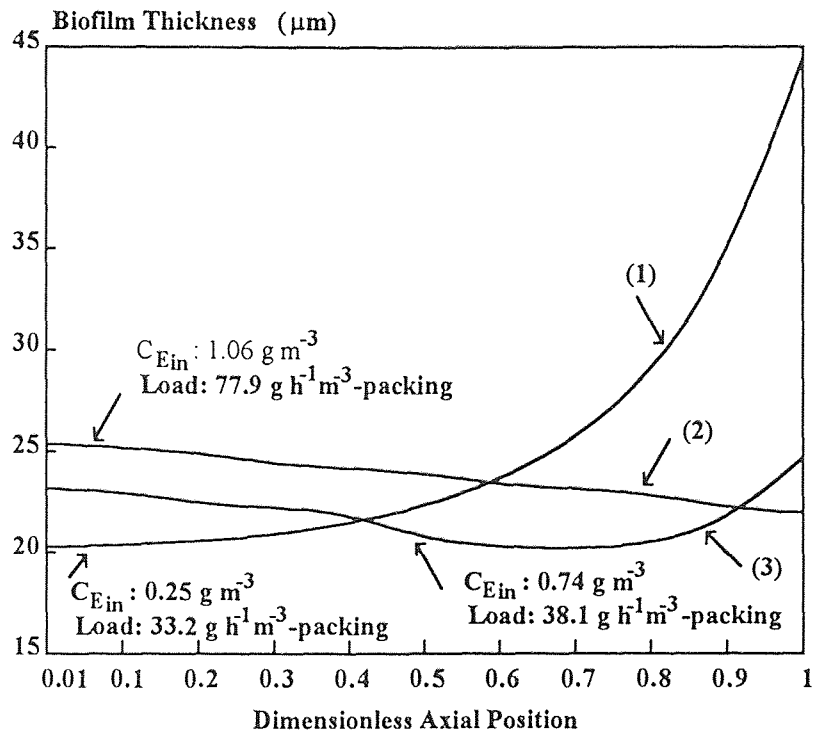


Figure 18 Axial profiles of active biofilm thickness at different inlet pollutant concentrations, loads, and τ . The values of V_p for the three curves are: (1) $638\ m^3$; (2) $980\ cm^3$; and (3) $556\ m^3$.

From the forgoing discussion, it becomes clear that oxygen plays a critical role in the biofiltration of the compounds studied in this thesis, and that the active biolayer thickness is small at all times. This last fact explains why no pressure drop developed in the columns even after a year of continuous operation. It appears that since the penetration of oxygen in the biofilm is low, cells that are further inside very possibly die, due to lack of oxygen, and their volume is being taken by the newly growing cells. An

even stronger evidence for this explanation, is the fact that although no essential nutrients, like nitrogen and phosphorous, were supplied to the columns after the beginning of the experiments, growth was still occurring. This could be attributed to the lysis of the cells present in the inner layers of the biofilm, which supplied the living cells with the necessary nutrients (24). This reasoning leads to the conclusion that the assumption of no biomass accumulation in the biofilter, is a correct one.

In deriving the model, it has been assumed that the biofilm density, X_V , and the specific biolayer area, A_S , are constant throughout the column. These quantities depend on the actual (not the active) biolayer thickness. For example, it has been reported (46) that X_V increases as the actual biolayer thickness decreases. If the variation in the active biolayer thickness implies also a variation in the actual biofilm thickness, then the assumption of constant X_V and A_S is not, in general, justified. On the other hand, since for the cases considered here the variations in δ are not wide, it appears that the assumption of constant X_V and A_S , is well justified.

The existence of a validated model, can and should be able to be used in design calculations. These calculations may concern different things, but the most important is the size of the unit required for achieving a certain duty. For a given load, environmental regulations require a particular percent removal. For this reason, some calculations were performed in order to predict the required size of a biofilter which is to achieve a 95.5 percent removal of ethanol from air, when the load is either 21,146 or 560 g h⁻¹. The results are shown in Figure 19. The curves of this graph are not experimental points, but have been obtained from successive runs of the computer program that solves the model equations, and predicts the concentration profile along the column. The volume has been calculated for different values of ethanol concentration in the air supplied to the biofilter. These results are extremely interesting as they suggest that there is an inlet concentration with which one can achieve a minimum reactor volume, for the specific conversion one wants to get. This implies that if the actual concentration of the polluted airstream is

higher than that at which the minimum volume is achieved, then the incoming air stream may be mixed with clean air so that the optimum concentration is achieved in the inlet, and the column volume is minimized, thus reducing the capital cost of the unit. The existence of a minimum is once again the result of inhibitory kinetics. At high concentrations, the rates are low, and thus, very large volumes of filter bed are predicted to be required. Since the volumes are always high, as can be seen from Figure 19, finding the optimum one may have a very significant impact on the cost of the process.

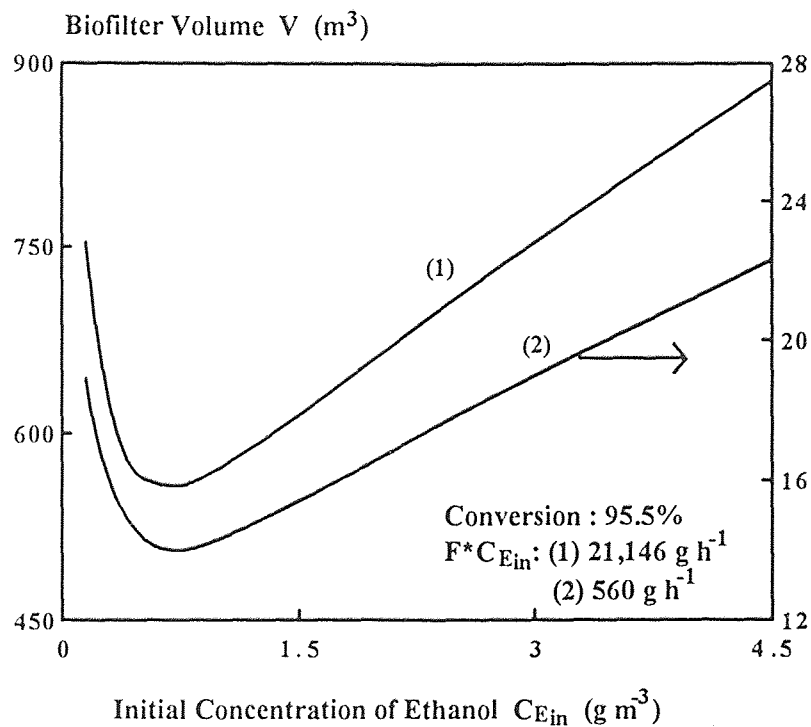


Figure 19 Predicted required biofilter volume at constant conversion and constant values of rate of mass of VOC supply.

The model has been also used in doing a sensitivity analysis of the effect of the kinetic and other model parameters. This work was done in order to examine the importance of these parameters, and derive results which could be useful for further studies. In this study, the removal rates were predicted for different values of the parameters. Figures 20 and 21 show the results of the sensitivity studies for the case of

butanol biofiltration. The x-axis represents the relative value of each parameter studied, and is defined as the ratio of its assumed value to the actual one used in the present work and shown in Table 3. The y-axis shows the relative value of the removal rate, R , being the value of the removal value corresponding to the new values of the parameter under consideration, divided by the removal rate of butanol achieved in the biofilter when the inlet concentration is equal to 1.01 g m^{-3} , the flow rate, $0.072 \text{ m}^3 \text{ h}^{-1}$, and the space time, 0.82 min . The model predicted removal rate for this case was $24.6 \text{ g h}^{-1} \text{ m}^{-3}$ -packing (Table 4). By observing these graphs, a number of interesting conclusions can be reached.

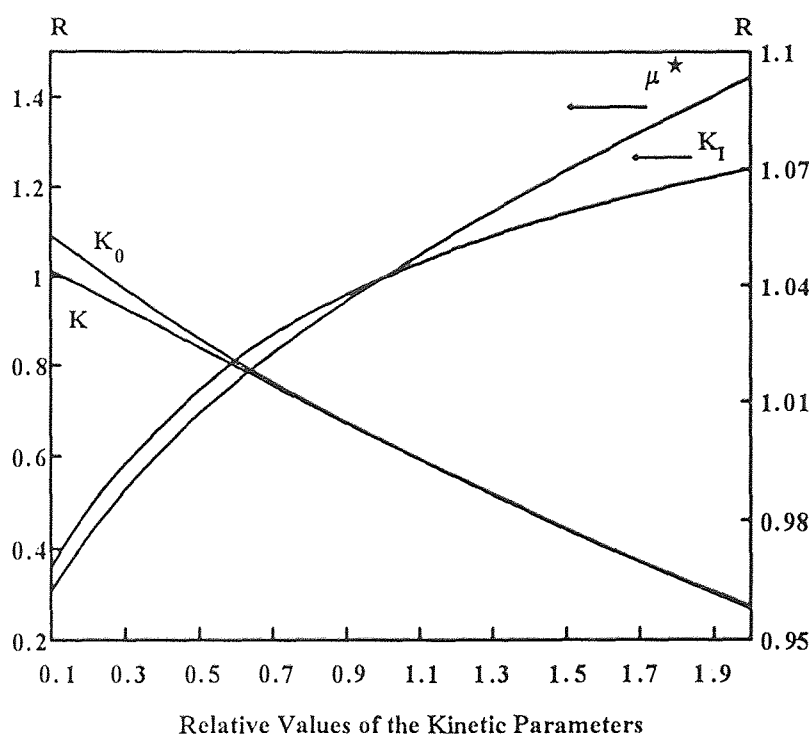


Figure 20 Sensitivity analysis of the effect of the kinetic parameters on the removal rate of butanol. Conditions for this graph are discussed in the text.

Figure 20 shows the effect of changes in the values of the kinetic parameters on the removal rate. It is interesting to notice here that the most important parameters in the kinetic expression appear to be the specific growth rate constant, μ^* , and the inhibitory constant, K_I . When these two parameters change, the predicted removal rates change

correspondingly, while variations in the rest of the parameters are practically unimportant. As it can be seen, even when the values of the constants K and K_0 are doubled, the resulting removal rate is only 4 percent less than its original value. Another conclusion is that when performing kinetic experiments for the determination of the parameters, one needs to be very careful in the estimation of the values of μ^* and K_I , while inaccuracies in the calculation of K and K_0 have a negligible impact. If now, one wanted to predict the behavior of a compound other than butanol, according to the model used in this study, then it could be concluded that if the new compound has μ^* and K_I values similar to those of butanol, it will be removed in the biofilter at rates similar to those of butanol, even if its values of K and K_0 are considerably different.

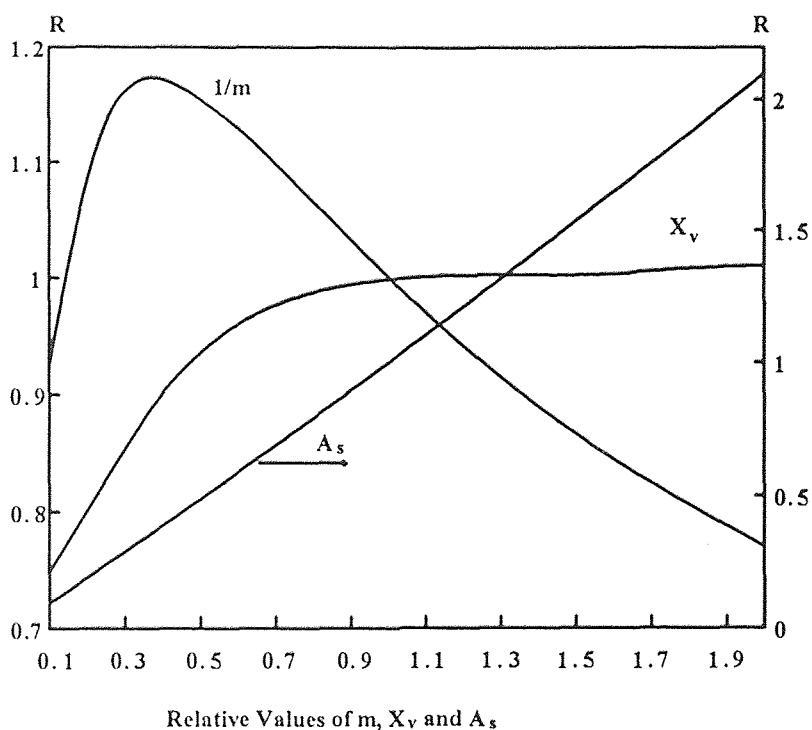


Figure 21 Sensitivity analysis of the effect of parameters A_s , X_v , and m on the removal rate of butanol. Conditions for this graph are discussed in the text.

Figure 21 shows the sensitivity of the removal rate to changes in the values of the biolayer surface area, A_s , the biofilm density, X_v , and the distribution coefficient, m . All

three of these parameters are very important in the prediction of the removal rate. The value of the biolayer surface area seems to be the most crucial, since the removal rate increases linearly with A_S , and small changes in the values of the latter can lead to considerable deviations in the removal rate values. The biofilm density is an important parameter only when its value is low, and its accurate knowledge for sizing a biofilter is important only if its value is less than 100 kg m^{-3} . Regarding the distribution coefficient, one can say that when the substance is very volatile (low $1/m$ value), then it is present in very low concentrations inside the biolayer. Consequently, the kinetics are non-inhibitory, and the removal rates are high. The less volatile a substance is, the higher the probability of being under inhibitory kinetics throughout the column, and this leads to lower removal rates. These last observations are interesting in cases where one wants to predict the removal rates for a substance having kinetic constants similar to those of butanol, but being less or more volatile than butanol. Also, for butanol itself, one can estimate the removal rate when there are temperature changes, which result to changes in the values of m , assuming that these temperature variations do not have a serious impact on the kinetics.

Exactly similar conclusions can be derived from Figures 22 and 23 which show the sensitivity of the removal rate with respect to changes in the kinetic parameters, as well as in the values of A_S , X_V , and m for the case of ethanol this time. For these graphs, the inlet ethanol concentration was taken as 3.63 g m^{-3} , the air flow rate as $0.024 \text{ m}^3 \text{ h}^{-1}$, and the space time as 2.33 min. As base line for the predicted removal rate a value of $22.4 \text{ g h}^{-1} \text{ m}^{-3}$ -packing was used (Table 5). For the case of m , there is again a critical relative value for which the maximum in the removal rate occurs, but is very low (0.01), and that is why it is not shown in the graph.

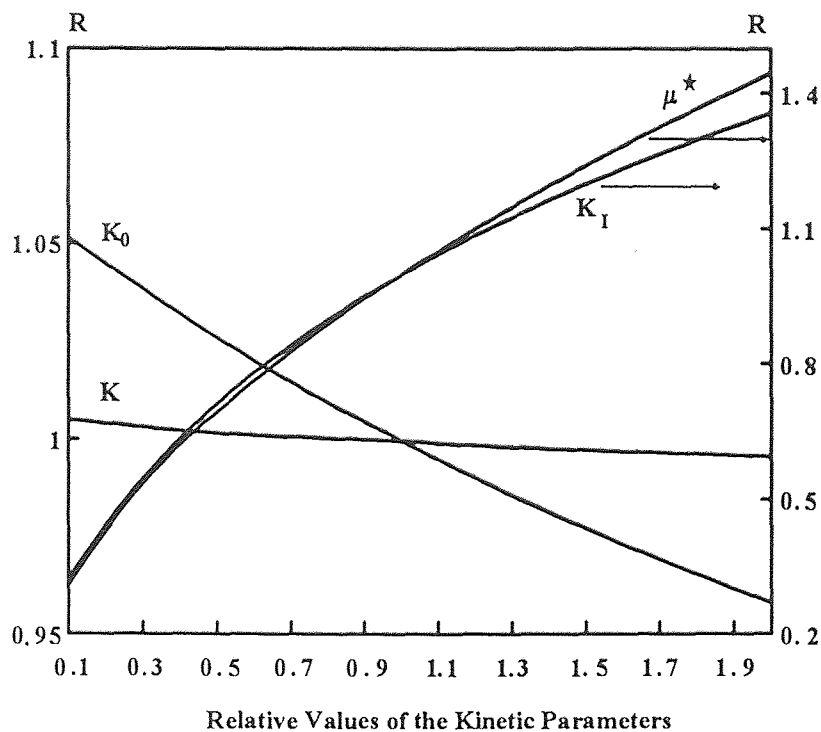


Figure 22 Sensitivity analysis of the effect of the kinetic parameters on the removal rate of ethanol. Conditions for this graph are discussed in the text.

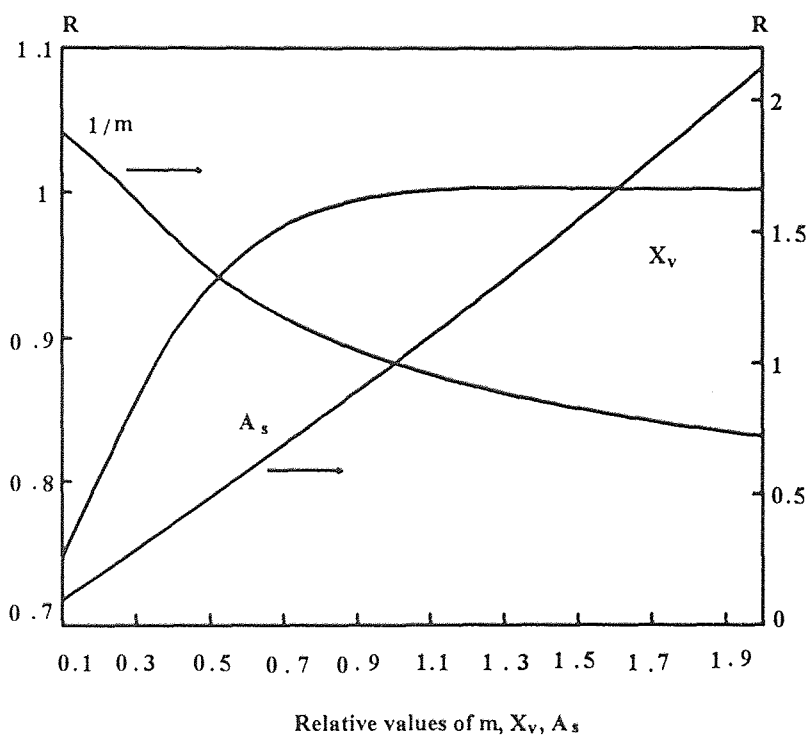


Figure 23 Sensitivity analysis of the effect of parameters A_S , X_V , and m on the removal rate of ethanol. Conditions for this graph are discussed in the text.

CHAPTER 7

CONCLUSIONS AND RECOMMENDATIONS

The results of this study prove that packed-bed biofilters removing a single pollutant respond very successfully under quantitative shock-loading conditions. These shocks may be due to changes either in the flow rate of the airstream, or the concentration of the pollutant in the air supplied to the biofilter. The results have also shown that under transient conditions, adsorption/desorption of the VOCs on the packing material occurs concurrently with biodegradation, and it is the adsorption process which is primarily responsible for the long transients exhibited by the biofilter columns.

Under qualitative shock-loading conditions it has been found that, although biofilters do not fail completely, they fail to achieve high removal rates, at least when the switch from one compound to the other is made infrequently.

Kinetic studies with the two model compounds studied (butanol and ethanol), have shown that both are degraded under inhibitory (Andrews) kinetics by the microbial consortia used in the study. Furthermore, it has been found that inhibition occurs at relatively low concentrations. More specifically, presence of ethanol or butanol in the air, at levels as low as 0.3 g m^{-3} leads to removal of these substances in the biolayers of the biofilter under inhibitory conditions.

The inhibitory kinetics lead to a number of interesting results which were obtained during the course of this study. Using a model which was developed in an earlier study (24), it was found that the thickness of the active part of the biofilm is always very small, and is determined by the depletion of oxygen. Variation of the active biofilm thickness along the biofilter columns, although not always significant, follows an increasing or decreasing trend which is closely related to the inhibitory kinetic characteristics. Due to inhibitory kinetics, it was also found that a given load requiring to be treated up to a

specified level can be dealt with a bed of minimum volume through possible dilution of the contaminated stream with pure air.

The steady state data obtained in this study, could be nicely predicted with a model which was originally developed for methanol biofiltration (24). This indicates that the model has a general applicability. Sensitivity studies with the model have shown that two of the four kinetic parameters need to be known accurately. The specific biofilm surface area, is another model parameter which was found to be very important for an accurate prediction of the process performance.

Of course, the present work does not make the study on shock-loading effects complete. The difficulty of the columns to respond more effectively after changes in the identity of the treated vapor, needs to be further investigated and explained. Future studies should possibly involve running the columns from the first day of their inoculation by using a mixture of butanol and ethanol vapors in the influent gas stream, and then switch each one of the compounds separately, for short time intervals. Another approach would be to start biofilter columns on one VOC only, but change its identity much sooner than was done in this study, and subject the biofilter to qualitative shocks more often.

Other possible issues for further study could be the ability, as well as the time needed for the biofilter to regain its former efficiency after it has been shut down for some time and then started up again. Another question is whether external supply of nutrients and oxygen to the biofilter could result to enhanced removal rates, and how frequently, if at all, the packing material should be replaced. A good understanding of all the above aspects can lead to the optimum use of biofilters, and to the achievement of the desired control of VOC emissions, under a minimum cost.

APPENDIX A

LIST OF SUPPLEMENTARY TABLES AND FIGURES

Table A-1 Experimental and regressed data from kinetic runs on ethanol.

Ethanol Initial Concentration (kg m ⁻³)	μ_{exp} (h ⁻¹)	μ_{regres} (h ⁻¹)	Yield Coefficient
0.144	0.109	0.113	0.375
0.301	0.201	0.189	0.246
0.350	0.210	0.206	0.446
0.475	0.228	0.237	0.495
0.600	0.234	0.255	0.311
0.709	0.275	0.264	0.430
0.899	0.270	0.270	0.449
1.10	0.294	0.268	0.363
1.31	0.240	0.261	0.358
1.80	0.240	0.239	0.376

$$\bar{Y}_E = 0.385$$

Standard error of regression estimate = $1.331 \cdot 10^{-2}$

Absolute average percent error = 4.26

Residual mean square = $2.434 \cdot 10^{-4}$

Table A-2 Experimental and regressed data from kinetic runs on butanol.

Butanol Initial Concentration (kg m ⁻³)	μ_{exp} (h ⁻¹)	μ_{regres} (h ⁻¹)	Yield Coefficient
0.11	0.084	0.061	0.380
0.19	0.090	0.096	0.420
0.28	0.108	0.126	0.357
0.52	0.174	0.174	0.574
0.63	0.198	0.184	0.530
0.91	0.186	0.192	0.487
1.85	0.162	0.163	0.462

$$\bar{Y}_B = 0.458$$

Standard error of regression estimate = $1.190 \cdot 10^{-2}$

Absolute average percent error = 7.70

Residual mean square = $2.265 \cdot 10^{-4}$

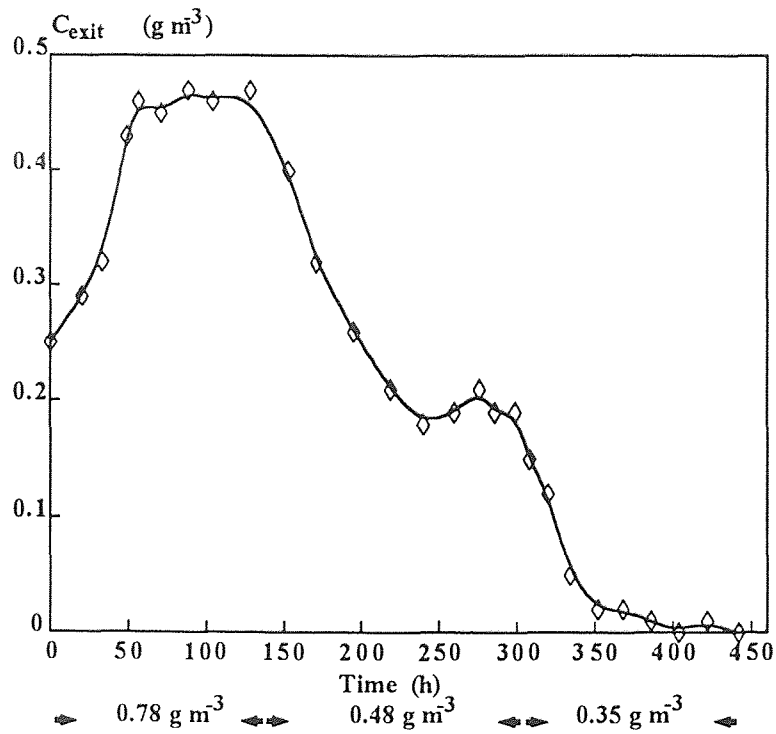


Figure A-1 Transient response of the butanol concentration in the biofilter exit when the butanol concentration in the incoming air stream is varied. Data from a biofilter exposed to butanol only. The space time was kept constant at 0.89 min ($F = 0.066 \text{ m}^3 \text{ h}^{-1}$).

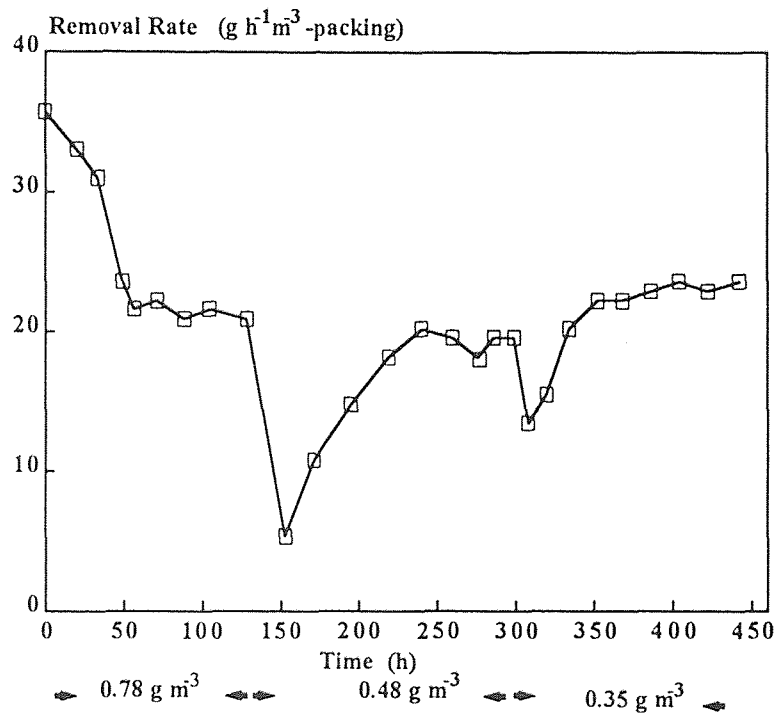


Figure A-2 Transient response of the butanol removal rate when the concentration in the inlet air is varied. This is an alternate representation of the data shown in Figure A-1.

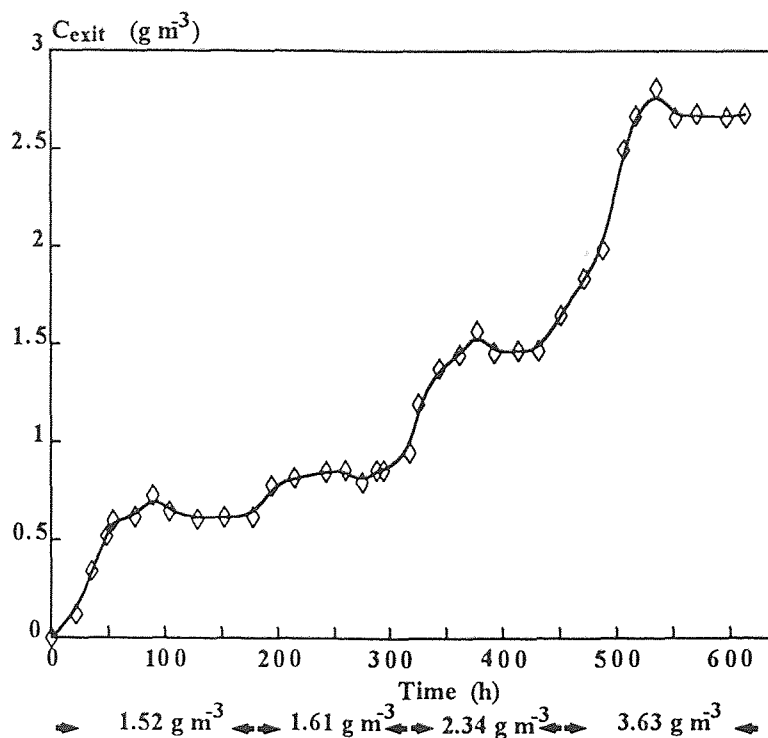


Figure A-3 Transient response of the ethanol concentration in the biofilter exit when the ethanol concentration in the incoming air stream is varied. Data from a biofilter exposed to ethanol only. The space time was kept constant at 2.33 min ($F = 0.024 \text{ m}^3 \text{ h}^{-1}$).

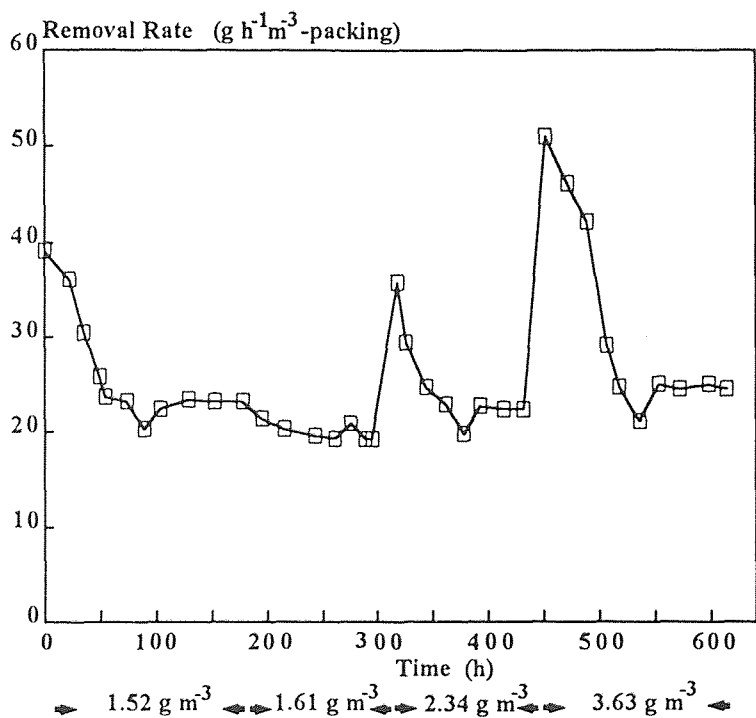


Figure A-4 Transient response of the ethanol removal rate when the concentration in the inlet air is varied. This is an alternate representation of the data shown in Figure A-3.

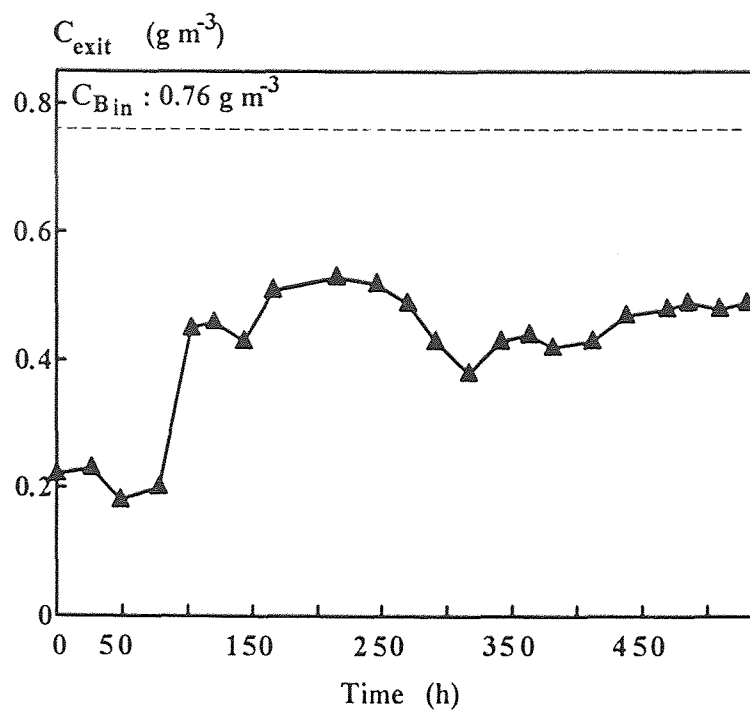


Figure A-5 Transient response of the butanol concentration at the exit of a biofilter which was switched from ethanol to butanol. The space time was kept constant at 2.33 min ($F = 0.024 \text{ m}^3 \text{ h}^{-1}$).

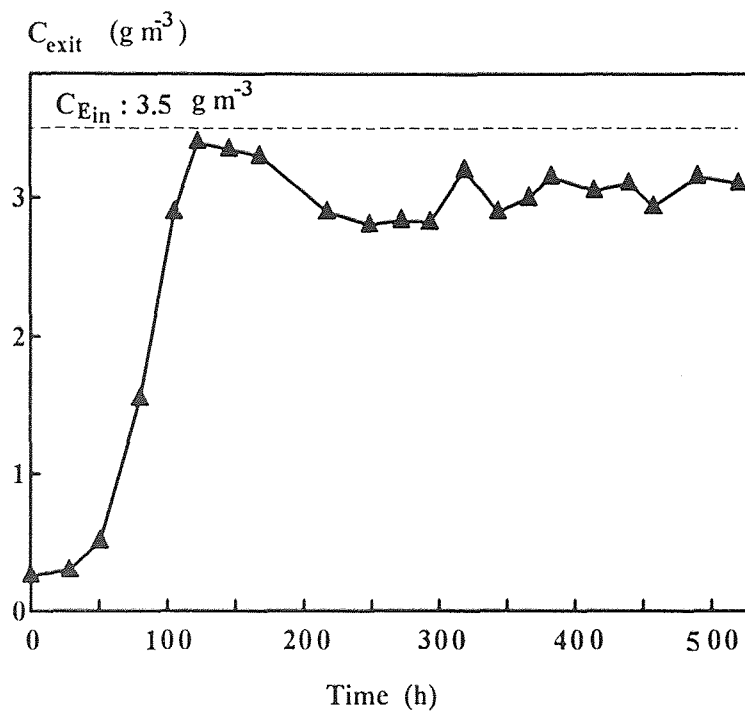


Figure A-6 Transient response of the ethanol concentration at the exit of a biofilter which was switched from butanol to ethanol. The space time was kept constant at 2.45 min ($F = 0.024 \text{ m}^3 \text{ h}^{-1}$).

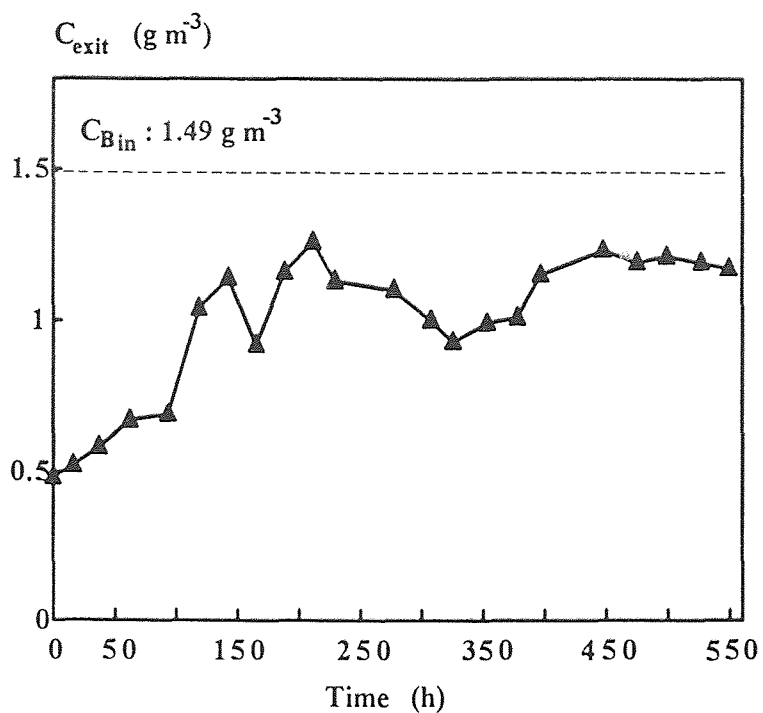


Figure A-7 Transient response of the butanol concentration at the exit of a biofilter which was switched from ethanol to butanol. The space time was kept constant at 2.33 min ($F = 0.024 \text{ m}^3 \text{ h}^{-1}$).

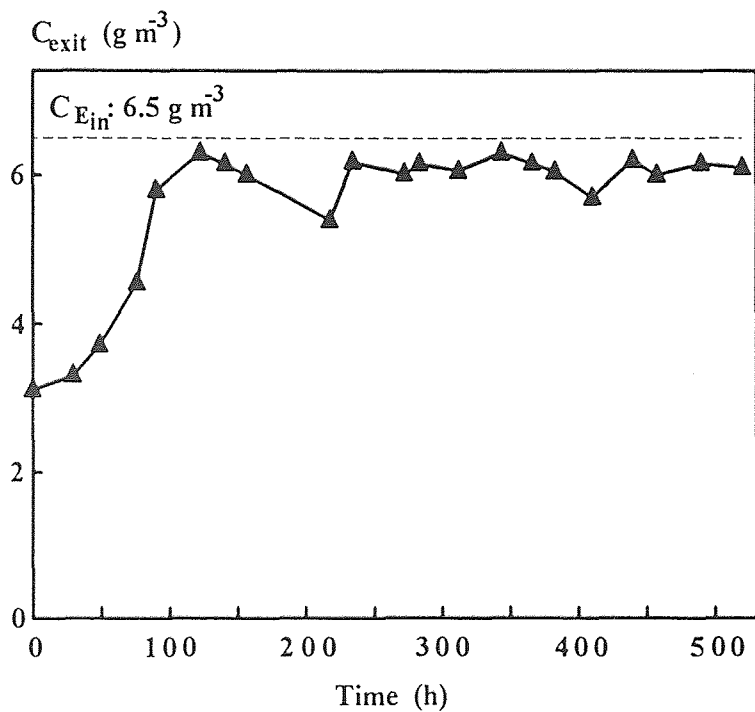


Figure A-8 Transient response of the ethanol concentration at the exit of a biofilter which was switched from butanol to ethanol. The space time was kept constant at 2.45 min ($F = 0.024 \text{ m}^3 \text{ h}^{-1}$).

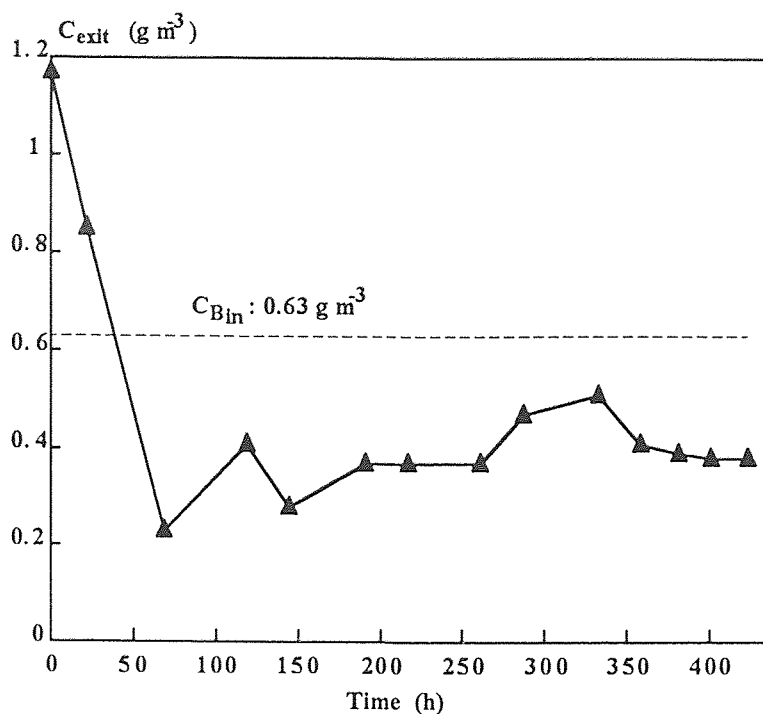


Figure A-9 Transient response of the butanol concentration at the exit of a biofilter which was switched from ethanol to butanol. The space time was kept constant at 1.86 min ($F = 0.030\ m^3\ h^{-1}$).

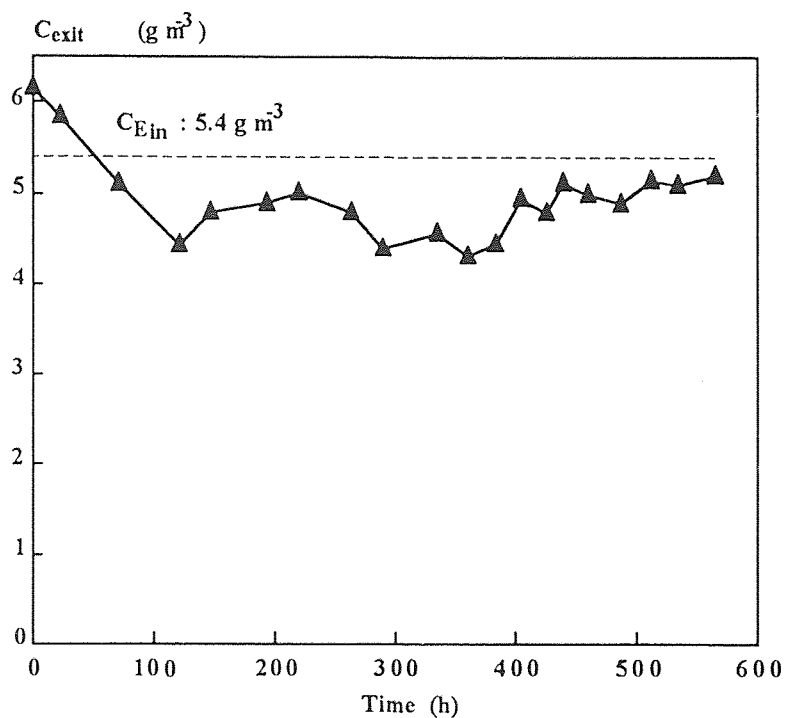


Figure A-10 Transient response of the ethanol concentration at the exit of a biofilter which was switched from butanol to ethanol. The space time was kept constant at 1.96 min ($F = 0.030\ m^3\ h^{-1}$).

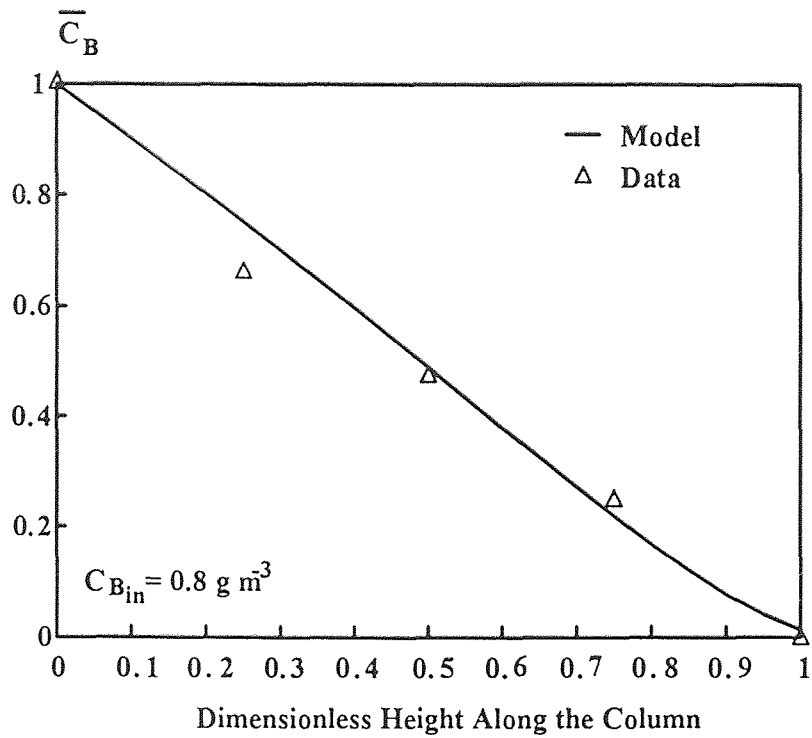


Figure A-11 Concentration profile of butanol vapor in the air along a biofilter column at constant air flowrate of $0.024 \text{ m}^3 \text{ h}^{-1}$.

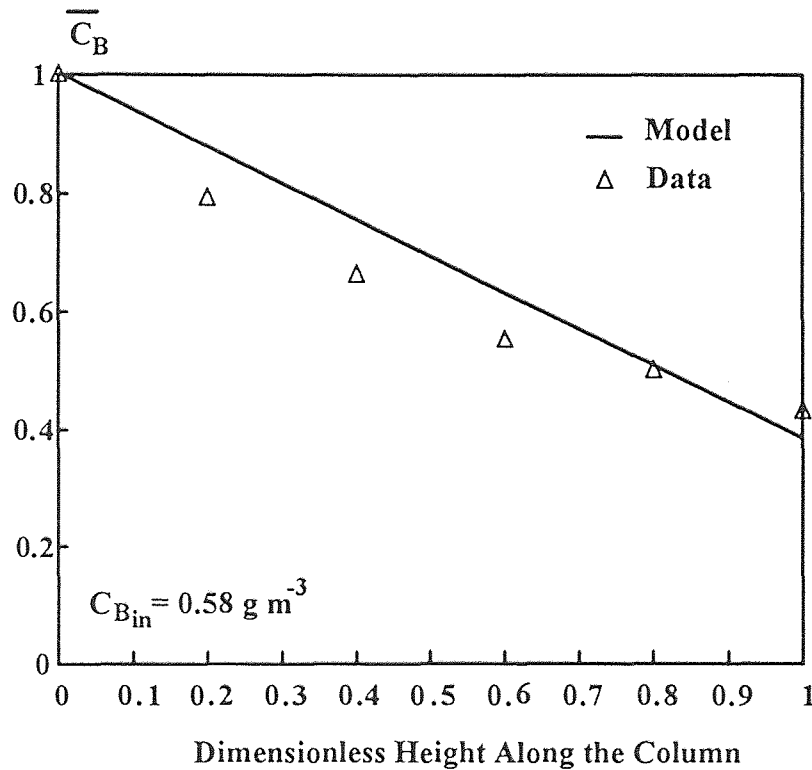


Figure A-12 Concentration profile of butanol vapor in the air along a biofilter column at constant air flowrate of $0.072 \text{ m}^3 \text{ h}^{-1}$.

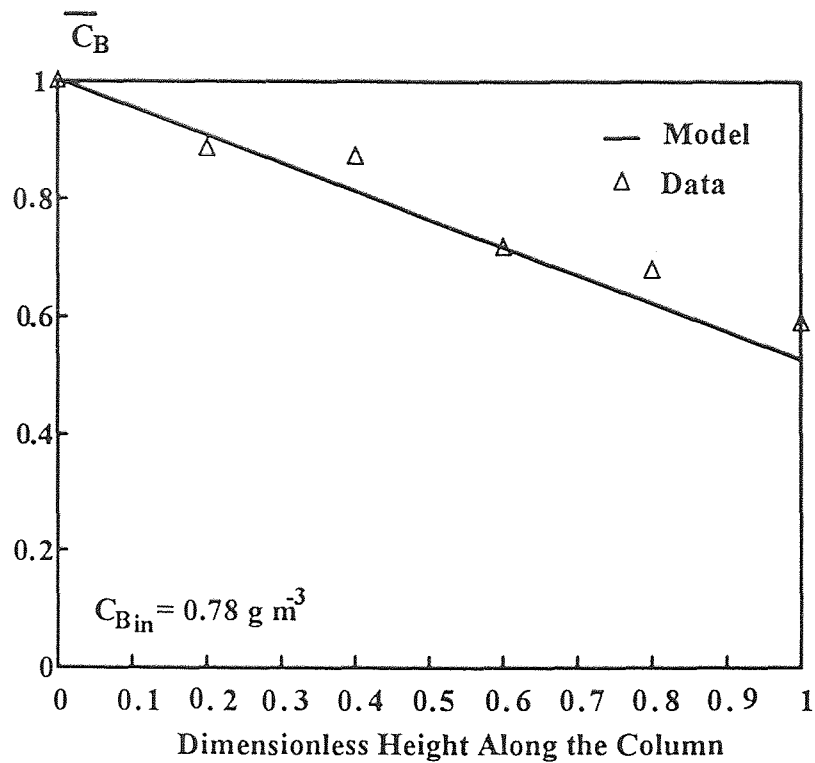


Figure A-13 Concentration profile of butanol vapor in the air along a biofilter column at constant air flow rate of $0.066 \text{ m}^3 \text{ h}^{-1}$.

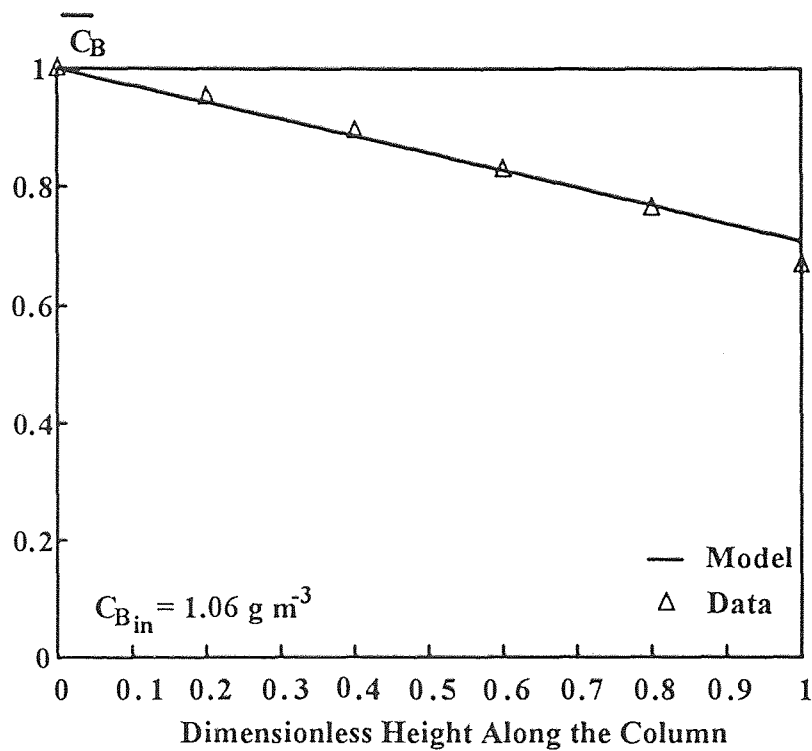


Figure A-14 Concentration profile of butanol vapor in the air along a biofilter column at constant air flowrate of $0.072 \text{ m}^3 \text{ h}^{-1}$.

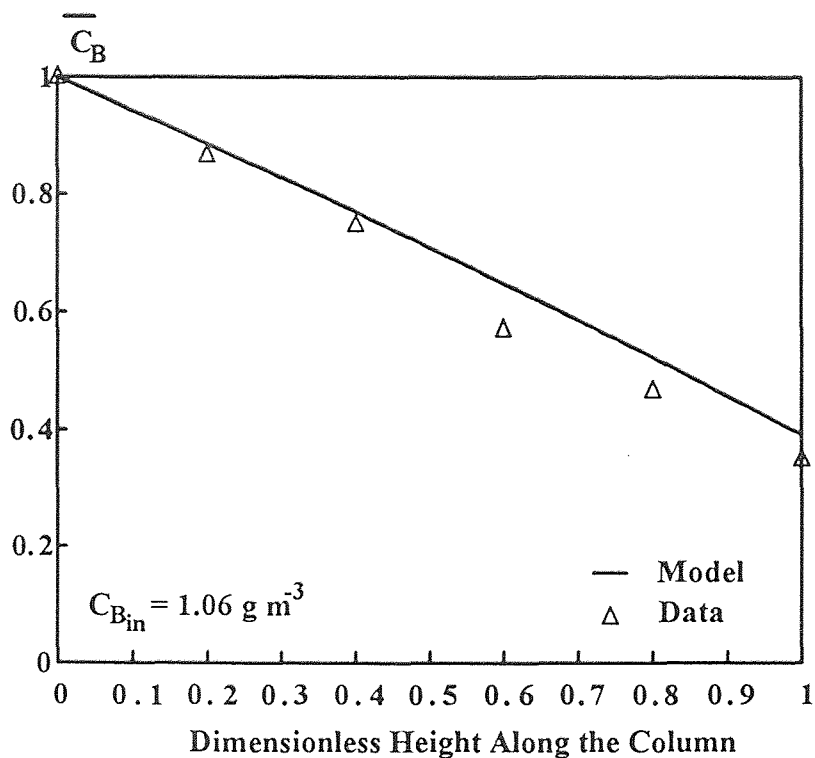


Figure A-15 Concentration profile of butanol vapor in the air along a biofilter column at constant air flowrate of $0.036 \text{ m}^3 \text{ h}^{-1}$.

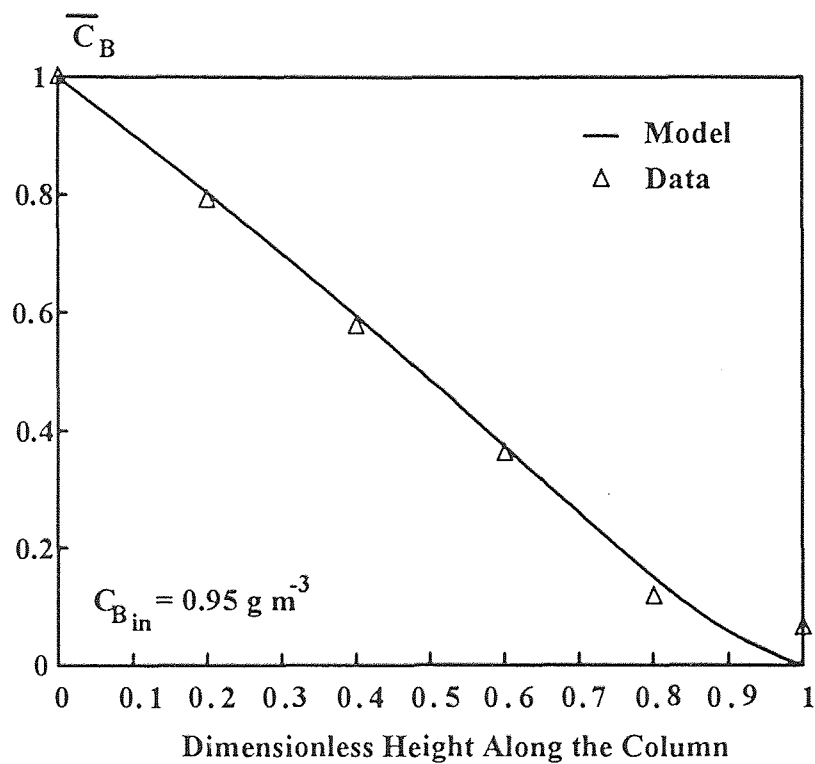


Figure A-16 Concentration profile of butanol vapor in the air along a biofilter column at constant air flowrate of $0.024 \text{ m}^3 \text{ h}^{-1}$.

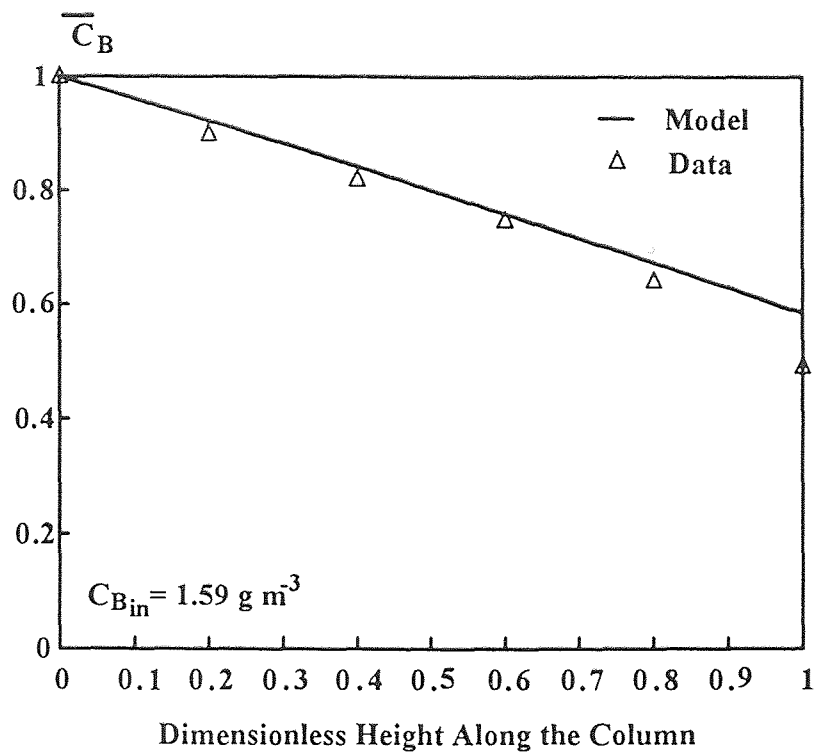


Figure A-17 Concentration profile of butanol vapor in the air along a biofilter column at constant air flowrate of $0.030 \text{ m}^3 \text{ h}^{-1}$.

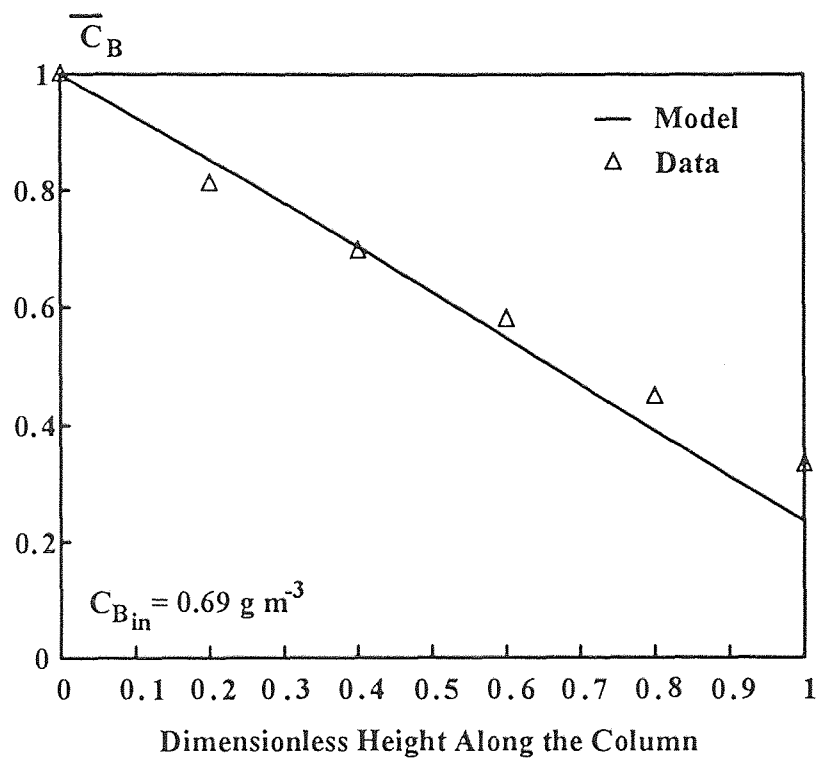


Figure A-18 Concentration profile of butanol vapor in the air along a biofilter column at constant air flowrate of $0.048 \text{ m}^3 \text{ h}^{-1}$.

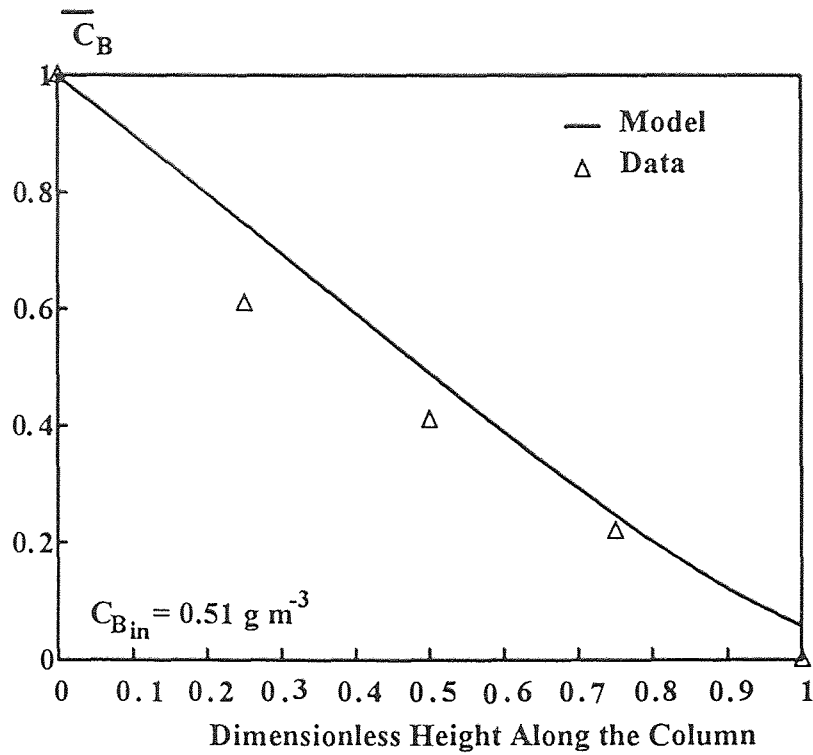


Figure A-19 Concentration profile of butanol vapor in the air along a biofilter column at constant air flowrate of $0.072 \text{ m}^3 \text{ h}^{-1}$.

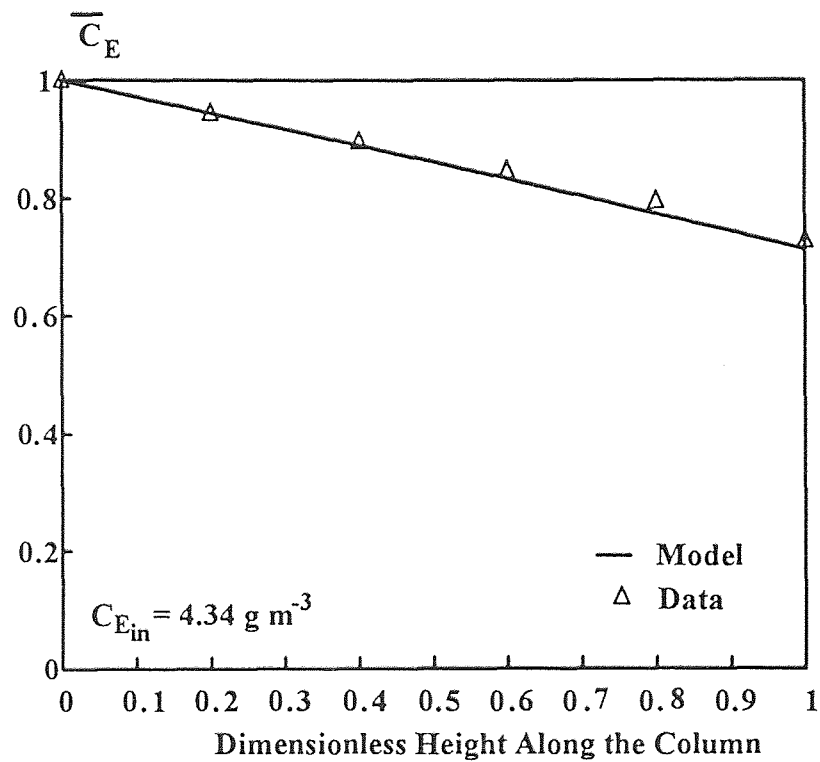


Figure A-20 Concentration profile of ethanol vapor in the air along a biofilter column at constant air flowrate of $0.015 \text{ m}^3 \text{ h}^{-1}$.

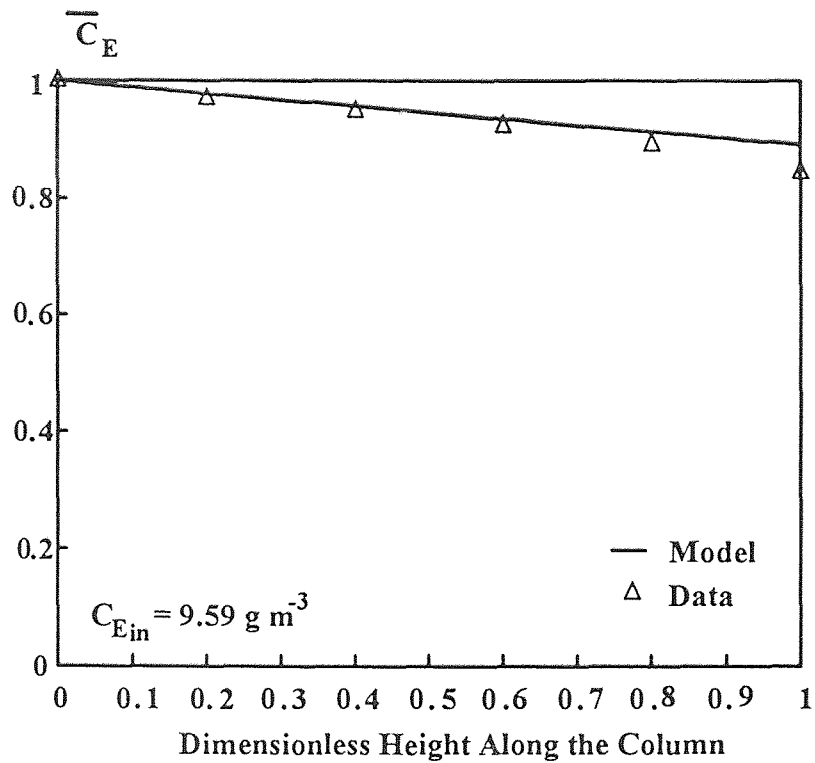


Figure A-21 Concentration profile of ethanol vapor in the air along a biofilter column at constant air flowrate of $0.015 \text{ m}^3 \text{ h}^{-1}$.

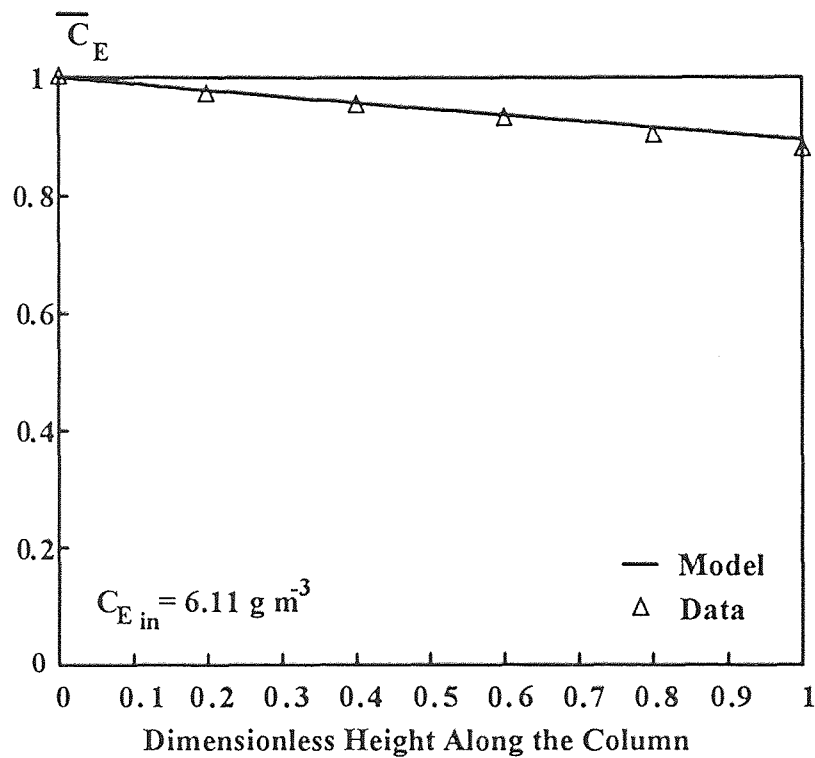


Figure A-22 Concentration profile of ethanol vapor in the air along a biofilter column at constant air flow rate of $0.024 \text{ m}^3 \text{ h}^{-1}$.

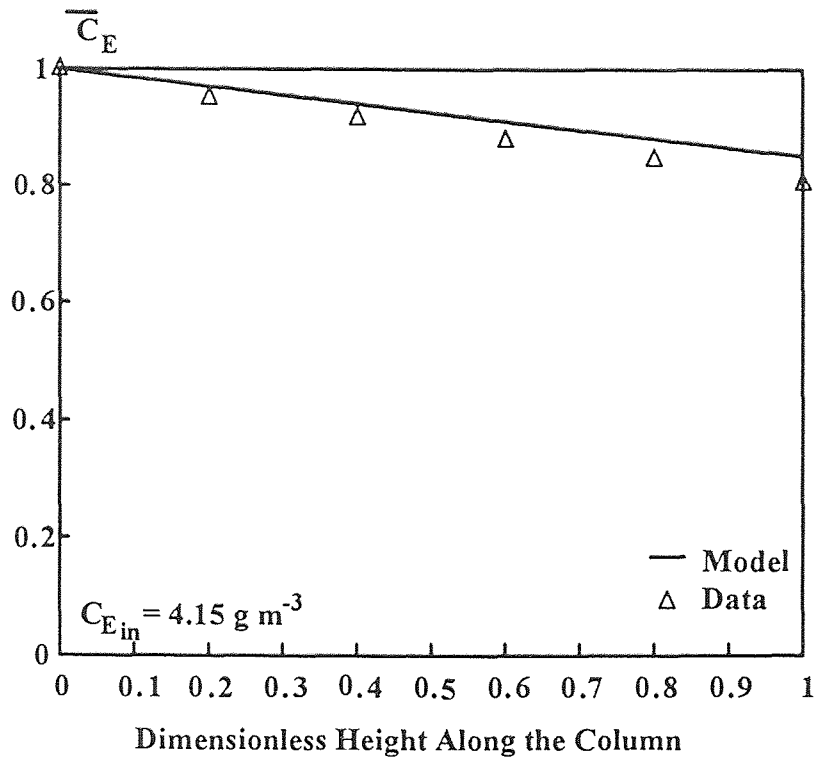


Figure A-23 Concentration profile of ethanol vapor in the air along a biofilter column at constant air flow rate of $0.030 \text{ m}^3 \text{ h}^{-1}$.

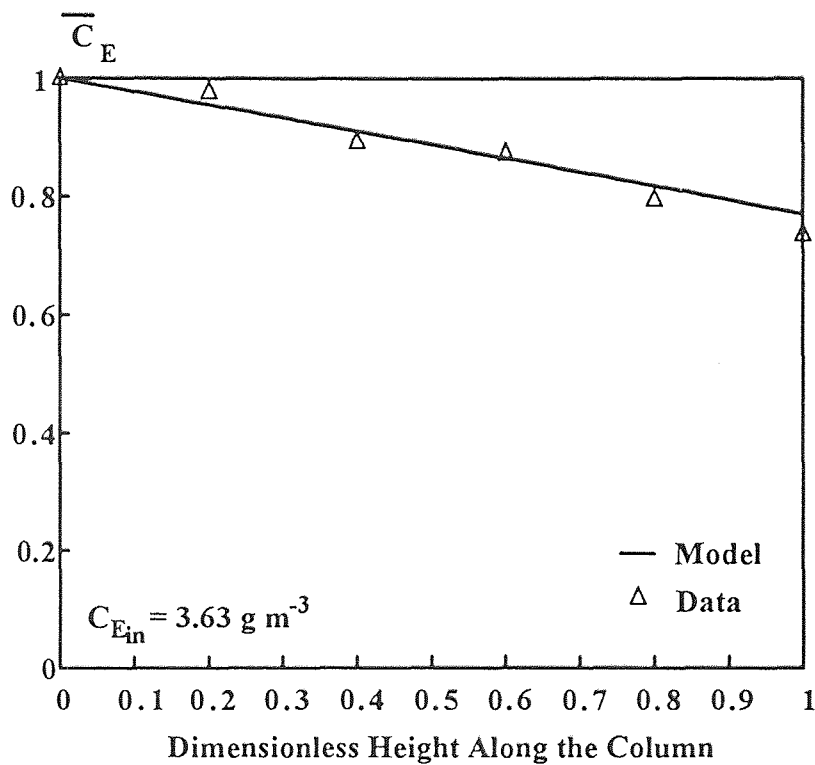


Figure A-24 Concentration profile of ethanol vapor in the air along a biofilter column at constant air flow rate of $0.024 \text{ m}^3 \text{ h}^{-1}$.

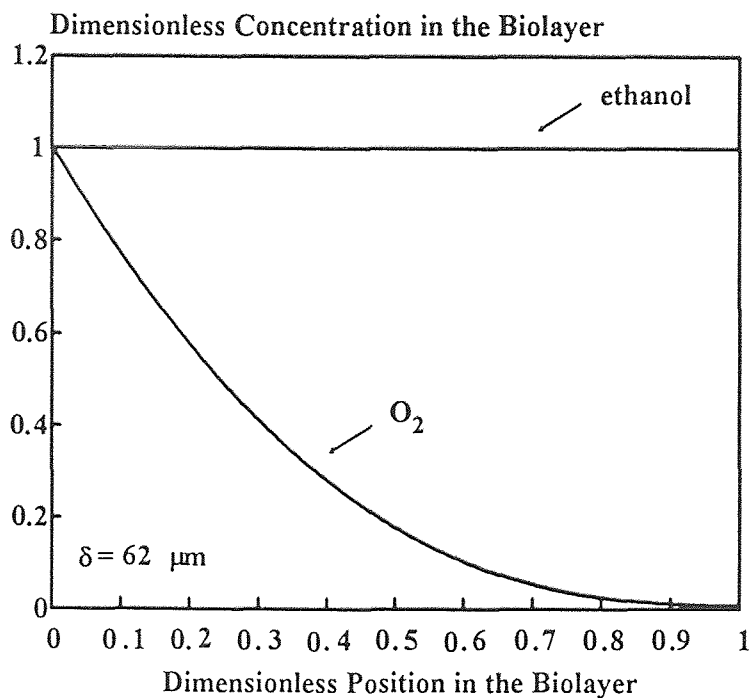


Figure A-25 Model predicted concentration profiles in the biolayer at the middle point of the biofilter. The experimental conditions were, air flow rate $0.012 \text{ m}^3 \text{ h}^{-1}$, and inlet ethanol concentration 9.59 g m^{-3} .

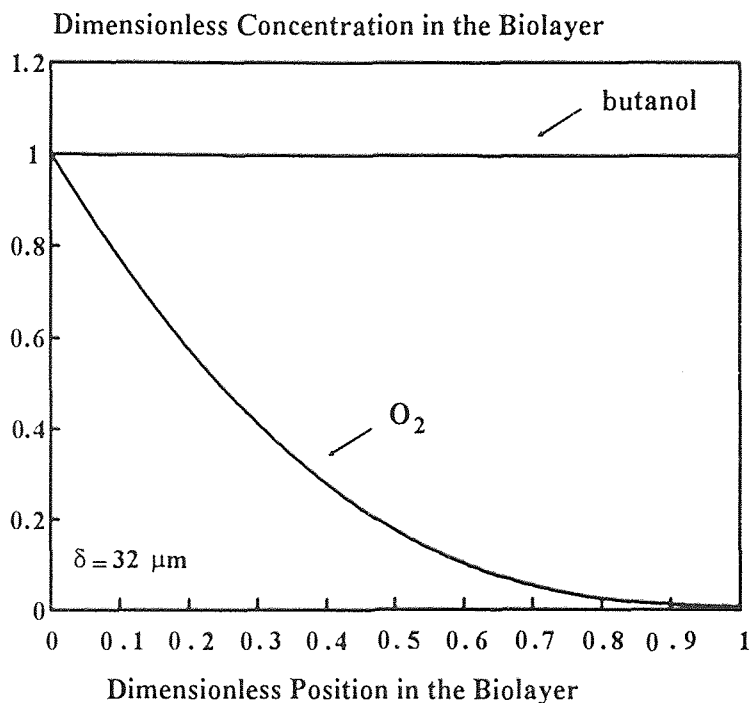


Figure A-26 Model predicted concentration profiles in the biolayer at the middle point of the biofilter. The experimental conditions were, air flow rate $0.030 \text{ m}^3 \text{ h}^{-1}$, and inlet butanol concentration 1.59 g m^{-3} .

APPENDIX B

COMPUTER CODE USED FOR SOLVING THE STEADY-STATE BIOFILTRATION MODEL EQUATIONS

```

c*****
c Purpose : program for solving the model equations
c           at steady state
c Method  : Model Equations based on the Oxygen are
c           solved by multiple shooting technique
c*****
      INTEGER LDY,NEQNS,NMAX
      PARAMETER (NEQNS=2,NMAX=21,LDY=NEQNS,NHMAX=21)
c
      PARAMETER (n=10)
      REAL height(n+1),gas(n+1,1)
c
      INTEGER I,MAXIT,NFINAL,NINIT,NOUT
      REAL  FCNBC,FCNEQN,FCNJAC,FLOAT,TOL,
& X(NMAX),XLEFT,XRIGHT,Y(LDY,NMAX),H(NHMAX)
      EXTERNAL BVPMS,FCNBC,FCNEQN,FCNJAC
c
      EXTERNAL  F
      EXTERNAL tdate
c
      COMMON /gas/deri,an
      COMMON /sur/ sur
      COMMON /cg/ cg
      COMMON /prm/ ak,al,g,e1,e2,w
      COMMON /del/ del
      COMMON /acg0/ acg01
c
c
      OPEN(6,file='bbv1.out',status='new')
c
      CALL TODAY
      cg = 1.0
c
c
      sur = 38.0
c
c gas
c
c
      delz = 1./float(n)
      z = 0.0
      height(1) = z
      gas(1,1) = cg
c
      index = 1000

```

```

c
  do 100 igas = 2,n+1
    del = 17.0
    WRITE(6,55) z
55  FORMAT(' ',Height = ',5x, f7.2)
c
  6  CALL prm (index,ak,al,g,e1,e2,an,w)
    index = 2000
c
  WRITE(6,1)
  1  FORMAT('LIQUID PHASE CONC. ALONG THE FILM OF
& THE BIOLAYER')
  WRITE(6,*)
  WRITE(6,*)
  WRITE(6,2)
  2  FORMAT(' ' X ' ' ' ' meoh (ppm) ' ,
& ' ' O2 (PPM) ' ,/)
  WRITE(6,*)
c
c
c BOUNDARY CONDITIONS
c
  XLEFT = 1.0e-3
  XRIGHT = 1.0
  TOL = 1.0E-4
  MAXIT = 20
  NINIT = NMAX
c
c INITIAL SHOOTING POINTS
c
c
c
  DO 10 I=1,NINIT
  X(I)=XLEFT+FLOAT(I-1)/FLOAT(NINIT-1)*(XRIGHT-XLEFT)
  Y(1,I)=30.0
  Y(2,I)=-0.01
10  CONTINUE
c
c CALL IMSL SUBROUTINE
c
  CALL BVPMS (FCNEQN,FCNJAC,FCNBC,NEQNS,XLEFT,XRIGHT
& ,TOL,TOL,MAXIT,NINIT,X,Y,LDY,NMAX,NFINAL,X,Y,LDY)
c
  sof = y(1,ninit)*0.26
  cob = al*w*(cg-1)+1
  smf = ((sof/0.26-e2*cob)/al+e1*cg)*952.

```



```

uplm1 = e2*cob/100*0.26
uplm2 = e1*cg/100*952.
alcg = cg*acg01
c
del = del/1e-6
c
IF (sof.ge.0.0.and.sof.le. uplm1)THEN
GO TO 5
ELSEIF (smf.ge.0.0.and.smf.le. uplm2) THEN
GO TO 5
ELSEIF (alcg.le.0.5.and.del.le.150.0)THEN
del = del + 0.1
GO TO 6
ELSEIF (alcg.gt.0.5.and.del.le.150.0)THEN
del = del + 1.0
GO TO 6
ELSEIF (del.gt.150)THEN
del = 150.
GO TO 6
ELSE
ENDIF
c
5 DO 4 I = 1,NINIT
so = y(1,I)*0.26
cob = al*w*(cg-1)+1
sm = ((so/0.26-e2*cob)/al+e1*cg)*952.
WRITE(6,*) X(I),sm,so
4 CONTINUE
3 FORMAT(' ',F7.3,3x,e10.6,3x,f10.6)
deri = y(2,1)/al
c
c CALCULATE GAS PHASE CONCENTRATION
c
CALL RK4(F,z,cg,delz)
height(igas) = z
gas(igas,1) = cg
IF(cg.le.0.01)THEN
cg = 0.01
ELSE
ENDIF
WRITE(6,33) height(igas), gas(igas,1)
100 CONTINUE
c
WRITE(6,123)
WRITE(6,22)

```

```

22 FORMAT(//,5x,'    Gas Phase Concent. Profile',/)
   WRITE(6,13)
13  FORMAT (' ',8x,'Height ', ' Concentration',/)
   DO 44 igas=1,n+1
   WRITE(6,33) height(igas), gas(igas,1)
44  CONTINUE
33  FORMAT(' ',F14.6,3x,F14.6)
c
c
   CALL lsq1 (gas, alsq)
   WRITE(6,66) alsq
66  FORMAT(' sum of sq. = ', 4x, f10.6)
c  WRITE(6,123)
c
123 FORMAT(' _____',/)
   STOP
   END
c*****
   SUBROUTINE TODAY
   EXTERNAL TDATE
   CALL TDATE (IDAY, MONTH, IYEAR)
   WRITE(6,123)
   WRITE (6,66) month,iday,iyear
66  FORMAT(' Date of Simulation: ',i2,',',i2,',',I4,/)
23  FORMAT(' _____',/)
   RETURN
   END

c*****
c purpose : solve the gas phase concentration profile
c           using the fourth order runge kutta method
c*****
   SUBROUTINE RK4(F,z,cg,H)
   H2 = 0.5*H
   START = z
   F1 = F(z,cg)
   F2 = F(z+H2,cg+H2*F1)
   F3 = F(z+H2,cg+H2*F2)
   F4 = F(z+H,cg+H*F3)
   cg = cg+H*(F1+2.*F2+2.*F3+F4)/6.
   z = z+H
   RETURN
   END

c
c*****

```

```

c purpose : give the function for RK method, in the gas phase
c      balance
c*****
c      FUNCTION F(z,cg)
c      COMMON/gas/deri,an
c      F= an*deri
c      RETURN
c      END
c*****
c purpose : compare the model predicitions with the exp. and
c      minimize the error to find the best surface area.
c*****
c
c      Least Square Subroutine for first 4 sets of
c      data sets
c
c      SUBROUTINE lsq1 (ycal, alsq)
c      REAL    ycal(11,1),yexp(5)
c      DATA yexp/.847,.665,.492,.312,.131/
c      x2 = ycal(3,1)-yexp(1)
c      x3 = ycal(5,1)-yexp(2)
c      x4 = ycal(7,1)-yexp(3)
c      x5 = ycal(9,1)-yexp(4)
c      x6 = ycal(11,1)-yexp(5)
c      alsq = (x2**2+x3**2+x4**2+x5**2+x6**2)
c      RETURN
c      END
c
c      SUBROUTINE lsq2 (ycal, alsq)
c      REAL    ycal(21,1),yexp(4)
c      DATA yexp/.788,.615,.481,.346/
c      x2 = ycal(6,1)-yexp(1)
c      x3 = ycal(11,1)-yexp(2)
c      x4 = ycal(16,1)-yexp(3)
c      x5 = ycal(21,1)-yexp(4)
c      alsq = (x2**2+x3**2+x4**2+x5**2)
c      RETURN
c      END
c
c      SUBROUTINE lsq3 (ycal, alsq)
c      REAL    ycal(21,1),yexp(3)
c      DATA yexp/.521,.292,.0/
c      x2 = ycal(8,1)-yexp(1)
c      x3 = ycal(14,1)-yexp(2)
c      x4 = ycal(21,1)-yexp(3)

```

```

alsq = (x2**2+x3**2+x4**2)
RETURN
END

```

c

```

SUBROUTINE lsq4 (ycal, alsq)
REAL    ycal(11,1),yexp(1)
DATA yexp/.60/
x2 = ycal(11,1)-yexp(1)
alsq = (x2**2)
RETURN
END

```

c

```

SUBROUTINE lsq5 (ycal, alsq)
REAL    ycal(21,1),yexp(4)
DATA yexp/.5774,.3501,.0118,.0/
x2 = ycal(6,1)-yexp(1)
x3 = ycal(11,1)-yexp(2)
x4 = ycal(16,1)-yexp(3)
x5 = ycal(21,1)-yexp(4)
alsq = (x2**2+x3**2+x4**2+x5**2)
RETURN
END

```

c

```

SUBROUTINE lsq6 (ycal, alsq)
REAL    ycal(21,1),yexp(4)
DATA yexp/.8137,.6917,.5578,.3375/
x2 = ycal(6,1)-yexp(1)
x3 = ycal(11,1)-yexp(2)
x4 = ycal(16,1)-yexp(3)
x5 = ycal(21,1)-yexp(4)
alsq = (x2**2+x3**2+x4**2+x5**2)
RETURN
END

```

c

```

SUBROUTINE lsq7 (ycal, alsq)
REAL    ycal(21,1),yexp(4)
DATA yexp/.9385,.79,.5616,.4157/
x2 = ycal(6,1)-yexp(1)
x3 = ycal(11,1)-yexp(2)
x4 = ycal(16,1)-yexp(3)
x5 = ycal(21,1)-yexp(4)
alsq = (x2**2+x3**2+x4**2+x5**2)
RETURN
END

```

```

c*****

```

```

SUBROUTINE FCNEQN (NEQNS,X,Y,P,DYDX)
INTEGER NEQNS
REAL X,Y(NEQNS),P,DYDX(NEQNS)
c
COMMON /cg/ cg
COMMON /prm/ ak,al,g,e1,e2,w
c
cob = al*w*(cg-1)+1
alp = -e2*cob+al*e1*cg
bet1 = al**2+al*alp+g*alp**2
bet2 = al+2.*alp*g
bet3 = al**2*ak
c
DYDX(1) = Y(2)*p
DYDX(2) = (bet3*y(1)/(bet1+p*bet2*Y(1)+p*Y(1)**2*G))*
& (alp+p*y(1))/(1.+p*y(1))*p
RETURN
END
c
SUBROUTINE FCNBC(NEQNS,YLEFT,YRIGHT,P,F)
INTEGER NEQNS
REAL YLEFT(NEQNS),YRIGHT(NEQNS),P,F(NEQNS)
c
COMMON /cg/ cg
COMMON /prm/ ak,al,g,e1,e2,w
c
cob = al*w*(cg-1)+1
c
F(1) = YLEFT(1)-cob*E2*p
F(2) = YRIGHT(2)
RETURN
END
c
SUBROUTINE FCNJAC(NEQNS,X,Y,P,DYDPDY)
INTEGER NEQNS
REAL X,Y(NEQNS),P,DYDPDY(NEQNS,NEQNS)
c
COMMON /cg/ cg
COMMON /prm/ ak,al,g,e1,e2,w
c
cob = al*w*(cg-1)+1
alp = -e2*cob+al*e1*cg
bet1 = al**2+al*alp+g*alp**2
bet2 = al+2.*alp*g
bet3 = al**2*ak

```

```

c
  x1 = bet1+p*bet2*y(1)+p*g*y(1)**2
  x2 = 1.+y(1)*p
  x3 = alp+2.*y(1)*p
  x4 = p*bet2+2.*g*y(1)*p
c
  DYPDY(1,1) = 0
  DYPDY(1,2) = 1.0*p
  DYPDY(2,1) = bet3*(x1*x2*x3-y(1)*(p*y(1)+alp)*(x1
& *p+x2*x4))/x1**2/x2**2*p
  DYPDY(2,2) = 0.0
  RETURN
  END

c*****
  SUBROUTINE prm (index,ak,al,g,e1,e2,an,w)
  COMMON /del/ del
  COMMON /sur/ sur
  COMMON /acg0/ acg01
c
c 1-methanol
c 2-oxygen
c
  del = del*1e-6
c
  b0 = 100e3
c
  xv = b0/1000
  fd = 1-0.43*xv**0.92/(11.19+0.27*xv**0.99)
c
  df1 = 0.77e-9 *3600.*fd
  df2 = 2.41e-9 *3600.*fd
  ayl = 0.458
  ay2 = 0.232
  akii1 = 0.857*1000
  akss1 = 0.952*1000
  amu1 = 0.579
  akss2 = 0.26
c
  ACG01 = 0.93
  aug = 0.030
  vv = 980.0e-6
c
  acg02 = 275
c

```

```

amm1 = .00036
amm2 = 34.4
if(index.eq.1000)then
CALL SVARI(sur,b0,vv,df1,df2,ay1,ay2,AKII1,
& AKSS1,amu1,akss2,acg01,acg02,aug, amm1,amm2,phi)
ELSE
ENDIF
c
ak = amu1*del**2*b0/df1/ay1/akss1
al = df1*ay1*akss1/ay2/akss2/df2
g = akss1/akii1
e1 = acg01/amm1/akss1
e2 = acg02/amm2/akss2
an = df1*sur*akss1*vv/del/aug/acg01
w = akss2*df2*acg01/akss1/df1/acg02
c
WRITE(6,123)
WRITE(6,1)
1 FORMAT (' ', ' Parameters Used :', '/')
WRITE(6,2) ak, g
WRITE(6,3) e1, AN
2 FORMAT (' ', ' k = ',e14.3,3x,'gama = ',3x,f7.3)
3 FORMAT (' ', ' Eps1 = ',f14.6,3x,'n = ',3x,f7.3)
WRITE(6,4) al,delta*1e6
WRITE(6,5) e2,w
4 FORMAT (' ', 'lamda = ',e14.3,5x,'delta (mic.m)=' ,
& f10.6,/)
5 FORMAT (' ', ' Eps2 = ',e14.3,3x,'omega = ',3x,e14.3,/)
12 FORMAT(' _____',/)
RETURN
END
c*****
SUBROUTINE SVARI(sur,b0,vv,df1,df2,ay1,ay2,AKII1,AKSS1,
& amu1,akss2,acg01,acg02,aug, amm1,amm2,phi)
c
WRITE(6,123)
WRITE(6,1)
1 FORMAT (' ',//, ' VARIABLES IN THE MODEL',/)
WRITE(6,19) Aug
19 FORMAT (' ', 'Gas Flow Rate (m3/hr) =', e14.3)
WRITE(6,3) vv*1e6
3 FORMAT (' ', 'Volume of the column(cm3) =', f14.3)
WRITE(6,4) SUR
4 FORMAT (' ', 'Biolayer Sur.Area( m2/m3) =', f14.3)
WRITE(6,44) b0

```

```

44 FORMAT (' ', 'Biomass Conc. (g/m3)      =', e14.3)
c  WRITE(6,5) del*1e3
c 5 FORMAT (' ', 'Film thickness (mm)      =', f14.3)
  WRITE(6,2) ACG01
  WRITE(6,22) ACG02
  2 FORMAT (' ', 'Inlet conc. (g/m3 of air)(m) =', f14.3)
22 FORMAT (' ', 'Inlet conc. (g/m3 of air)(o) =', f14.3)
  WRITE(6,31) ay1
31 FORMAT (' ', 'Yield Coefficient (m)      =', f14.3)
  WRITE(6,32) ay2
32 FORMAT (' ', 'Yield Coefficient (o)      =', f14.3)
  WRITE(6,51) df1*1e9/3600
  WRITE(6,54) df2*1e9/3600
51 FORMAT (' ', 'Diff. Coefficient (m)*1e9 =', f14.3)
54 FORMAT (' ', 'Diff. Coefficient (o)*1e9 =', f14.3)
  WRITE(6,56) amm1
56 FORMAT (' ', 'Dist. Coeff.      (m)      =', e14.3)
  WRITE(6,566) amm2
566 FORMAT (' ', 'Dist. Coeff.      (o)      =', e14.3)
  WRITE(6,123)
  WRITE(6,*) '      Andrews and other Parameters'
  WRITE(6,6) akii1,akss1,amu1, akss2
  6 FORMAT(' ', ' Ki1 (g/m3) =', e14.3, 3x, 'Ks1 (g/m3) =',
& ' ', f7.3, '/', ' Sp. Growth Rate-1 (1/hr) =', f14.3, 3x, '/', ' ',
& ' aKd (g/m3) =', f7.3, '/')
123 FORMAT(' _____;')
  RETURN
  END

```


REFERENCES

1. Moretti, E.C., and N. Mukhopadhyay. "VOC Control: Current Practices and Future Trends." *Chemical Engineering Progress* 89(7) (1993):20-26.
2. Leson, G., D.S. Hodge, F. Tabatabai, and A.M. Winer. "Biofilter Demonstration Projects for the Control of Ethanol Emissions." *Presented at the 86th Annual A&WMA Meeting, Denver, CO* (1993): Paper No. 93-WP-52C.04.
3. Wooley, J., W.W. Nazaroff, and A.T. Hodgson. "Release of Ethanol to the Atmosphere During Use of Consumer Cleaning Products." *J. Air Waste Manage. Assoc.* 40 (1990):1114-1120.
4. Dharmavaram, S. "Biofiltration: A Lean Emissions Abatement Technology." *Presented at the 84th Annual A&WMA Meeting, Vancouver, BC*(1991): Paper No. 91-103.2.
5. Bohn, H.L. "Consider Biofiltration for Decontaminating Gases." *Chemical Engineering Progress* 88(4) (1992): 34-40.
6. Leson, G., and A.M. Winer. "Biofiltration: An Innovative Air Pollution Control Technology for VOC Emissions." *J. Air & Waste Manage. Assoc.* 41(8) (1991): 1045-1054.
7. Bohn, H.L. "Biofiltration: Design Principles and Pitfalls." *Presented at the 86th Annual A&WMA Meeting, Denver, CO* (1993): Paper No. 93-TP-52A.01.
8. Ergas, S.J., E.D. Schroeder, and D.P.Y. Chang. "VOC Emission Control from Wastewater Treatment Facilities Using Biofiltration." *Proceedings of the 84th Annual A&WMA Meeting, Vancouver, BC* (1991): Paper No. 91-105.4.
9. Pomeroy, R.D. "Controlling Sewage Plant Odors." *Consulting Engineer* 20 (1963): 101-108.
10. Carlson, D.A., and C.P. Leiser. "Soil Beds for the Control of Sewage Odors." *J. Wat. Pollut. Contr. Fed.* 38 (1966): 829-840.
11. Ottengraf, Simon P.P. "Exhaust Gas Purification." *Biotechnology*. W. Shonborn, Ed. v. 8. VCH Verlagsgesellschaft, Weinheim, Germany (1986): 425-452.
12. Ottengraf, S.P.P., and A.H.C. van den Oever. "Kinetics of Organic Compound Removal from Waste Gases with a Biological Filter." *Biotechnol. Bioeng.* 25 (1983):3089-3102.

13. Ottengraf, S.P.P, J.J.P.M. Meesters, A.H.C. van den Oever, and H.R. Rozema. "Biological Elimination of Volatile Xenobiotic Compounds in Biofilters." *Bioprocess Engineering* 1 (1986): 61-69.
14. Diks, R.M.M, and S.P.P. Ottengraf. "Verification Studies of a Simplified Model for the Removal of Dichloromethane from Waste Gases Using a Biological Trickling Filter (Part I)." *Bioprocess Engineering* 6 (1991): 93-99.
15. Diks, R.M.M, and S.P.P. Ottengraf. "Verification Studies of a Simplified Model for the Removal of Dichloromethane from Waste Gases Using a Biological Trickling Filter (Part II)." *Bioprocess Engineering* 6 (1991): 131-140.
16. Diks, R.M.M, and S.P.P. Ottengraf. "Process Technological View on the Elimination of Chlorinated Hydrocarbons from Wastegases." *Man and his Ecosystem*. L.J. Brassier, and W.C. Mulder, Eds. *Proceedings of the 8th World Clean Air Congress, The Hague, The Netherlands* 4 (1989): 406-410.
17. Ottengraf, S.P.P. "Biological Systems for Waste Gas Elimination." *Trends in Biotechnology* 5 (1987): 132-136.
18. Lith, C.V., S.L. David, and R. Marsh. "Design Criteria for Biofilters." *Trans IChemE* 68(Part B) (1990): 127-132.
19. Lith, C.V. "Biofiltration, an Essential Technique in Air Pollution Control." *Man and his Ecosystem*. L.J. Brassier, and W.C. Mulder, Eds. *Proceedings of the 8th World Clean Air Congress, The Hague, The Netherlands* 4 (1989):393-398.
20. Kambell, D.H., J.T. Wilson, H.W. Reed, and T.T. Stocksdale. "Removal of Aliphatic Hydrocarbons in a Soil Bioreactor." *J. Air Pollut. Contr. Assoc.* 37(10) (1987): 1236-1240.
21. Utgikar, V., R. Govid, Y. Shan, S. Safferman, and R.C. Brenner. "Biodegradation of Volatile Organic Chemicals in a Biofilter." *In Emerging Technologies in Hazardous Waste Management II*. D.W. Tedder, and F.G. Pokland, Eds. ACS Symposium Series 468 (1991): 233-260.
22. Hartmans, F, and T. Tramper. "Dichloromethane Removal from Waste Gases with a Trickle-Bed Bioreactor." *Bioprocess Engineering* 6(3) (1991): 83-92.
23. Ockeloen, H.F., T.J. Overcamp, and C.P.L. Grady, Jr. "A Biological Fixed-Film Simulation Model for the Removal of Volatile Organic Air Pollutants." *Presented at the 85th Annual A&WMA Meeting, Kansas City, MO* (1992): Paper No. 92-116.05.

24. Shareefdeen, Z., B.C. Baltzis, Y. Oh, and R. Bartha. "Biofiltration of Methanol Vapor." *Biotechnol. Bioeng.* 41 (1993): 512-524.
25. Baltzis, B.C., and Z. Shareefdeen. "Modeling and Preliminary Design Criteria for Packed Bed Biofilters." *Presented at the 86th Annual A&WMA Meeting, Denver, CO* (1993): Paper No. 93-TP-52A.03.
26. Baltzis, B.C., and Z. Shareefdeen. "Biofiltration of VOC Mixtures: Modeling and Pilot Scale Experimental Verification." *To be presented at the 87th Annual A&WMA Meeting, Cincinnati, OH* (1994).
27. Deshusses, M.A., and G. Hamer. "The Removal of Volatile Ketone Mixtures from Air in Biofilters." *Bioprocess Engineering* 9 (1993):141-146.
28. Smith, P.J., P. Biswas, M.T. Swidan, and R.C. Brenner. "Treatment of Volatile Organic Compounds in Waste Gases Using a Trickling Biofilter System: A Modeling Approach." *Presented at the 86th Annual A&WMA Meeting, Denver, CO* (1993): Paper No. 93-TP-52A.05.
29. Ergas, S.J., E.D. Schroeder, and D.P.Y. Chang. "Control of Air Emissions of Dichloromethane, Trichloroethene, and Toluene by Biofiltration." *Presented at the 86th Annual A&WMA Meeting, Denver, CO* (1993): Paper No. 93-WA-52B.
30. Togna, A.P., and S. Frisch. "Field Pilot Study of Styrene Biodegradation Using Biofiltration." *Presented at the 86th Annual A&WMA Meeting, Denver, CO* (1993): Paper No. 93-WP-52C.03.
31. van derVaart, P.R., M.W. Vatauvuk, and A.H. Wehe. "The Cost Estimation of Thermal and Catalytic Incinerators for the control of VOCs." *J. Air Waste Manage Assoc.* 41(4) (1991): 497-501.
32. Ottengraf, S.P.P., and J.H.G. Konings. "Emission of Microorganisms from Biofilters." *Bioprocess Engineering* 7 (1991): 89-96.
33. Ottengraf, S.P.P., A.H.C. Van den Oever, and I.J.C.M. Kempenaars. "Waste Gas Purification in a Biological Filter Bed." *Prog. Ind. Microbiol.* 20 (1987): 157-167.
34. Paul, P.G., and C. Roos. "Biological Waste Air Treatment with the Biobox." *Man and his Ecosystem.* Brassier, and W.C. Mulder, Eds. *Proceedings of the 8th World Clean Air Congress, The Hague, The Netherlands* 4 (1989):399-404.
35. Luong, J.H.T. "Generalization of Monod Kinetics for Analysis of Growth Data with Substrate Inhibition." *Biotechnol. Bioeng.* 29 (1987): 242-248.

36. Bailey, J.E., and D.F. Ollis. *Biochemical Engineering Fundamentals*. Second Edition. New York: McGraw-Hill (1986).
37. Williamson, K., and P.L. McCarty. "A Model of Substrate Utilization by Bacterial Films." *J. Wat. Pollut. Contr. Fed.* 48 (1976): 9-24.
38. Fan, L.S., R. Leyva-Ramos, K.D. Wisecarver, and B.J. Zelner. "Diffusion of Phenol Through a Biofilm Grown on Activated Carbon Particles in a Draft-Tube Tree-Phase Fluidized-Bed Bioreactor." *Biotechnol. Bioeng.* 35 (1990): 279-286.
39. Williamson, K., and P.L. McCarty. "Verification Studies of the Biofilm Model for Bacterial Substrate Utilization." *J. Wat. Pollut. Contr. Fed.* 48 (1976): 281-296.
40. Livingston, A.G. "Biodegradation of 3,4-Dichloroaniline in a Fluidized-Bed Bioreactor and a Steady State Biofilm Kinetic Model." *Biotechnol. Bioeng.* 38 (1991):260-272.
41. Reid, R.C., J.M. Prausnitz, and T.K. Sherwood. *The Properties of Gases and Liquids*. New York: McGraw-Hill (1977).
42. Sherwood, T.K, R.L. Pigford, and C.R. Wilke. *Mass Transfer*. New York: McGraw-Hill (1975).
43. Yaws, C., H.C. Yang, and X. Pan. "Organic Compounds in Water." *Chemical Engineering* 98(11) (1991): 179-185.
44. Lyman, W.J., W.F. Reehl, and D.H. Rosenblatt. *Handbook of Chemical Property Estimation Methods*. Washington, DC: American Chemical Society (1990): 12-15.
45. Fogler, H. Scott. *Elements of Chemical Reaction Engineering*. Englewood Cliffs, New Jersey: Prentice-Hall (1986).
46. Shareefdeen, Z. "Engineering Analysis of a Packed-Bed Biofilter for Removal of Volatile Organic Compound (VOC) Emissions." *PhD Thesis, New Jersey Institute of Technology*, Newark, NJ (1994).